Detection and Quantification of Stem Cells in Human Salivary Glands

Ву

Mariia Mielkozorova

Master of Science – Dental Sciences (Thesis)

Faculty of Dental Medicine and Oral Health Sciences

McGill University

Montreal

April 15th, 2024

A thesis submitted to

McGill University

In partial fulfilment of the requirements of the degree of Master's in dental sciences

First published on May 12th, 2025

© Mariia Mielkozorova, 2024

Table of Contents

List of Tables2					
List of Figures		5			
List of Abbrevia	tions	12			
Abstract		13			
Resume		15			
Acknowledgeme	nts	18			
Preface and Con	tribution of Authors	20			
1. Introduction		21			
1.1 Understa	anding basic structure, components and functions of Salivary Glands	21			
1.2 Salivary	Glands Diseases and The Impact on Human Life	22			
1.3 Salivary	Gland Cell Types	23			
1.3.1	Stem Cell Origin and Function.	24			
1.3.2	Stem Cell Therapy	26			
1.4 Salivary	Glands Markers	28			
1.5 Rational	le, Objectives and Hypothesis	28			
2. Materials and	Methods	31			
2.1 Literatur	re review	31			
2.2 Obtainir	ng Salivary Tissues from Patients	31			
2.3 Preparat	tion of Formalin Fixed Paraffin Embedded (FFPE) human salivary slides	33			
2.4 Immuno	ofluorescence staining	33			
2.4.1	Primary and Secondary Antibodies.	33			
2.4.2	Single Staining	34			
2.4.3	Co-staining	35			
2.4.4	Evaluation of staining	36			
2.5 MATLA	AB Code Development and Functionality	37			
2.5.1	Design and Development of the Algorithm	38			

2.5.2 Implementing the Algorithm in a User-Friendly Interface Application	40		
2.6 Statistical Test.	43		
3. Results	44		
3.1 Literature Search Results	44		
3.2 Immunofluorescence staining			
3.3 Quantitative and Qualitative Data Analysis			
4. Discussion	84		
5. Conclusions	88		
5.1 Future Directions.	89		
6. References	90		

List of Tables

Introduction

Table 1. List of existent treatments for salivary gland diseases. Adapted from Lombaert (2016).

Materials and Methods

Table 2. List of patients included in the study with their specifications.

Results

Table 3. Papers which were included in rapid literature review showing the tested markers.

Table 4. Curve fitting values for the predictive model of ratio of CD34+ stem cell quantity to total number of cells in the tissue. Basing on the R-square values, we can hypothesize that fit is relatively good with a couple of major deviations.

Table 5. Curve fitting values for the predictive model of ratio of CD90+ stem cell quantity to total number of cells in the tissue. Based on the R-square values, the overall quality of the fit is lower.

List of Figures

Introduction

Figure 1. Depiction of the locations of the three major salivary glands in human (A) and mouse (B). SMG: submandibular gland; SLG: sublingual gland; PG: parotid gland

Figure 2. Types of cells present in generic Salivary Glands

Methods

Figure 3. Algorithm schematics for custom MATLAB-based code designed and executed from raw data to processed images with cells count and labelling.

Figure 4. Steps of the image adjustments using the custom MATLAB code. (A) Single staining, (1a-1d) red channel adjustments, (2a-2d) blue channel adjustments, (e) merged image without post processing, (f) merged final image with post processing. (B) Double staining, (1a-1d) red channel adjustments, (2a-2d) green channel adjustments, (3a-3d) green channel adjustments, (e) merged image without post processing, (f) merged image with post processing with enhanced contrast, (g) final image with post processing. 20X magnification.

Figure 5. First window of the Application. Image selection phase of process.

Figure 6. Second window in the Application. Quantification of the nuclei in the processed image.

Figure 7. Third step in the Application. Labelling the quantified nuclei according to the channel and Data export.

Results

Figure 8. Data summarized from the results of the search for rapid literature review. Sections on how the papers were extracted, retrieved and included in the final data processing are presented in PRISM flow chart.

Figure 9. A) The retrieved articles by year B) The most common markers tested in the obtained studies.

Figure 10. Diagram pie charts showing a) distribution of stem cell markers which were tested for presence in studies using the human cells/tissues b) distribution of stem cell markers which were tested for presence in studies using the rodent cells/tissues c) stem cell markers which were tested positive in studies using the human cells/tissues d) stem cell markers which were tested positive in studies using the human cells/tissues

Figure 11. Diagram pie charts showing a) stem cell markers tested negative in the included studies using the human cells/tissues b) stem cell markers tested negative in the included studies using the rodent cells/tissues.

Figure 12. Bar plots showing a) comparison of quantity of total number of markers tested and their actual expression in studies using the rodent cells/tissues b) comparison of quantity of total number of markers tested and their actual expression in studies using the human cells/tissues.

Figure 13. Expression of markers AQP5 and CD34 in 20x magnification (left) and 40x magnification (right)

Figure 14. Expression of markers AQP5 and CD90 in 20x magnification (left) and 40x magnification (right)

Figure 15. Expression of markers α –SMA and CD34 in 20x magnification (left) and 40x magnification (right)

Figure 16. Expression of markers α –SMA and CD90 in 20x magnification (left) and 40x magnification (right)

Figure 17. Expression of markers α–SMA and Vimentin in 20x magnification (left) and 40x magnification (right)

- Figure 18. Expression of markers CK7 and CD34 in 20x magnification (left) and 40x magnification (right)
- Figure 19. Expression of markers CK7 and CD90 in 20x magnification (left) and 40x magnification (right)
- Figure 20. Bar plot showing the ratio of stem cells with positive expression of marker CD90 to total number of cells in the tissue slide in all 12 patients
- Figure 21. Bar plot showing the ratio of stem cells with positive expression of marker CD34 to total number of cells in the tissue slide in all 12 patients
- Figure 22. Bar plot showing the ratio of stem cells with positive expression of marker Vimentin to total number of cells in the tissue slide in all 12 patients
- Figure 23. CD34 marker expression in 12 patients in relation to the acinar cells
- Figure 24. CD34 marker expression in 12 patients (excluding patient 11) in relation to the acinar cells
- Figure 25. CD34 marker expression in 12 patients in relation to the ductal cells
- Figure 26. CD34 marker expression in 12 patients in relation to the myoepithelial cells
- Figure 27. CD90 marker expression in 12 patients in relation to the acinar cells
- Figure 28. CD90 marker expression in 12 patients (excluding patient 11) in relation to the acinar cells
- Figure 29. CD90 marker expression in 12 patients in relation to the ductal cells
- Figure 30. CD90 marker expression in 12 patients in relation to the myoepithelial cells
- Figure 31. Vimentin marker expression in 12 patients in relation to the myoepithelial cells

 The highest ratios in this plot we observed in Patients 2,3 and 11. No relevance was noticed in relation to the clinical conditions or demographic factors.

Figure 32. Scatter plot with data from all 12 patients representing the ratio between total cell number and CD34 positive stem cell quantity in the in the tissue slide

Figure 33. Ashby plot with data from all 12 patients representing the ratio between total cell number and CD34 positive stem cell quantity in the in the tissue slide. Each patient's data points are represented as a distinct cluster on the plot, with the position of the cluster indicating the patient's overall ratio of stem cells to total number of cells

Figure 34. Scatter plot with data from all 12 patients divided into three groups (Healthy, Benign Tumor, Cancer), representing the ratio between total cell number and CD34 positive stem cell quantity in the in the tissue slide

Figure 35. Ashby plot with data from all 12 patients divided into three groups (Healthy, Benign Tumor, Cancer), representing the ratio between total cell number and CD34 positive stem cell quantity in the in the tissue slide. Each patient's data points are represented as a distinct cluster on the plot, with the position of the cluster indicating the patient's overall ratio of stem cells to total number of cells

Figure 36. Scatter plot with data from all 12 patients divided into two groups (<50 years old, >50 years old), representing the ratio between total cell number and CD34 positive stem cell quantity in the in the tissue slide

Figure 37. Ashby plot with data from all 12 patients divided into two groups (<50 years old, >50 years old), representing the ratio between total cell number and CD34 positive stem cell quantity in the in the tissue slide. Each patient's data points are represented as a distinct cluster on the plot, with the position of the cluster indicating the patient's overall ratio of stm cells to total number of cells

Figure 38. Scatter plot with data from all 12 patients divided into two groups (Female, Male), representing the ratio between total cell number and CD34 positive stem cell quantity in the in the tissue slide

Figure 39. Ashby plot with data from all 12 patients divided into two groups (Male, Female), representing the ratio between total cell number and CD34 positive stem cell quantity in the in the tissue slide. Each patient's data points are represented as a distinct cluster on the plot, with the position of the cluster indicating the patient's overall ratio of stem cells to total number of cells

Figure 40. Scatter plot with data from all 12 patients representing the ratio between total cell number and CD90 positive stem cell quantity in the in the tissue slide

Figure 41. Ashby plot with data from all 12 patients representing the ratio between total cell number and CD90 positive stem cell quantity in the in the tissue slide. Each patient's data points are represented as a distinct cluster on the plot, with the position of the cluster indicating the patient's overall ratio of stem cells to total number of cells

Figure 42. Scatter plot with data from all 12 patients divided into three groups (Healthy, Benign Tumor, Cancer), representing the ratio between total cell number and CD90 positive stem cell quantity in the in the tissue slide

Figure 43. Ashby plot with data from all 12 patients divided into three groups (Healthy, Benign Tumor, Cancer), representing the ratio between total cell number and CD90 positive stem cell quantity in the in the tissue slide. Each patient's data points are represented as a distinct cluster on the plot, with the position of the cluster indicating the patient's overall ratio of stem cells to total number of cells

Figure 44. Scatter plot with data from all 12 patients divided into two groups (<50 years old, >50 years old), representing the ratio between total cell number and CD90 positive stem cell quantity in the in the tissue slide

Figure 45. Ashby plot with data from all 12 patients divided into two groups (<50 years old, >50 years old), representing the ratio between total cell number and CD90 positive stem cell quantity in the in the tissue slide. Each patient's data points are represented as a distinct cluster on the plot, with the position of the cluster indicating the patient's overall ratio of stm cells to total number of cells

Figure 46. Scatter plot with data from all 12 patients divided into two groups (Female, Male), representing the ratio between total cell number and CD90 positive stem cell quantity in the in the tissue slide

Figure 47. Ashby plot with data from all 12 patients divided into two groups (Male, Female), representing the ratio between total cell number and CD34 positive stem cell quantity in the in the tissue slide. Each patient's data points are represented as a distinct cluster on the plot, with the position of the cluster indicating the patient's overall ratio of stem cells to total number of cells

Figure 48. Curve fitting for the data from all 12 patients divided into three groups (Healthy, Benign Tumor, Cancer), representing the ratio between total cell number and CD34 positive stem cell quantity in the in the tissue slide.

Figure 49. Curve fitting for the data from all 12 patients divided into three groups (Healthy, Benign Tumor, Cancer), representing the ratio between total cell number and CD90 positive stem cell quantity in the in the tissue slide.

Figure 50. Bar plot showing the total overlap count of stem cells with 3 types of SG cells without separation for each type in the tissue slide in all 12 patients

Figure 51. Overlap of epithelial markers with stem cell marker CD34 in all 12 patients.

Figure 52. Overlap of epithelial markers with stem cell marker CD90 in all 12 patients.

List of Abbreviations

α-SMA	Alpha smooth muscle actin				
AQP5	Aquaporin-5				
CK7	Cytokeratin 7				
FFPE	Formalin fixed paraffin embedded				
HIER	Heat induced antigen retrieval				
MSCs	Mesenchymal stem cells				
PBS	Phosphate-buffered saline				
SGSCs	Salivary gland stem cells				
PBS	Phosphate-buffered saline				
SMG	Submandibular salivary gland				

Abstract

Salivary glands diseases can significantly reduce the quality of life and have a negative impact on the regular daily activities. As all body tissues, certain stem cells might reside within salivary glands, and play a crucial role in maintaining tissue homeostasis, repair and regeneration of an injured tissue. It is important to determine the origin of salivary glands stem cells in order to estimate their potential and function. The analysis of salivary glands stem cells holds valuable promises for further understanding of salivary diseases and advancing the regenerative therapies, however, there are several challenges to address before turning these perspectives into real practice. Stem cell therapy has emerged as a ground-breaking field of regenerative medicine, that can be beneficial in the treatment of various medical conditions, such as degenerative diseases, injuries, and different body disorders. While stem cell therapy has been proven effective in certain conditions, it is still progressing continuously. The challenges in the field of stem cells lie in multiple directions, starting from identification and isolation of specific stem cell populations when multiple types coexist and understanding their regulatory mechanisms. In addition to the complexity of translating the laboratory findings into clinically applicable therapy which may require years of analysis and validation. Although, finding the ideal stem cells for therapy is still in progress, the mesenchymal stem cells are considered the main candidate.

Recently, the interest in identifying and characterizing salivary stem cells has emerged. Determining certain salivary stem cell markers will undoubtedly be a crucial step in the advancement of stem cell therapy. These markers are very important diagnostic tools to distinguish between benign and malignant tumors and to diagnose certain salivary autoimmune diseases, such as Sjogren's syndrome. Certain markers can be used as prognostic indicators to help clinicians predict the aggression level of certain tumor types which might guide the treatment accordingly.

In this study the co-expression of certain stem cell markers, such as CD90, CD34 and Vimentin was examined with certain typical salivary gland cell markers, such as AQP5, CK7 and α -SMA. For the detection of stem cells located in the submandibular salivary glands of 12 patients, immunofluorescence staining was performed with following analysis using the custom created application based on the MATLAB code. The results which were analyzed with statistical tools revealed the presence of certain stem cells in human submandibular salivary tissue, and the ratios of salivary to stem cells were compared. The patients were divided by sex, age and medical conditions (healthy, with benign tumor and with cancer).

Our findings revealed a definite correlation between disease status and the quantity of stem cells present. However, establishing a clear relationship between age and stem cell quantity proved to be inconclusive due to the heterogeneous clinical conditions and demographic profiles of our patients. Although statistical analysis yielded nonsignificant results (p value > 0.05), notable trends emerged. Stem cell expression in the healthy group consistently fell within a certain range, whereas the group of patients with benign tumors exhibited lower stem cell expression compared to other groups. Conversely, stem cell expression in the cancer group displayed significant variability, likely attributable to its larger size and heterogeneous composition in terms of age and sex distribution. Furthermore, higher expression of the hematopoietic stem cell marker CD34 in cancer patients underscored its role in cancer stem cell populations.

Obtained results would serve as a proof of stem cells presence in salivary glands and will provide perspectives for future research directions. Our future directions aim to compare stem cell numbers in major salivary gland and to study the impact of specific negative habits, such as smoking and alcohol consumption on the quantity and location of certain stem cells.

Résume

Les maladies des glandes salivaires peuvent réduire considérablement la qualité de vie et avoir un impact négatif sur les activités quotidiennes régulières. Comme tous les tissus corporels, certaines cellules souches peuvent résider dans les glandes salivaires et jouer un rôle crucial dans le maintien de l'homéostasie des tissus, la réparation et la régénération d'un tissu blessé. Il est important de déterminer l'origine des cellules souches des glandes salivaires afin d'estimer leur potentiel et leur fonction. L'analyse des cellules souches des glandes salivaires est porteuse de promesses précieuses pour mieux comprendre les maladies salivaires et faire progresser les thérapies régénératives. Cependant, il reste plusieurs défis à relever avant de transformer ces perspectives en pratique réelle.

La thérapie par cellules souches est devenue un domaine révolutionnaire de la médecine régénérative, qui peut être bénéfique dans le traitement de diverses conditions médicales, telles que : les maladies dégénératives, les blessures et différents troubles corporels. Même si la thérapie par cellules souches s'est avérée efficace dans certaines conditions, elle continue de progresser continuellement. Les défis dans le domaine des cellules souches vont de plusieurs directions, à commencer par l'identification et l'isolement de populations spécifiques de cellules souches lorsque plusieurs types coexistent et par la compréhension de leurs mécanismes de régulation. En plus de la complexité de traduire les résultats de laboratoire en thérapie cliniquement applicable qui peut nécessiter des années d'analyse et de validation. Bien que la recherche des cellules souches idéales pour le traitement soit encore en cours, les cellules souches mésenchymateuses sont considérées comme les principales candidates.

Récemment, l'intérêt pour l'identification et la caractérisation des cellules souches salivaires est apparu. La détermination de certains marqueurs de cellules souches salivaires

constituera sans aucun doute une étape cruciale dans l'avancement de la thérapie par cellules souches. Ces marqueurs sont des outils de diagnostic très importants pour distinguer les tumeurs bénignes des tumeurs malignes et pour diagnostiquer certaines maladies auto-immunes salivaires, comme le syndrome de Sjögren. Certains marqueurs peuvent être utilisés comme indicateurs pronostiques pour aider les cliniciens à prédire le niveau d'agressivité de certains types de tumeurs, ce qui pourrait guider le traitement en conséquence.

Dans notre étude, nous avons examiné la co-expression de certains marqueurs de cellules souches, tels que CD90, CD34 et Vimentine, avec certains marqueurs cellulaires typiques des glandes salivaires, tels que AQP5, CK7 et α-SMA. Nos résultats révèlent la présence de certaines cellules souches dans le tissu salivaire sous-maxillaire humain sain, et nous avons comparé les ratios cellules salivaires/cellules souches à l'aide d'un logiciel personnalisé. De plus, nous avons analysé ces ratios en comparant plusieurs groupes de tissus en fonction de leur âge et de leur sexe.

Les résultats obtenus serviraient de preuve de la présence de cellules souches dans les glandes salivaires et ouvriraient des perspectives pour de futures orientations de recherche. Nos orientations futures visent à comparer le nombre de cellules souches dans les principales glandes salivaires et à étudier l'impact d'habitudes négatives spécifiques, telles que le tabagisme et la consommation d'alcool, sur la quantité et la localisation de certaines cellules souches. Pour la détection des cellules souches situées dans les glandes salivaires submandibulaires de 12 patients, une coloration par immunofluorescence a été réalisée avec l'analyse suivante à l'aide de l'application créée sur mesure et basée sur le code MATLAB. Les résultats analysés à l'aide d'outils statistiques ont révélé la présence de certaines cellules souches dans le tissu salivaire submandibulaire humain, et les ratios cellules salivaires/cellules souches ont été comparés. Les

patients ont été répartis en fonction de leur sexe, de leur âge et de leur état de santé (sains, atteints d'une tumeur bénigne ou d'un cancer).

Nos résultats ont révélé une corrélation certaine entre l'état de la maladie et la quantité de cellules souches présentes. Cependant, l'établissement d'une relation claire entre l'âge et la quantité de cellules souches s'est avéré peu concluant en raison de l'hétérogénéité des conditions cliniques et des profils démographiques de nos patients. Bien que l'analyse statistique ait donné des résultats non significatifs (valeur p > 0,05), des tendances notables sont apparues. L'expression des cellules souches dans le groupe sain se situait systématiquement dans une certaine fourchette, tandis que le groupe de patients atteints de tumeurs bénignes présentait une expression des cellules souches plus faible que les autres groupes. À l'inverse, l'expression des cellules souches dans le groupe de patients atteints de cancer présentait une variabilité significative, probablement attribuable à sa taille plus importante et à sa composition hétérogène en termes d'âge et de répartition par sexe. En outre, l'expression plus élevée du marqueur de cellules souches hématopoïétiques CD34 chez les patients cancéreux a souligné son rôle dans les populations de cellules souches cancéreuses.

Les résultats obtenus serviront de preuve de la présence de cellules souches dans les glandes salivaires et fourniront des perspectives pour les orientations futures de la recherche. Nos orientations futures visent à comparer le nombre de cellules souches dans les principales glandes salivaires et à étudier l'impact d'habitudes négatives spécifiques, telles que le tabagisme et la consommation d'alcool, sur la quantité et la localisation de certaines cellules souches.

Acknowledgements

I would like to begin my gratitude by saying hugest thank you to my supervisor Dr. Simon Tran. Thanks to him, my incredible journey in Canada began, thanks to him I have an opportunity to pursue science and do what makes me happy. Since the war started in my country Ukraine, I couldn't believe that I will continue my path in science, especially in one of the best universities in Canada. I would like to say thank you to Professor Yuri Monchak, who I met on second course of my bachelor's degree back at home and in time of need when I asked for his help, he connected me with Dr. Simon Tran and incredible administrative workers of McGill University. My big gratitude is to Dr. Svetlana Komarova, who was of great support since I only began planning my start at McGill University and she still is. I am looking forward to working with you and achieving great goals we set our minds on. I thank Dr. Ola Maria for her professional advice and her support, for teaching me and for the understanding of each other we had while generating ideas and processing results.

I thank my dear colleagues from Dr Tran's lab, Janaki Iyer, who is my big sister and I will always appreciate and remember how kind and caring you were to a stranger through these two years; Uyen Cao, we were crying and laughing together and I wish you be happy and believe in your power; Sangeeth Pilai, you were kind to me from the first day I stepped scared in the laboratory and you were of a big support, you are an example for me, how you can become great and still be so humble about it and I appreciate the opportunity to learn from you as well; Yuli Zhang, you were patient and helpful to me, your kind soul makes you out of this world; Akshaya Upadhyay, thank you, I have learnt valuable lesson from you which will help me in my future career; Dr. Younan Liu, thank you for your hard work and continuous help.

I would like to give special thanks to Lander Manrique, you are my biggest support, you were always there for me, giving important advice and working side by side with me.

I would like to thank the Canadian governmental agencies, CIHR and FRQ for their support and for creating financial support programs for Ukrainian students so we have an opportunity to study and obtain knowledge we couldn't dream of.

Most importantly, I would like to say thank you to my mother and my father, I am grateful for pushing me despite all my fears and we are all support for each other, I love you more than anything and every day of my life I will be trying to do more and get out of my skin so you will be proud.

Preface and Contributions of Authors

Mariia Mielkozorova was responsible for performing Immunofluorescence staining on the FFPE salivary gland tissue slides, performing the evaluation of the staining, the study direction and performance, and results analysis. Akshaya Upadhyay and Sangeeth Pilai mentored and assisted in preparing the salivary tissue, choosing appropriate antibodies, and assessing the quality of results. Lander Manrique assisted with writing the custom code for MATLAB, developing the project and editing the manuscript. Dr Ola Maria assisted with the correction of the French version of the abstract. Dr. Ola Maria assisted with assessing the quality of images, cell counting, evaluating the histology of salivary tissues and editing the manuscript. All other work was performed by Mariia Mielkozorova under the supervision of Dr. Simon Tran. The project was funded by the Canadian Institutes of Health Research (CIHR grant 159577) and Fonds de Recherche du Quebec Sante.

1. Introduction

1.1 Understanding basic structure, components and functions of Salivary Glands

Salivary glands are relatively small structures in the human body which are usually overlooked while talking about successful maintenance of the organism, although they play a very important role in supporting the quality and stability of everyday life [1]. Their significance in our body combines irreplaceable functions to a fundamental role in maintaining oral health and starting the first step of digestion. The point in understanding their importance lays in understanding their basic structure, analysing the components and unique functions.

Salivary glands are located throughout the oral cavity (Figure 1). There are three pairs of major salivary glands: parotid, submandibular and sublingual, and many minor salivary glands [2]. Parotid glands are the largest of the major salivary glands and are located near the ears. The components of all three glands are relatively similar with a few differences [3]: the parotid is mainly composed of serous cells (production of enzyme-rich saliva), the submandibular, which is located under the mandible, is composed of serous and mucous cells (mixed saliva) and the sublingual, which is located under the tongue, consists mainly of mucous cells (mucous saliva) [4]. These different types of saliva get mixed in the mouth to form human saliva that starts the digestion process.

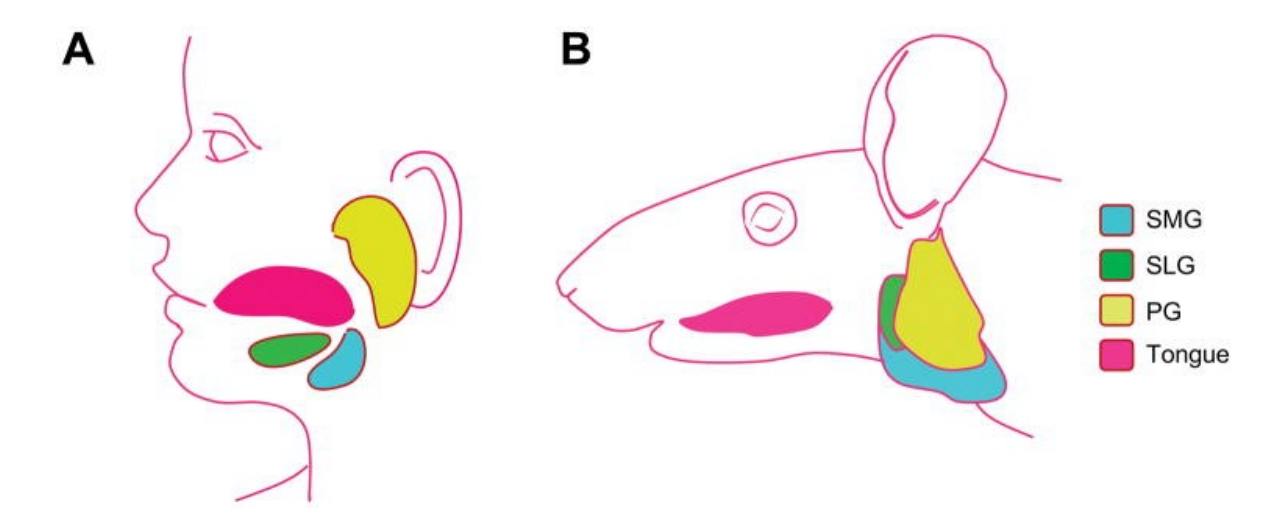


Figure 1. Depiction of the locations of the three major salivary glands in human (A) and mouse (B). SMG: submandibular gland; SLG: sublingual gland; PG: parotid gland [3].

1.2 Salivary Glands Diseases and The Impact on Human Life

Salivary glands as any other organ of the human body are susceptible to various diseases which can significantly reduce the quality of life. Certain diseases can cause difficulty in swallowing, mastication, and speech, making them very discomfortable and painful.

There are recognised various diseases that can lead to such complications, among which are such as salivary gland sialoliths - stones which obstruct the normal flow of the saliva, causing pain and discomfort. They can obstruct the ductal part of the gland and may cause injury to its epithelial cells, leading to reduced salivary secretion. Another common disease which is found widespread is Sjogren's syndrome. It is an autoimmune disorder which affects salivary and lacrimal glands, leading to reduction of saliva and tear production. Both acinar and ductal cells within the affected glands get damaged and eventually further destroyed if disease management measures are not implemented [5].

Therefore, it is very important to study the salivary glands components and functions to be able to understand the pathology of each glandular disease.

1.3 Salivary Gland Cell Types

Salivary glands consist of several types of specialized cells, each of which have unique roles in contributing to the saliva formation.

Acinar salivary cells are the main cellular component that produces and secretes saliva. These cells produce different enzymes, electrolytes and water, and pack these components into secretory granules in order to release them into the ductal system. Acinar cells are typically rounded or pyramidal shaped cells, depending on whether they form serous or mucous acini. Acinar cells have a granular cytoplasm, well-developed endoplasmic reticulum, and Golgi apparatus, which are involved in the protein synthesis process. Serous and mucous acini produce different types of saliva. Serous cells produce enzyme-rich watery saliva while mucous cells produce thick mucin-rich saliva.

Ductal cells form the duct system of the salivary gland and their main role is to modify and transport saliva secreted by acinar cells to the oral cavity. They reabsorb sodium ions and water then secrete potassium ions and concentrate the initially formed saliva. Ductal cells are organized in three different types of ducts: intercalated, striated, and excretory as shown in Figure 2. The intercalated ducts are formed of cuboidal epithelial cells, the striated ducts are formed of taller cells with basal striations due to the presence of mitochondria, and the excretory ducts are formed of columnar or high cuboidal epithelial cells.

Myoepithelial cells have special criteria that allow them to contract, to expel saliva from the acinar cells to the ductal system. Upon receiving the stimulating signal, myoepithelial cells contract to squeeze acinar cells and facilitate saliva secretion. Such contraction is happening due to the presence of actin and myosin filaments, which form the typical components of all human muscles. Myoepithelial cells are located on the basement membrane on the acinar cells, "wrapping" around them, to create an additional supportive layer [1].

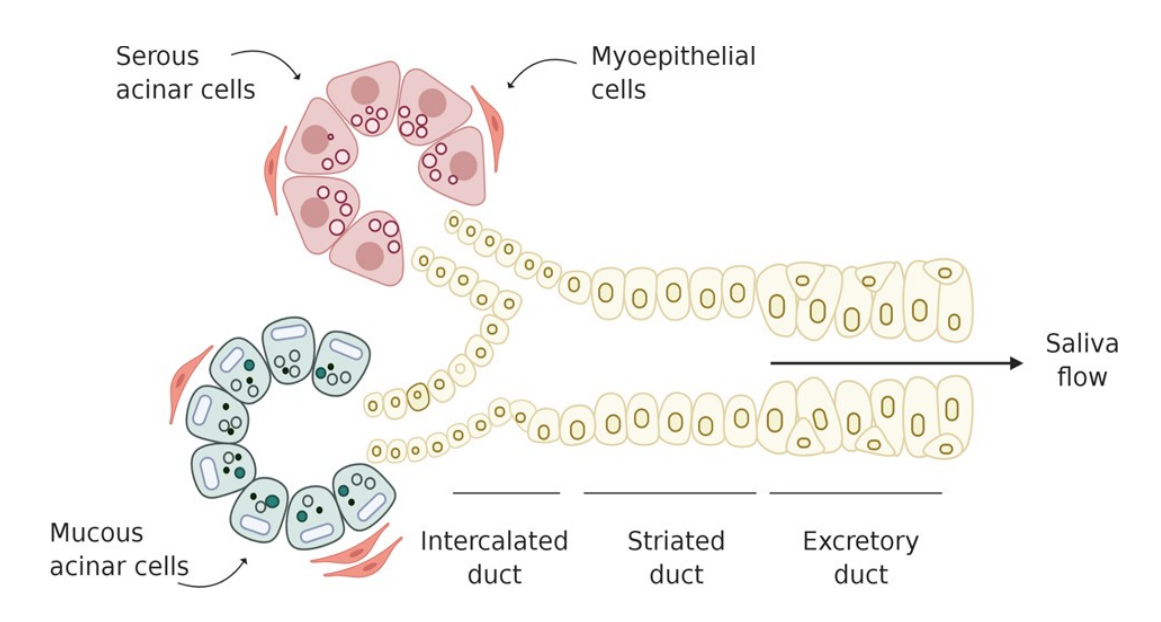


Figure 2. Types of cells present in generic Salivary Glands [6].

1.3.1 Stem Cells Origin and Function

Stem cells play an important role in maintaining tissue homeostasis, repair and tissue regeneration. It is crucial to determine the origin of salivary gland stem cells to study their potential functions.

During embryogenesis, salivary gland precursor cells are located in an area that becomes the future oral cavity. These precursor cells differentiate into various salivary cell types which include resident salivary stem cells which possess the regenerative capacity. In the next stages of human growth, adult stem cells reside in a tissue-localized pool of stem cells, which plays an important role in tissue regeneration, maintain homeostasis and perform repair of damaged tissues.

These stem cells are typically located in specific niches that maintain ideal microenvironments to support stem cells and provide necessary signalling molecules, growth factors and cytokines, to regulate the stem cells behaviour, influence their self-renewal, and differentiation [3].

Salivary glands harbor several types of the stem cells, each of which having their specific role, properties, and functions. Such types are salivary gland stem cells (SGSCs), mesenchymal stem cells (MSCs) and epithelial progenitor cells. SGSCs are resident stem cells specific to salivary glands and their main function is to maintain salivary tissue homeostasis, repair and regeneration. SGSCs can differentiate into acinar and ductal salivary cells. Mesenchymal stem cells might be found within the salivary glandular tissue. MSCs have the ability to differentiate into different salivary cell types and can contribute to the salivary tissue regeneration. Epithelial stem cells are responsible for generating specific epithelial cells, such as acinar and ductal cells. They are essential for the maintenance of the epithelial architecture within the glands and for responding to tissue damage [7].

Salivary gland stem cells are essential for maintaining the normal architecture and function of the glands. They continuously replace damaged or aging cells, ensuring that the glands can produce and secrete saliva effectively. In response to injury or damage, that is caused by infections, radiation therapy, or autoimmune disorders, stem cells residing within salivary glands become activated, undergo division and differentiate into the necessary cell types to repair the damaged tissue and restore the salivary gland function [8].

The regenerative capacity of salivary gland stem cells has attracted significant interest in the field of regenerative medicine. Researchers have been exploring their potential therapeutic use in the treatment for certain conditions, such as Sjögren's syndrome, radiation-induced xerostomia, and salivary gland tumors [9].

While the study of salivary gland stem cells holds a promise to provide better understanding of salivary gland diseases and provide potential therapy, there are several challenges to overcome before turning these perspectives into clinical practice. These challenges are related to identifying and isolating specific stem cell populations residing within salivary glands, as multiple types of stem cells may possibly coexist, stem cells regulatory mechanisms are not fully understood and the fact that transition of research findings into clinically applicable therapies is a complex process that requires years of testing and validation.

1.3.2 Stem Cell Therapy

There is no unified approach for the treatment of these salivary gland disorders. There are multiple options of how these diseases are managed by the researchers and clinicians (Table 1).

Treatment modality	Specific approaches or methods	Known limitations	
Palliative	Saliva substitutes	Effectiveness is limited & short-term	
(Symptomatic	Nutritional counseling	Oral tissues continue to display	
relief)		deleterious changes	
		Patient compliance is highly variable	
Pharmacologic	Sialogogues	Effects are systemic	
	Immunomodulatory drugs	Multiple doses/day required	
		Interact with other drugs	
		Patient compliance is highly variable	
Gene Therapy	Adeno-associated viruses (AAVs)	Effect depends on the extent of gland	
	Oligonucleotides	damage	
	Plasmids	Effect can be ablated by immune	
		response	
		Response to treatment is often of	
		limited duration	
Cell-based	Salivary gland progenitors	Treatment must be optimized	
therapies	Induced pluripotent stem cells	(cell type, route of administration,	
	(iPSCs)	dose, etc)	
	Mesenchymal stem cells (MSCs)	Cells must engraft and survive for	
		ongoing effect	
		Mechanisms of action are diverse	

Table 1. List of existent treatments for salivary gland diseases. Adapted from Lombaert (2016)

Stem cell therapy has emerged as a ground-breaking field of regenerative medicine, holding promises for the treatment of various medical conditions, including degenerative diseases, injuries, and disorders affecting different parts of the body. While some stem cell therapies have already been established as effective treatments, others are still in the developmental stages.

For salivary glands, stem cell therapy is still emerging. Studies aim to harness the regenerative potential of stem cells to repair damaged salivary gland tissue and improve the quality of life for individuals suffering from different salivary gland disorders.

In case of Sjogren's syndrome, SGSCs and MSCs can be isolated, cultured, and transplanted into the affected glands to promote tissue repair and regeneration. Preliminary studies have shown encouraging results, with improvements in salivary flow rates and symptoms relief. Xerostomia is a chronic condition that can result from radiation therapy for head and neck cancers, where radiation damages salivary tissue to a variable degree, depending on the radiation dose [10-15]. Clinical trials have explored the transplantation of SGSC and MSCs into the irradiated salivary glands. These stem cells could promote tissue repair, reduce inflammation, and enhance saliva production [11, 16-19].

While stem cell therapy for salivary gland disorders is a new promising field that shows a potential for treating conditions that have "no cure", several specific challenges and areas of ongoing research do exist. Besides the regulatory research approvals challenges, defining the optimized and best fitting stem cells to employ as a therapy is another big challenge. In addition, finding the best delivery method to minimize the invasiveness of the existing techniques is the biggest challenge.

1.4 Salivary Glands Markers

Markers are specific molecules or proteins, which are expressed by specific cells and can allow researchers and clinicians to identify, characterize, localize, and target these specific cells within any human tissue. Recently, the interest to identify and characterize the stem cells located in salivary glands has been increasing. Using specific markers might help to determine a salivary-specific stem cell therapy. In addition, markers serve as a precise diagnostic tool that can distinguish between benign and malignant tumors or diagnose certain autoimmune diseases, such as Sjogren's syndrome. Furthermore, some markers have been used as prognostic indicators, helping clinicians to predict the aggressiveness of certain tumors and direct the treatment accordingly [17].

The most common markers for different salivary gland cells are: Aquaporin 5 (AQP5) for the acinar cells, Cytokeratin 5 (CK5) or Cytokeratin 7 (CK7) for the ductal cells, alpha smooth muscle actin (α-SMA) for myoepithelial cells, and for stem cells C-Kit, CD44, Musashi-1 are among the most commonly used markers [1]. Furthermore, a literature review was performed to determine other markers not often used in human studies that could be potentially reliable as diagnostic tools or to confirm the presence of stem cells within the submandibular salivary glands.

1.5 Rationale, Objectives, and Hypothesis

As a graduate student at McGill University, Faculty of Dental Medicine and Oral Health Sciences, the main goal of the research we conducted is to improve access to oral care, to improve current oral care interventions, and/or to address oral diseases.

This research project aims to provide new possible ways for easier detection of stem cells for future treatment strategies and understanding the stem cell presence in healthy and irradiated salivary glands.

This thesis addresses the following issue by providing information about precise localization and frequency of stem cells occurrence in relation to the main salivary cell types which are responsible for the saliva production, transportation and overall maintenance of health of oral and life quality. We also aim to compare the ratio of stem cells to salivary gland cells in different age groups and in healthy versus irradiated salivary glands.

Several objectives have been outlined to address the potential directions for stem cell therapy researchers in future:

- 1. Choosing the appropriate stem cell markers:
- a) Determining certain markers by accessing the current literature-available methods of stem cells detection.
- b) Understanding, by using the histological structure of salivary glands, which types of stem cells are more likely to be present in the adult human submandibular salivary tissue.
- c) Visualizing the presence of stem cells using immunofluorescence method.
- d) Establishing a protocol for proper, effective and consistent detection of stem cells in adult human submandibular salivary glands tissue.
- 2. Detecting stem cell markers:
- a) Performing immunofluorescence staining using the accurately chosen antibodies.
- b) Stem cell detection and counting in respect to acinar, ductal and myoepithelial cells.
- 3. Creating custom code in MATLAB for making the process of detection of different cell types more accessible, reliable, and smarter for future research:

- a) Developing the code for image correction.
- b) Creating the code for separation of color channels and converting image for automatic cell counting.
- c) Implementing developed code in a user-friendly application for future smart image processing.

The rationale for using markers which were chosen for this study lies in the literature review which was performed in order to access the current published data, which will be explained in detail in the next sections.

The main hypothesis of the project is that the typical human submandibular salivary gland cells can be co-localized with stem cells, which might be adding to their regeneration and repair.

2. Materials and Methods

2.1 Literature review

Rapid literature review was performed on October 5th, 2023, in Medline (Ovid), Web of Science and Embase (Ovid) to access the data present in the literature regarding ways to detect stem cells in salivary gland tissue. For the search strategy were combined a) different types of stem cells, b) types of glands, making an accent on the submandibular glands, c) types of cells present in the salivary glands (acinar, ductal, and myoepithelial cells) and d) marker or biomarker as a MESH term and a keyword. Studies, which were retrieved using the established search strategy, were screened by the first author of the project and were included if within that study they performed immunofluorescence staining and used markers to target stem cells. Both human and animal studies were included, as with this review the differences and similarities between the expression of stem cell markers in both subjects were accessed.

2.2 Obtaining Salivary Tissues from Patients

Twelve human submandibular salivary glands were obtained from Montreal General Hospital and McGill University Health Centre, both located in Montreal, Quebec, Canada. All gland tissues were extracted due to the clinical conditions mentioned in the Table N. Execution of this project was performed with approval from the McGill Faculty of Medicine Institutional Review Board (IRB study number A05-M62-05B).

Patient co	de	Tissue collection date	Age	Gender	Clinical Condition	Gland type
FS7	1	February 2023	25	M	Surgery for mandibular	SMG
					reconstruction	
AS7	2	April 2023	45	M	Odontogenic keratocyst	SMG
MYS7	3	May 2023	70	M	Tongue cancer	SMG
PtS7	4	June 2023	81	F	CVA/Stroke injury, possible	SMG
					history of neurodegenerative	
					disease	
MAD 03-	5	2003	38	M	Metastatic papillary thyroid cancer	SMG
2042						
MAD 02-	6	2002	52	M	Metastatic squamous cell carcinoma	SMG
1012						
MAD 03-	7	2003	52	M	Carcinoma of the floor of mouth	SMG
1500						
MAD 04-	8	2004	54	M	Right floor of mouth cystic	SMG
172					sublingual tumor, carcinoma of	
					minor salivary gland, adenoid	
					cystic carcinoma	
MAD 03-	9	2003	48	F	Squamous cell carcinoma of	SMG
1680					larynx	
MAD 04-	10	2004	59	F	Floor of mouth squamous cell	SMG
167					cancer with evidence of bony	
					involvement	
Oct23Pt1	11	October 2023	28	F	Central Giant Cell Granuloma	SMG
					(mandible)	
Oct23Pt2	12	October 2023	24	F	Ameloblastoma(mandible)	SMG

Table 2. List of patients included in the study with their specifications.

2.3 Preparation of Formalin Fixed Paraffin Embedded (FFPE) human salivary slides

In order to obtain FFPE slides, each gland tissue was cut, fixed in 40% paraformaldehyde for 24 hours then washed and preserved in PBS. Afterwards, tissue in PBS was sent to the Cancer Center of McGill University to be embedded in paraffin and cut to create tissue slides.

2.4 Immunofluorescence staining

Immunofluorescence staining is considered to be an important immunochemical technique which allows to localization and detection of certain proteins within cells and tissues [20]. The main principle of immunofluorescence staining relies on the use of specific antibodies corresponding to the targeted protein of interest. These antibodies are labeled with fluorophores, which emit light when introduced to their appointed wavelength.

The rationale for using immunofluorescence staining in this project was its relative simplicity and being highly specific in detection of cellular targeted proteins. The use of this novel semi-quantitative technique allows for the examination and analysis of FFPE slides, which are a common practice in research and in the medical pathology laboratories, which makes this technique clinically applicable the medical practice.

2.4.1 Primary and Secondary Antibodies

The following primary anti-human antibodies were used in this study: rabbit monoclonal [EPR5368] to alpha smooth muscle actin (1:300) (AbCam ab124964), rabbit monoclonal [EPR3747] to aquaporin 5 (1:250) (AbCam ab92320), purified mouse anti-human CD90 (1:100) (Thermofisher AB_2203304), recombinant anti-cytokeratin 7 antibody [EPR17078] - cytoskeleton marker (1:100) (ab181598) and CD34 (Thermofisher MA1-10202 QBEND/10).

As a negative control staining with only secondary antibodies was used, emitting the described steps with primary antibodies tissue preparation.

The secondary antibodies used were Alexa Fluor 488 and Alexa Fluor 594 for the corresponding antibodies, as per the manufacturer's instructions, and DAPI was used for staining the nuclei.

2.4.2 Single Staining

Single staining was performed with the following protocol that was established in Dr. Tran's laboratory. The staining steps were performed over three consecutive days. On the first day, FFPE slides were deparaffinized in citric solution by immersion for five minutes, two times. Following deparaffinization, rehydration was performed by immersing the slides in 100% Ethanol for 5 minutes, 2 times, then in 95% Ethanol for 5 minutes, then in 80% Ethanol, and 75% Ethanol for 5 minutes each, and finally in phosphate-buffered saline (PBS) 3 times for 5 minutes. This step is important as hydrated tissues allow for better antibody penetration.

The next step was the antigen retrieval with the heat induced antigen retrieval (HIER) method. The mounted tissue sample is heated in a buffer solution of Citric Acid (with a neutral pH=6-6.1) at 95° C to cleave the crossed-links and to preserve the protein conformation. Post antigen retrieval slides were let to cool down for 15 minutes to preserve properties of the glass then were washed with PBS for 5 minutes, 3 times.

The next step is blocking and permeabilization: for samples with intracellular targeted proteins, there is a need to make cell membranes more permeable, so the antibodies can pass through the membrane to reach the targeted protein. 0.3% Triton X-100 was used to cover the tissue sections for 10 minutes to perform the permeabilization step. In this step it is crucial to keep

delicate balance, as over-permeabilization can lead to loss of cellular integrity. Thereafter, slides were washed with PBS for 5 minutes, 3 times. The blocking step was performed to prevent binding to non-specific antibodies. For blocking, 0.3% hydrogen peroxide was used for 10 minutes, PBS wash for 5 minutes 3 times then, the Universal block solution overnight at 4°.

During the second day, the chosen primary antibodies were added to the tissue slides to target acinar cells, ductal cells, myoepithelial cells and stem cells. Tissue slides with primary antibodies were incubated overnight at 4° to allow for ideal binding of the antibody to the targeted protein.

On the third day, slides were washed with PBS for 5 minutes, 3 times and secondary antibodies were added after being diluted, for 1 hours in a dark room. Afterwards, slides were washed with PBS for 5 minutes, 3 times, then stained with DAPI for 10 minutes in a dark room, washed with PBS 5 minutes, 3 times and each covered with a covering slip. The mounting media contained antifade reagents to prevent fluorescent signals damage due to frequent exposure to light.

2.4.3 Co-staining

The co-staining was performed following the same protocol. On day two, before adding the primary antibodies to the tissue, it was necessary to dilute the two chosen primary antibodies together, verifying that the host species of the antibodies are different, to prevent cross-reactivity and false binding.

On day three, before adding the secondary antibodies, dilutions should be made according to the chosen primary antibodies and the corresponding color wavelength. Origins of the secondary antibodies should also be chosen to avoid cross-reactivity and incorrect secondary antibody

binding. All the previous and following steps of the staining protocol are the same as for single immunofluorescence staining technique.

In total, for each patient, 5 FFPE slides with 3 tissue sections per slide were processed. Staining was done for AQP5, CK7 and α -SMA antibodies co-stained with CD90, CD34 and Vimentin antibodies respectively. These combinations of cell-specific and stem cell-specific staining were used to access the localization and the frequency of stem cells in the submandibular salivary gland tissue.

2.4.4 Evaluation of Staining

After processing human tissue slides, they were evaluated with a light microscope ZEISS AXIO Imager. M2 (Carl Zeiss Jena, Germany). Slides were analyzed in RGB spectrum per each tissue section. Software ZEN 2 (blue edition-(Carl Zeiss Microscopy GmbH, 2011) was used for capturing images. Cells were counted manually in order to verify the trustworthiness of the developed custom code. The intensity of the staining was not evaluated in the study. Cells are considered positive if they were emitting blue, red or green light, respectively, without considering the area covered, as it was impossible to predict the direction of cell localization in the cut sections. Cells were counted using 20X magnification, 4 areas per patient were chosen randomly for each of the 12 patients included in this study. Additionally, age, sex and medical conditions groups of patients were taken into account, as a secondary goal of this project, we aimed at accessing the possible difference in the quantity of stem cells in different demographics.

2.5 MATLAB Code Development and Functionality

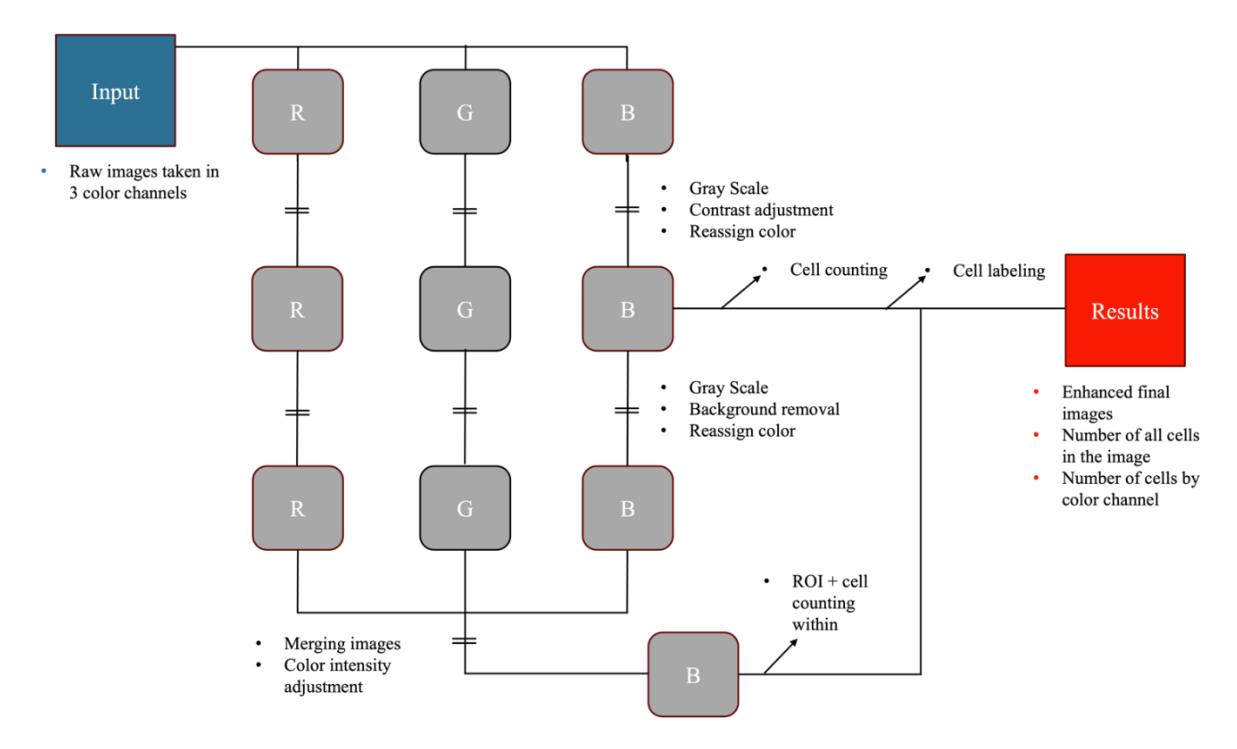


Figure 3. Algorithm schematics for custom MATLAB-based code designed and executed from raw data to processed images with cells count and labelling.

In order to create an automized "smart" working system for images processing, was developed a custom code using MATLAB software. There are two main goals for using the custom code in this project:

- For the purpose of creating unified results, the first step for the code was to develop a chain of commands, corresponding to separate images for a single staining and the costaining.
- 2) The next step was to evaluate color intensities and interactions in merged images to be able to analyze and access separate structures presented in the image, to count present cells and to evaluate the distribution of stem cells in correspondence to acinar, ductal and myoepithelial cells, respectively.

2.5.1 Design and Development of the Algorithm

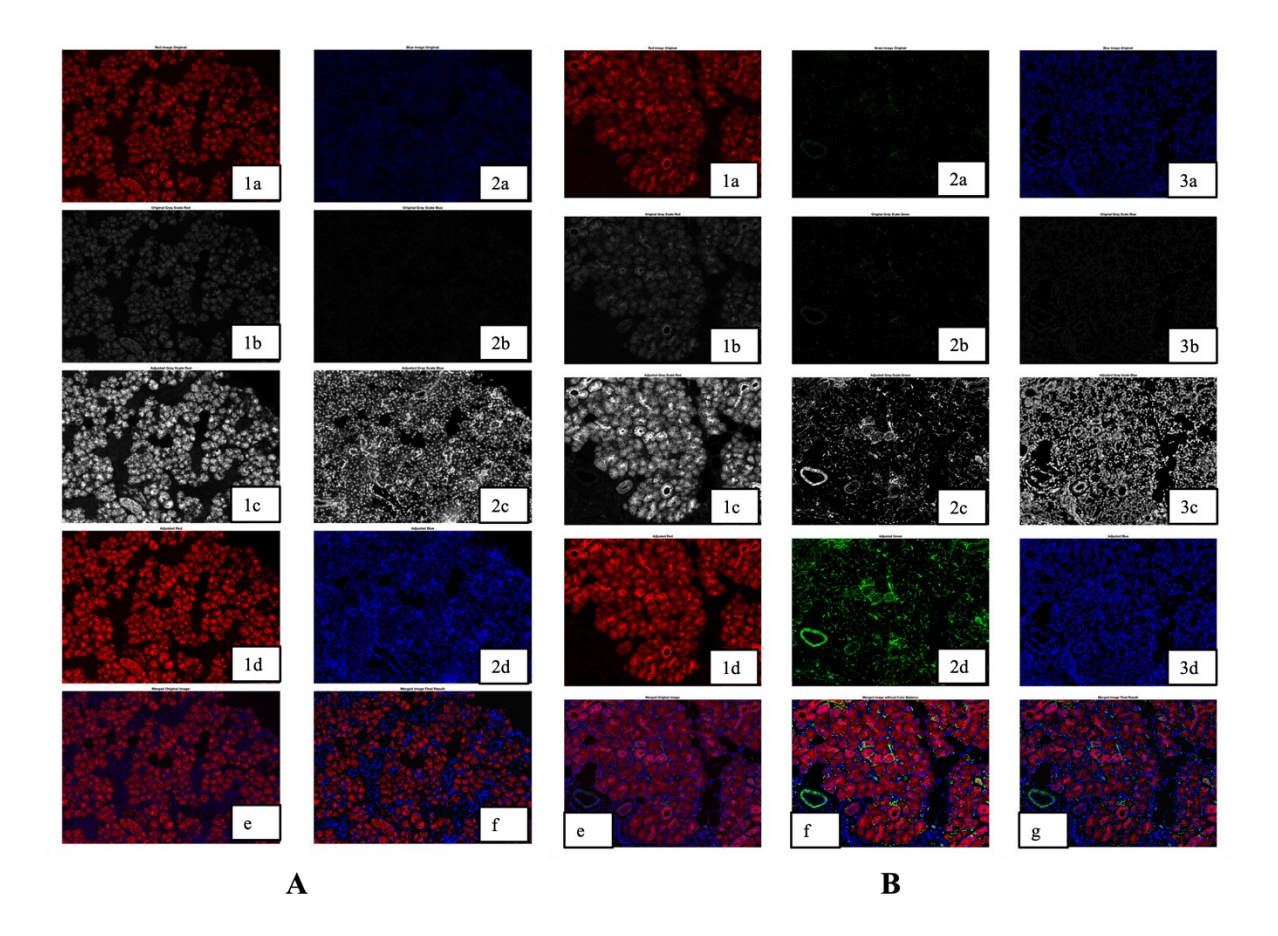


Figure 4. Steps of the image adjustments using the custom MATLAB code. (A) Single staining, (1a-1d) red channel adjustments, (2a-2d) blue channel adjustments, (e) merged image without post processing, (f) merged final image with post processing. (B) Double staining, (1a-1d) red channel adjustments, (2a-2d) green channel adjustments, (3a-3d) green channel adjustments, (e) merged image without post processing, (f) merged image with post processing with enhanced contrast, (g) final image with post processing. 20X magnification.

To retrieve relevant parameters from the acquired data, a custom image processing tool was designed and executed during this stage of the project. After the images were digitalized, the first step was to adjust the contrast. To augment the contrast in obtained images the function "imadjust" was used and applied to all three RGB channels which were converted into gray scale

prior to the adjustment. Masks for background removal were created for each channel, defining a proper threshold, creating the mask and applying it to the final image. Continuing, brightness adjustments were coded, specific for each channel. Lastly, the three channels respectively were merged and retrieved in the final separate image with desired parameters.

The next step was to perform cell counting by detecting the centroids from the blue channel (DAPI staining) converted into the gray scale, as the blue channel was responsible for the cell nuclei present in the tissue slide. Before performing such counting the background of the image was removed once again (in a similar manner as to previously stated) and then binarized using the 'imbinarize' function. The purpose of this process was to obtain binary bodies representative of the nuclei that could be found in the tissue section. One of the obstacles was to segment binary bodies of clustered nuclei. For the smaller clusters of approximately 10 nuclei, the watershed transform was applied for segmentation. For the larger clusters probability areas of nuclei were established (meaning likely size in pixels for centroid surface in the image), a grid of points was set, and then k-means clustering was performed to obtain the different nuclei constituting the large cluster. After the segmentation processes took place, binary bodies were retrieved, and their centroids were calculated (one centroid per nuclei) for further work.

Further analysis involved labeling the different nuclei that were found across each picture. Each centroid of the nuclei was to be labelled into one of the three following categories: red – for the epithelial cells, green – for the stem cells, yellow – for the absence of red or green channel expression but presence of the cell nuclei of the other, undetected type. This labelling was conducted going over each centroid and creating a probable area of expression defined by a common radius. If red expression was overlapping the centroid probable area, then it fell under the first label; if green expression was detected the second label was selected; and if no expression

was found it fell under the last category. Once the process was finalized the algorithm exported the final counts to excel automatically.

2.5.2 Implementing the Algorithm in a User-Friendly Interface Application

After designing the algorithm, it was implemented in an application, which was aimed for rapid and assisted processing of the images for data extraction purposes while promoting a user-friendly experience. On the first screen which the app displays, that is ran when the app is opened in the application, three buttons were located to select the input images. The application allows for 'TIFF', 'JPEG', 'JPG; and 'PNG' input formats. The images can be selected throughout the directory of the user's PC memory and plotted in the app marked by the labels separately to the three-color channels.

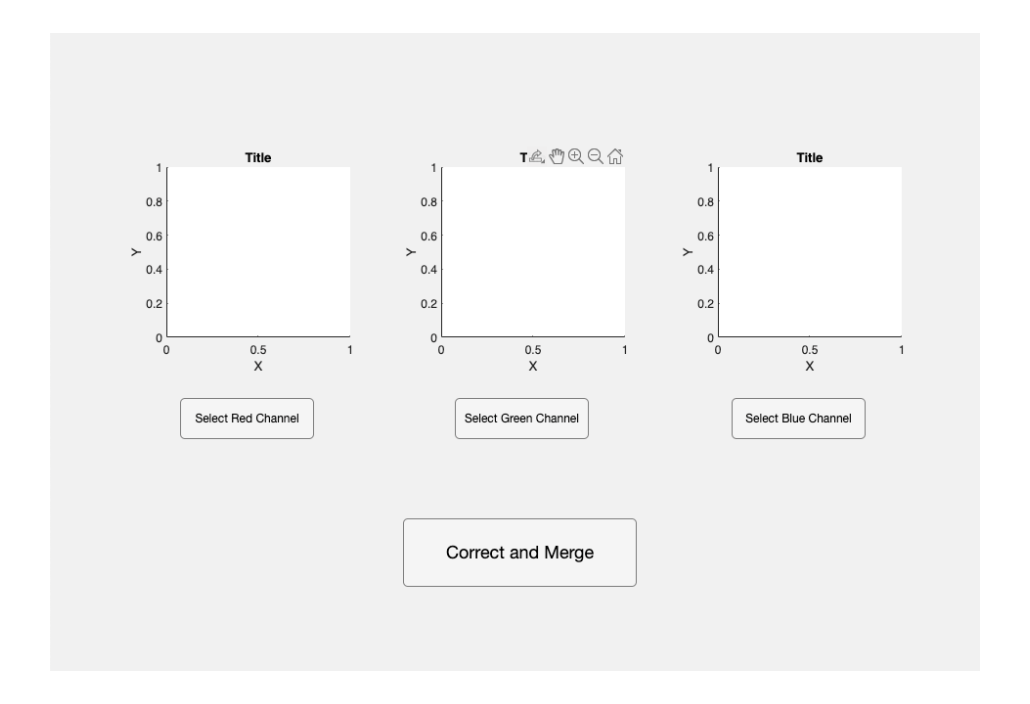


Figure 5. First window of the Application. Image selection phase of process.

After choosing the channels, image correction is done automatically, by pressing the button "Merge". Additionally, a function for the user to be able to designate chosen regions (ROIs) where

the nuclei are counted in separately was implemented. Following the merging and correction of the images, the next step is to quantify the total number of nuclei, as described above. Two specific interactive parameters were added to allow use of the application with input images with varying brightness and saturation levels: "Sensitivity" and "Segmentation". For these parameters that the user can alter, two slider objects were implemented in the app. The sensitivity slider is responsible for adjusting the number of centroids that are picked up, due to the fact that some images can display centroid surfaces that have similar intensity values to the background noise. The higher the sensitivity value is, the less the background noise repercusses in the final quantification of nuclei count. The segmentation slider allows for the selection for the probable size of the nuclei. This was done for the application to be able to handle different magnifications. This parameter helps to break down the larger clusters of the cells.

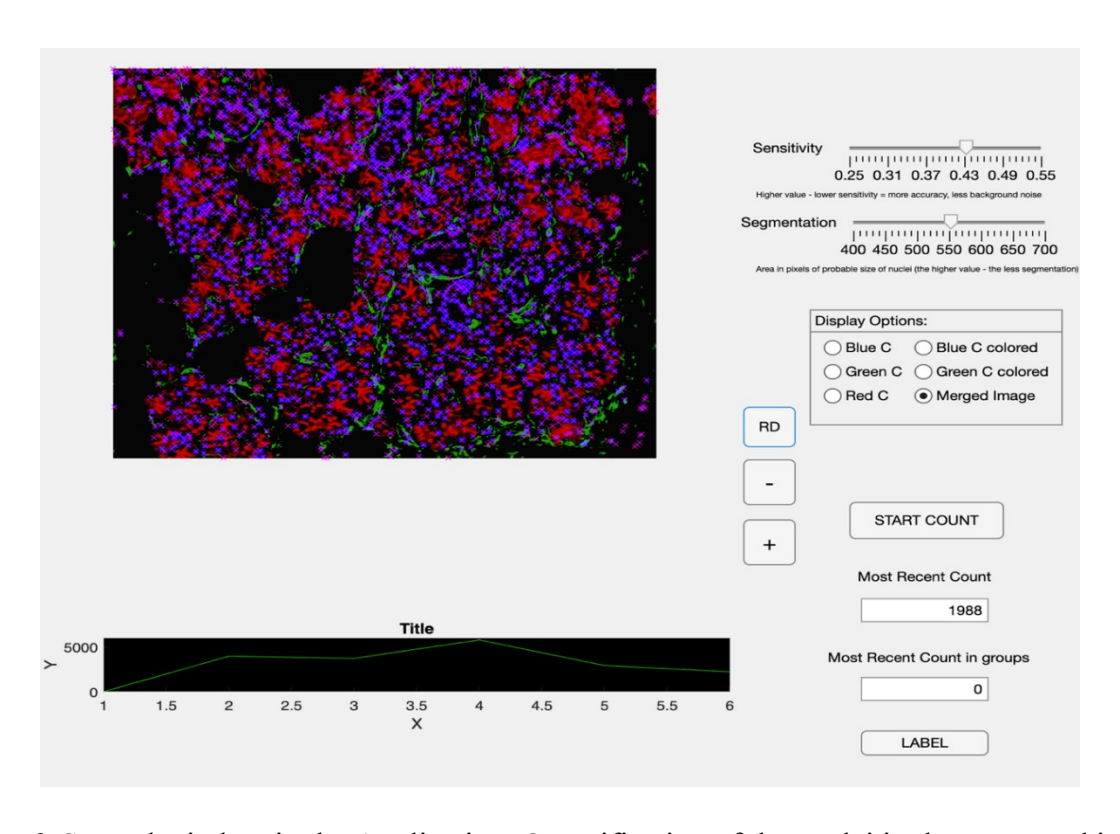


Figure 6. Second window in the Application. Quantification of the nuclei in the processed image.

Additionally, another button is used for the removal of the duplicates. This function is needed to correct for the over segmentation of the binary bodies created to represent the centroids. After receiving the final count plotted on top of the merged image or preferred channel (the display buttons object allows for different options), the final step in this application view is to press button "Label", in order to label cells by channels.

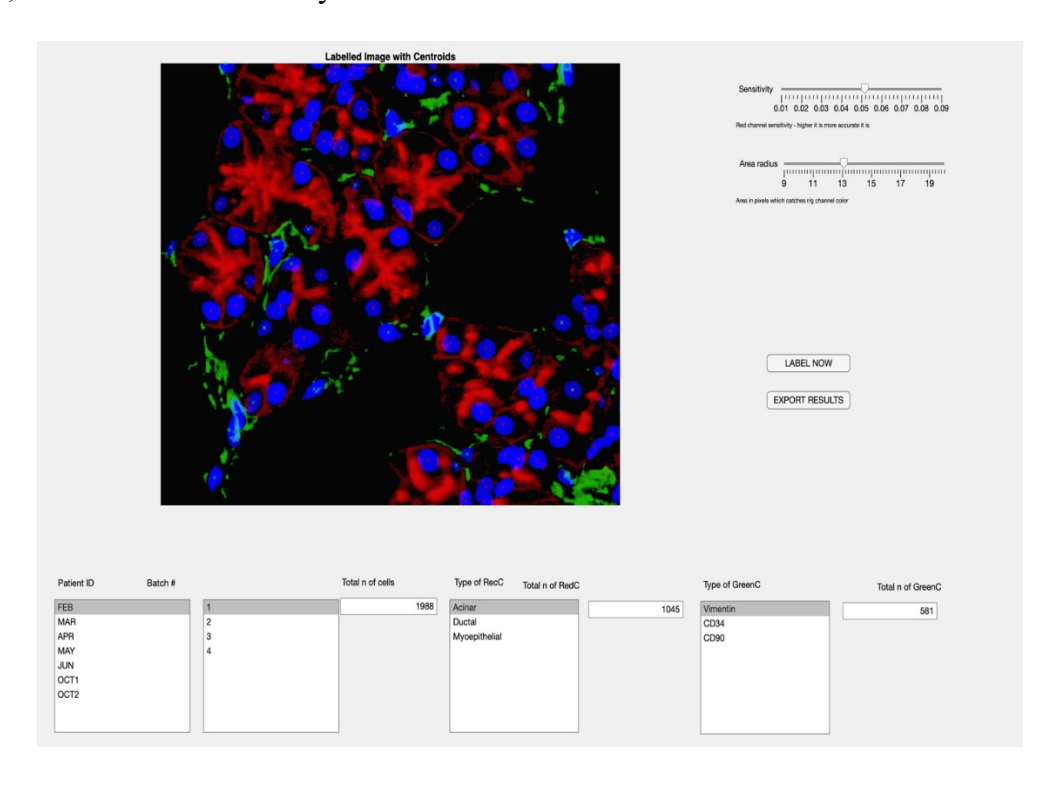


Figure 7. 3rd step in the Application. Labelling the quantified nuclei according to the channel and data exporting.

In this screen (Figure 7) there are two additional sliders "Sensitivity' and "Area radius". The slider "Sensitivity" helps to adjust the prevalent channel sensitivity. The higher the value is, the more accurate the results are. The "Area radius" slider is responsible for the radius in which nuclei will be identified being of one or another channel type. From this last window used can manually choose the patient whose images are processed by specifying: the batch (repetition) number, the number of total cells in the slide, the number of cells which were identified as Red

channel and their type (in case of our work three categories were acinar, ductal and myoepithelial cells) and the number of cells which were identified as Green channel and their type (in case of our work three categories were identified as the following stem cell markers Vimentin, CD34 and CD90). In order to export a table with all established and calculated information to the Excel file, the user can press the button: "Export results".

2.6 Statistical Test

Statistical analysis was conducted using the Microsoft Excel extension for Data Analysis. Various tests were performed to analyze the data difference and overlap of the different variables, those would be patient related variables (age, sex and health condition) and expression marker types. Anova: Single Factor, F-Test Two-Sample for Variances for testing the equality of variances and t-Test: Two-Sample Assuming Equal Variances or t-Test: Two-Sample Assuming Unequal Variances, depending on the outcomes of F-Test. A p-value of <0.05 was considered as an indication of statistical significance. Additionally, for several measured variables curve fitting was conducted for two variables at same the time in order to establish a potential relation between them. The fitting was carried out using the MATLAB built in 'curve fitter app' toolbox by using the one-degree polynomial function.

3. Results

3.1 Literature Search Results

During the literature review phase, a final count of 24 articles were retrieved from the literature and included for this study. Figure 8 depicts the process with its different phases that was carried out to retrieve such articles.

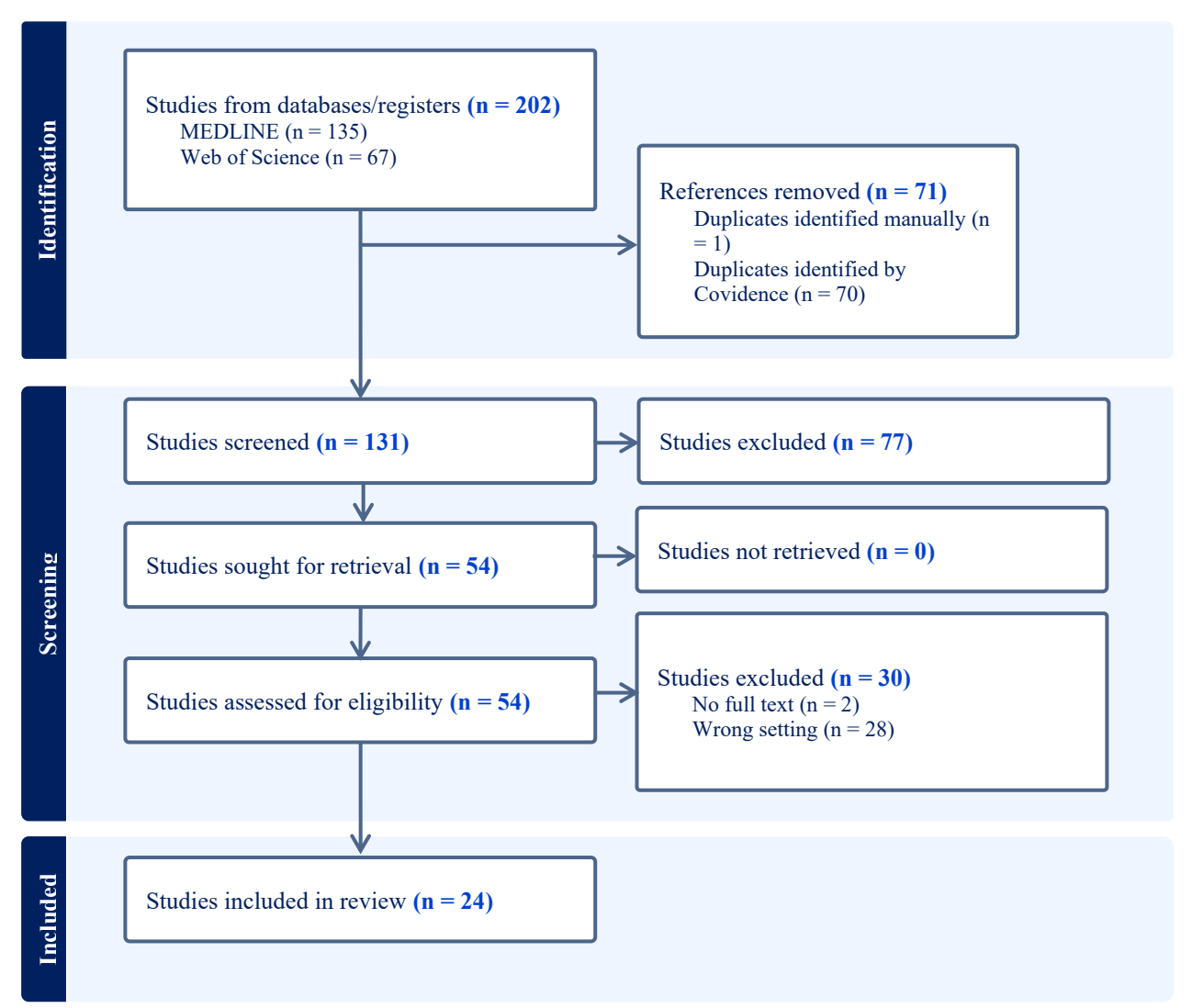


Figure 8. Data summarized from the results of the search for rapid literature review. Sections on how the papers were extracted, retrieved and included in the final data processing are presented in PRISM flow chart.

From the final list of retrieved studies, the types of multiple purpose markers and stem cell markers were documented. Table 3 is a summary of the utilized markers in each of the articles that met inclusion.

Author, year, reference	Model	All markers used	Stem cell markers
You et al, 2011[21]	Mice	ABCG2, Sca-1, vimentin, nestin	ABCG2, Sca-1, vimentin, nestin
Yi et al, 2016[22]	Human	E-Cad, α–SMA, LGR5, CD90, CK14, CK5, AQP5	LGR5, CD90
Usui et al, 2023[23]	Mice	c-Kit, CK5, AQP5	CK5, C-Kit
Togarrati et al, 2017[24]	Human	CD31, CD34, CD56, CD105, CD133, α–SMA, K5, Calponin, Vimentin, CD326, K18, Nestin, CD73, CD90, CD45, CD44, CD271, CD13, CD271, CD19, HLA-DR, CD33, CD14	CD34, CD73, CD90, CD45, CD31, CD44, CD271, CD13, CD105, CD271, CD133, vimentin, CD56, nestin, CD19, HLA-DR, CD33, CD14
Tiwari et al, 2012[25]	Human	E-cad, CK3, CK12, CD90, Vimentin, GFAP, s-100, Lysozyme, p63, CD90, Vimentin	CD90, Vimentin
Tatsuishi et al, 2009[26]	Human	CK, CK7, CK14, α–SMA, AQP3, amylase, Vimentin, CK18	Vimentin
Sato et al, 2007[27]	Human	CD29, CD38, CD44, CD45, CD49f, CD90, CD104, CD130, p75, CD133, ABCG2/BCRP1, CD34, cKit	CD29, CD38, CD44, CD45, CD49f, CD90, CD104, CD117, CD130, p75, CD133, ABCG2/BCRP1, CD34
Rotter et al, 2007[28]	Human	CD73, CD105, CD13, CD29, CD44, CD90, Stro- 1, CD34, CD45, CD106, Oct3/4	CD73, CD105, CD13, CD29, CD44, CD90, Stro-1, CD34, CD45 (not msc specific markers), CD106, Oct3/4
Redman et al, 2023[29]	Rat	caspase-3, c-Kit, Sca-1, Ki67, CK5, SOX2	c-Kit, Sca-1, CK5, Sox2
Redman et al, 2023[30]	Human	CA IV, CD34, CK5, Sca-1	CK5, Ska-1, CD34
Nelson et al, 2013[31]	Mice	AQP5, ECad, c-Kit, collagen IV, Fibronectin, K5, CK7, Laminin, mucin 10, α–SMA, ZO-1	c-Kit, K5
Nanduri et al, 2011[12]	Mice	c-Kit, CD133, CD49f, CD24	c-Kit, CD133, CD49f, CD24
Matsumoto et al, 2007[32]	Swine	CD49f, laminin, laminin a1, albumin, AFP, insulin, glucagon, GATA6, CK8, CK18, CK19, CD29, CD34, CD44, CD45, CD49c, CD90, cKit, PAS, SLA-1, CD106, CD46	CD29, CD90, CD44, SLA-1, CD106, CD46, CD34, CD117, CD45
Lu et al, 2015[33]	Mice	CD29, CD44, CD73, CD90, CD105, CD166, CD45, CD34, cKit	CD29, CD44, CD73, CD90, CD105, CD166, CD45, CD34, CD117
Lombaert et al, 2008[34]	Mice	c-Kit, Sca-1	Sca-1, c-Kit
Lee et al, 2018[35]	Human	CD14, CD34, CD44, CD45, CD49f, CD73, CD90, CD105, CD106, CD119, CD146	CD44, CD49f, CD73, CD90, CD105, CD14, CD34, CD45, CD106, CD119, CD146
Kasamatsu et al, 2012[36]	Human	CD73, CD90, CD105, CD31, CD34, CD45	CD73, CD90, CD105, CD45, CD34, CD31
Kang et al, 2023[37]	Mice	Sca-1, CD106, CD105, CD29, CD44, CD73	Sca-1, CD106, CD105, CD29, CD44, CD73
Jeong et al, 2013[38]	Human	CD49f, CD90, CD34, CD44, CD45, CD105,	CD44, CD105, CD49f, CD90, CD34, CD45
Takashi et al, 2020[39]	Mice	CD31, CD34, CD44, α–SMA, Sca-1, c-Kit, CD90, Ki-67	CD34, CD44, Sca-1, c-Kit, CD90, CD31
Furukawa et al, 2015[40]	Mice	Sca-1, CD44, CD90	Sca-1, CD44, CD90
El-Naseery et al, 2021[41]	Rat	α–SMA, AQP1, Sca-1, PCNA, ssDNA, caspase-3, CD105, CD34	CD105, Sca-1, CD34
Back et al, 2014[42]	Rat	CD90, anti-integrin a6b1, c-kit, laminin, CD44, CD45, nestin, Oct4, c-met, AQP5, Amy1, claudin-1, claudin-3, occludin, vimentin, Nkx6.1, insulin, c-peptide, CK18, CK19, CNN1, CD29, CD34, CD133, CD49f	CD90, anti-integrin a6b1, c-kit, laminin, CD44, CD45, nestin, Oct4, c-met, AQP5, amylase, claudin-1, claudin-3, occludin, vimentin, Nkx6.1, insulin, c-peptide, CK18, CK19, CD29, CD34, CD133
Andreadis et al, 2013[43]	Human	Nanog, Oct-3/4, SSEA-3, CD90, CD105, CD49f, CD81, nestin, CD146, Stro-1, c-Kit, CD45, CD271, AQ-1, CK7, CK8,	Nanog, Oct-3/4, SSEA-3, CD90, CD105, CD49f, CD81, nestin, CD146, Stro-1, C-Kit, CD45, CD271

CD271, AQ-1, CK7, CK8, CD146, Stro-1, C-Kit, CD45, CD271 Table 3. Papers which were included in rapid literature review showing the tested markers.

After accessing the articles, it was determined that many of them were published in 2023 (Figure 9A), suggesting the relevance of the information provided. Most common stem cell markers which were present in the selected studies are shown in the diagram (Figure 9B).

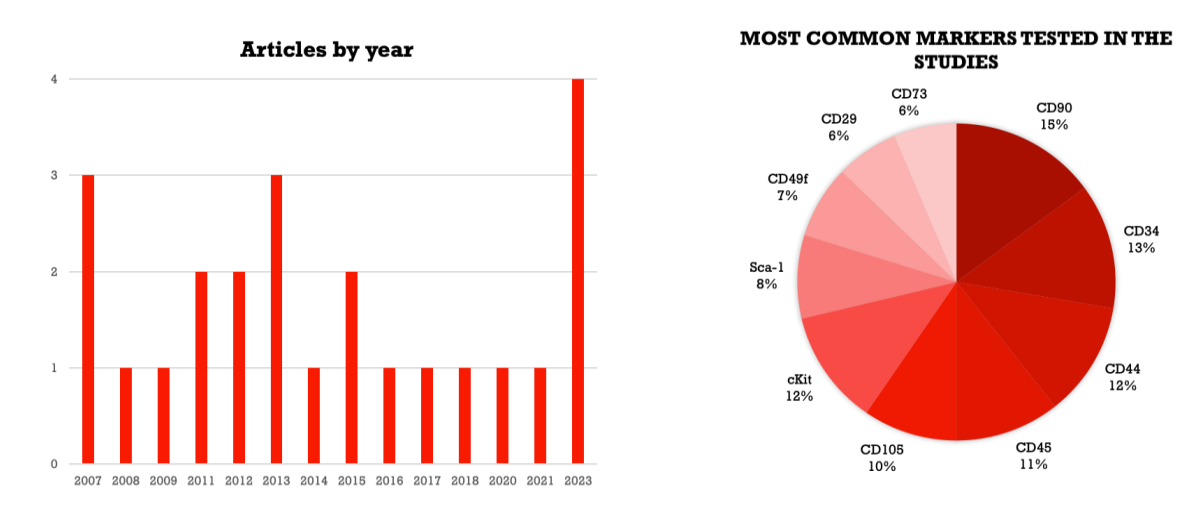


Figure 9. A) The retrieved articles by year B) The most common markers tested in the obtained studies.

From the selected articles, the following data was accessed: markers which were tested in human and rodent cells or tissues. For acinar, ductal, myoepithelial cells, but most importantly for stem cells, focusing on mesenchymal stem cells.

Continuing further exploration of the data, markers were divided by presence in rodent and human tissues/cells.

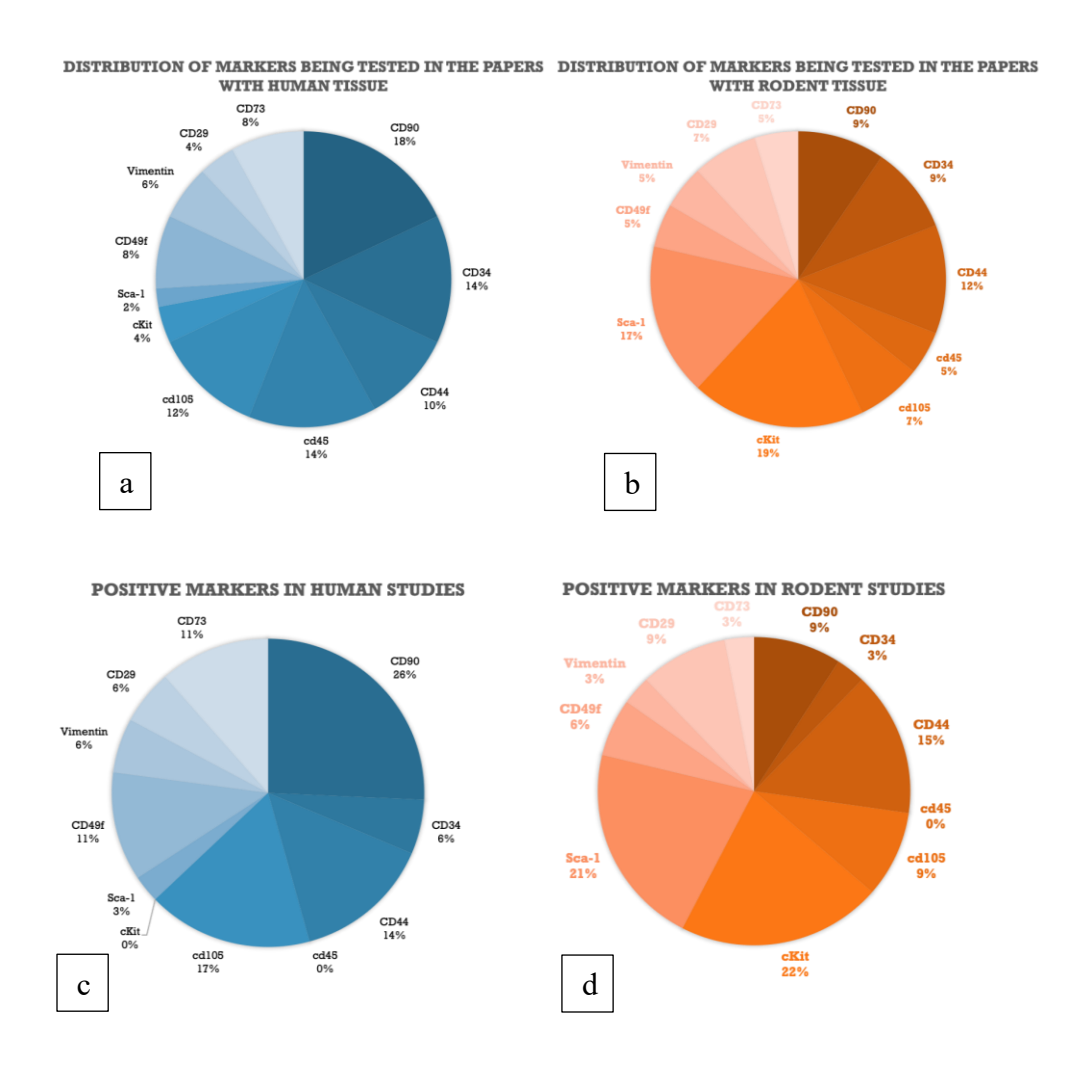


Figure 10. Diagram pie charts showing a) distribution of stem cell markers tested in the included studies using the human cells/tissues; b) distribution of stem cell markers tested in the included studies using the rodent cells/tissues; c) stem cell markers which were tested positive in studies using the human cells/tissues; d) stem cell markers tested positive in the included studies using the rodent cells/tissues.

Additionally, stem cell markers tested negative were accessed in the included studies, in both human and rodent tissues/cells (Figure 11).

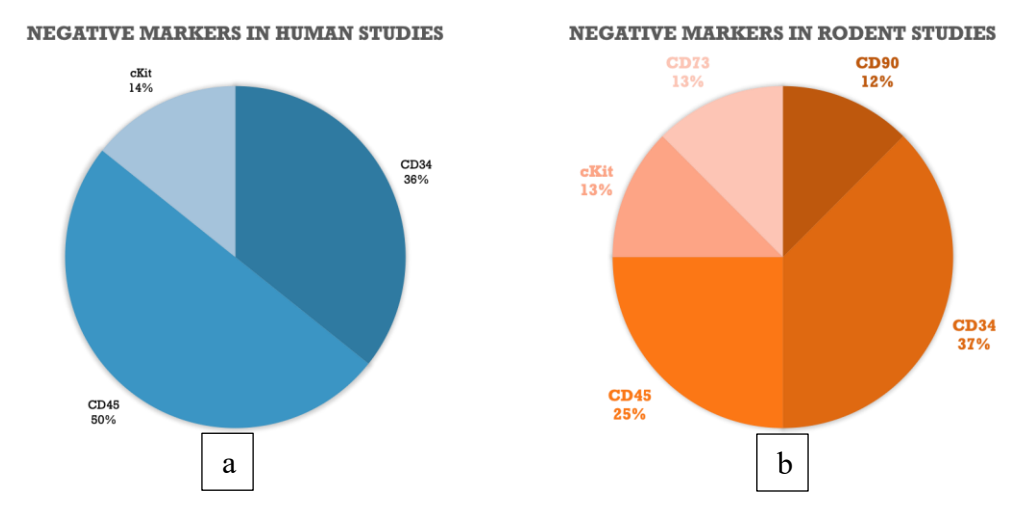


Figure 11. Diagram pie charts showing a) stem cell markers tested negative in the included studies using the human cells/tissues b) stem cell markers tested negative in the included studies using the rodent cells/tissues.

Lastly, the marker expression was determined between tested and actually expressed, in both human and rodent tissues/cells (Figure 12).

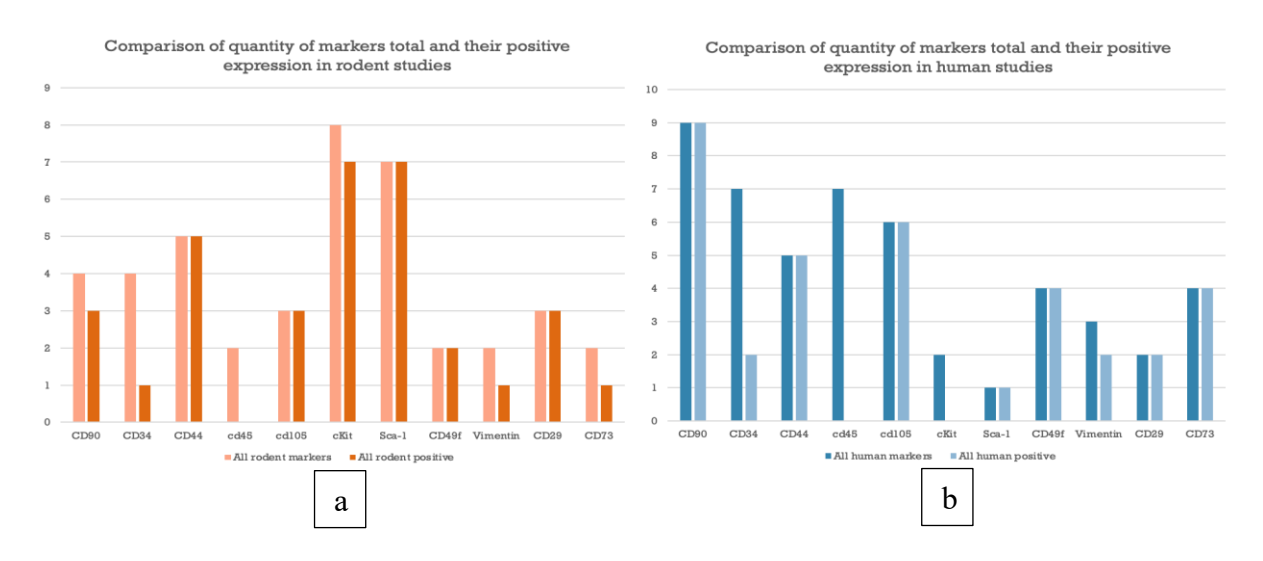


Figure 12. Bar plots showing a) comparison of quantity of total number of markers tested and their actual expression in studies using the rodent cells/tissues b) comparison of quantity of total number of markers tested and their actual expression in studies using the human cells/tissues.

3.2 Immunofluorescence Staining

Post performing the immunofluorescence staining, the images for 7 pairs of markers were obtained as follows: CD34+AQP5, CD34+CK7, CD34+ α -SMA, CD90+AQP5, CD90+CK7, CD90+ α -SMA and Vimentin+ α -SMA, which were further analyzed (Figure 13-19).

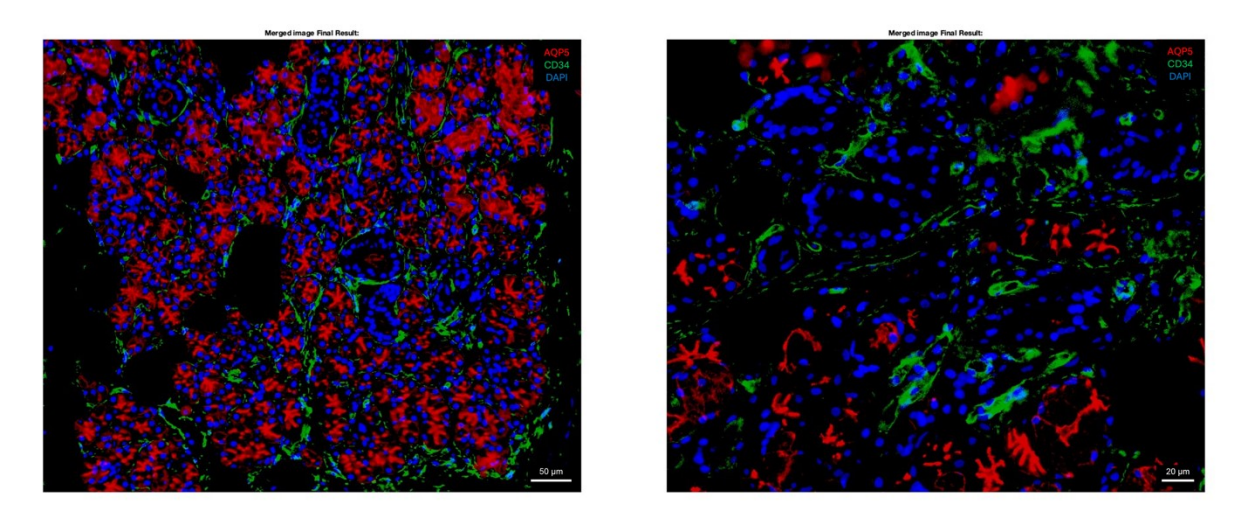


Figure 13. Expression of markers AQP5 and CD34 in 20x magnification (left) and 40x magnification (right).

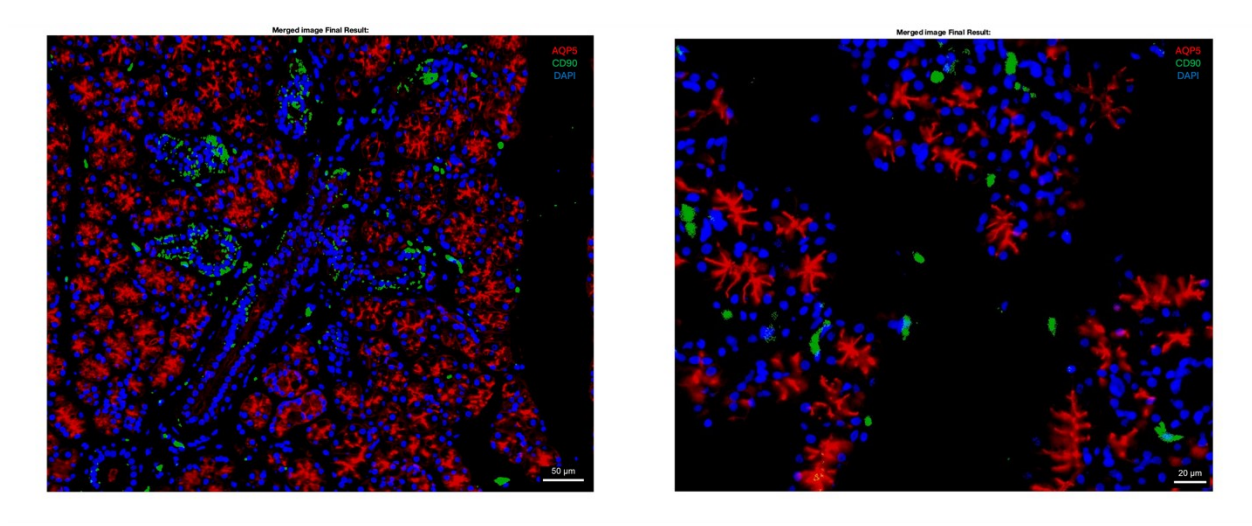


Figure 14. Expression of markers AQP5 and CD90 in 20x magnification (left) and 40x magnification (right).

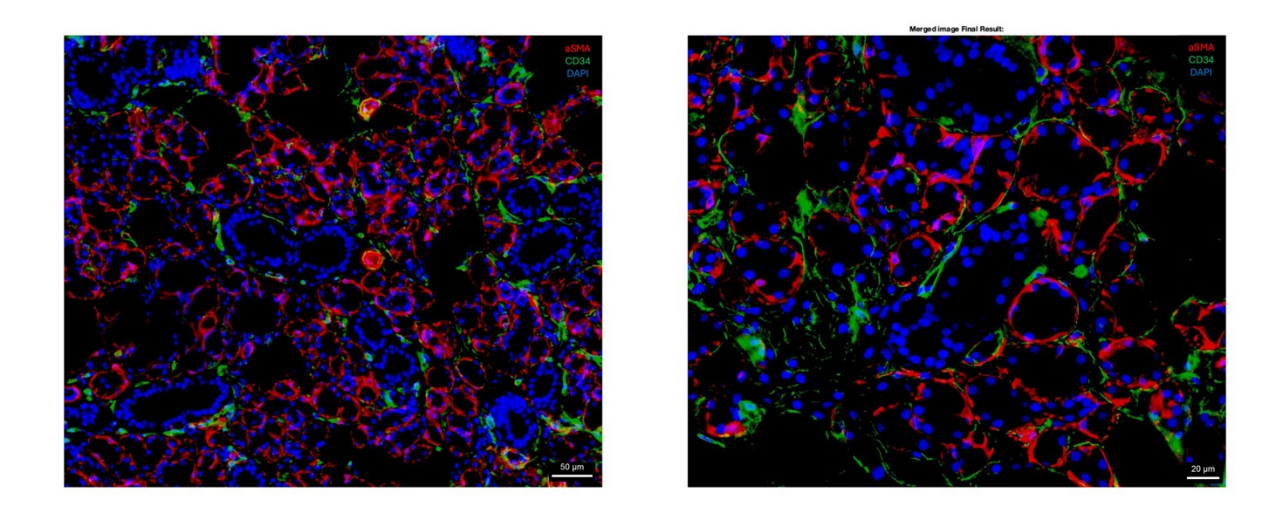


Figure 15. Expression of markers α –SMA and CD34 in 20x magnification (left) and 40x magnification (right).

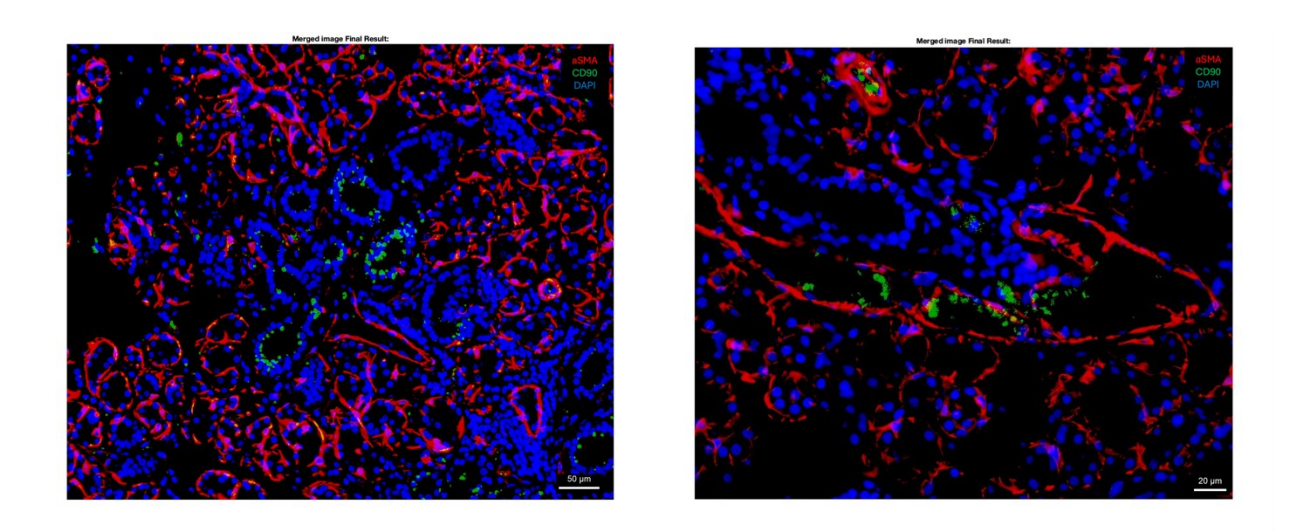


Figure 16. Expression of markers α –SMA and CD90 in 20x magnification (left) and 40x magnification (right).

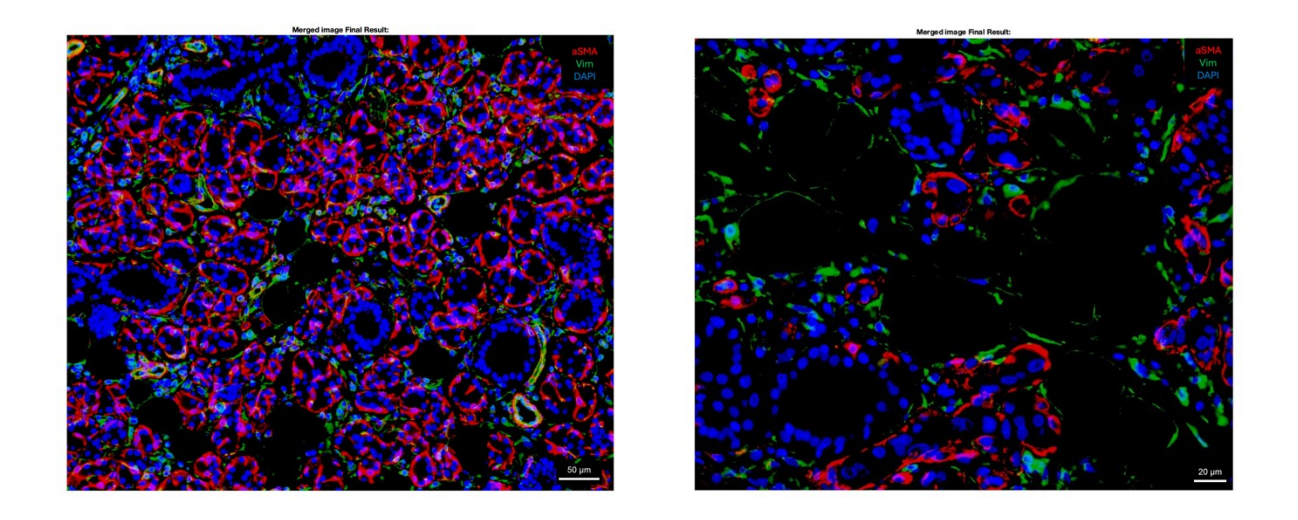


Figure 17. Expression of markers α –SMA and Vimentin in 20x magnification (left) and 40x magnification (right).

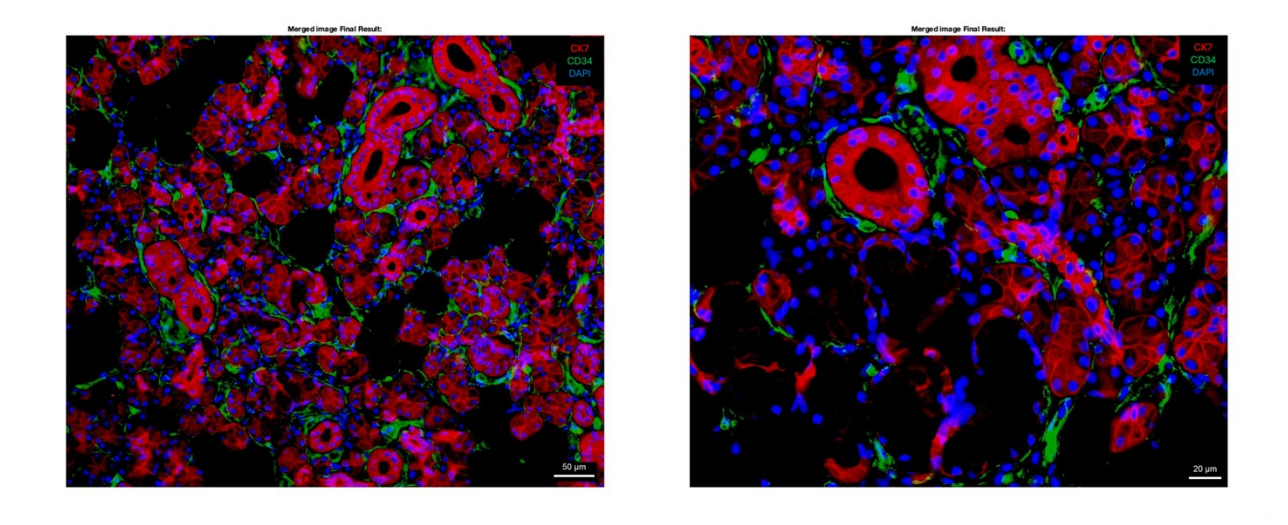


Figure 18. Expression of markers CK7 and CD34 in 20x magnification (left) and 40x magnification (right).

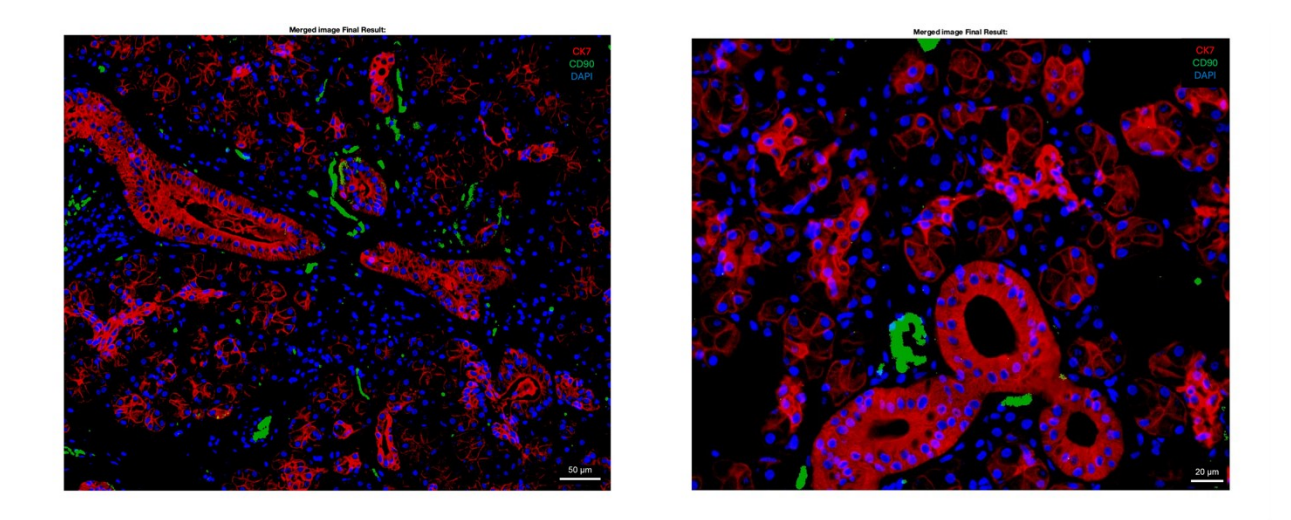


Figure 19. Expression of markers CK7 and CD90 in 20x magnification (left) and 40x magnification (right).

3.3 Quantitative and Qualitative Analysis of the Data

All the images which have been taken from the performed staining have shown the expression of stem cell markers. To obtain the qualitative and quantitative data the ratios of stem cell markers expressed compared to the total numbers of cells detected were calculated and plotted.

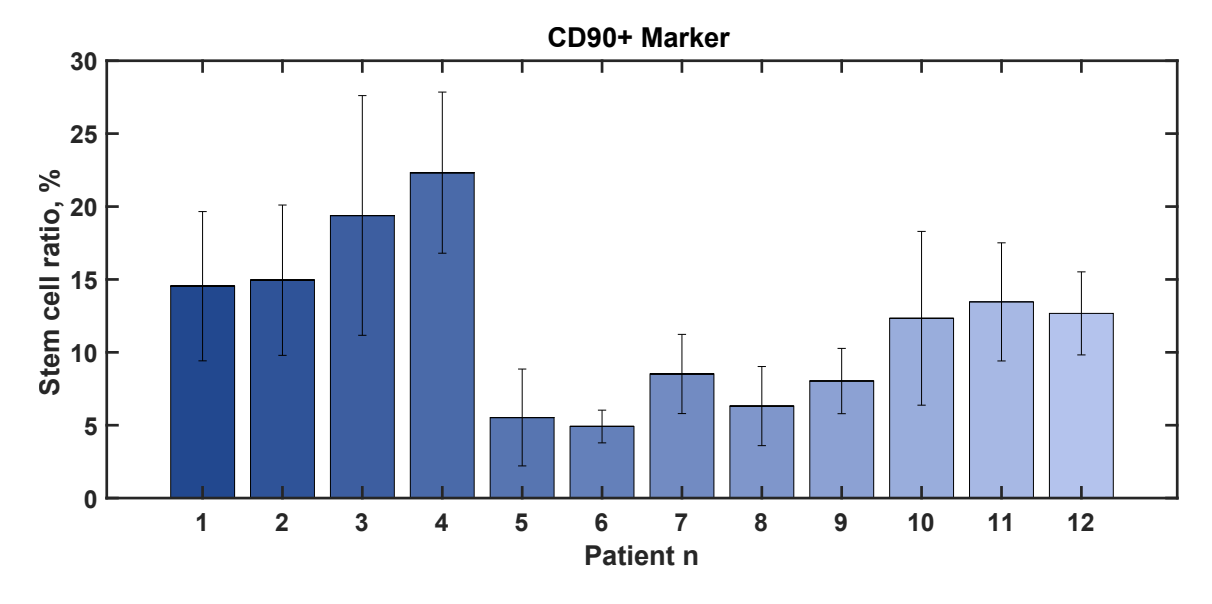


Figure 20. Bar plot showing the ratio of stem cells with positive expression of marker CD90 to total number of cells in the tissue slide in all 12 patients.

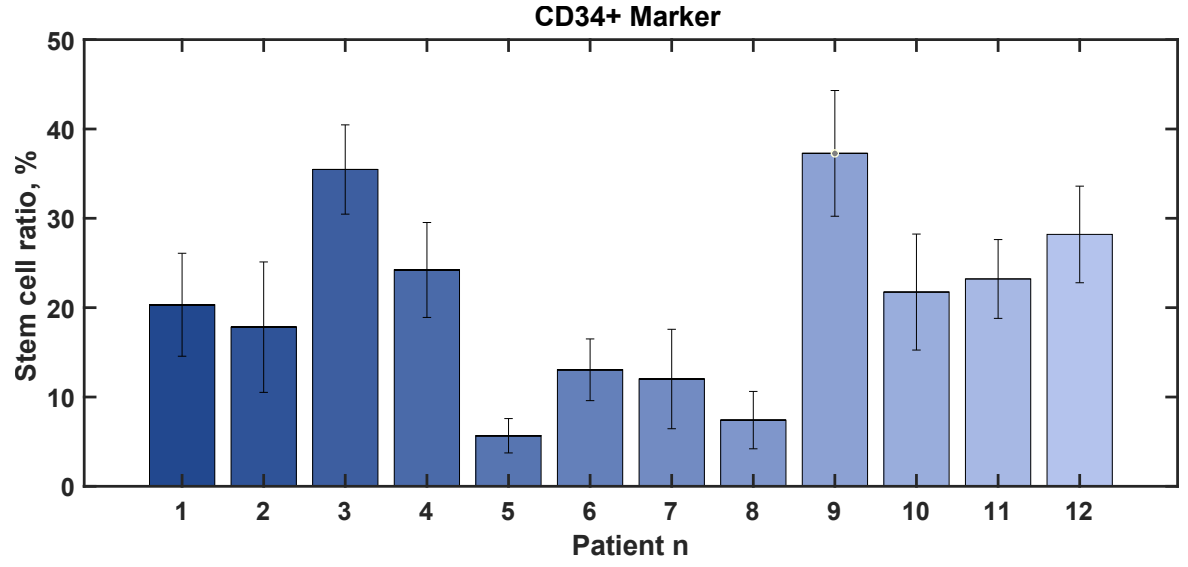


Figure 21. Bar plot showing the ratio of stem cells with positive expression of marker CD34 to total number of cells in the tissue slide in all 12 patients.

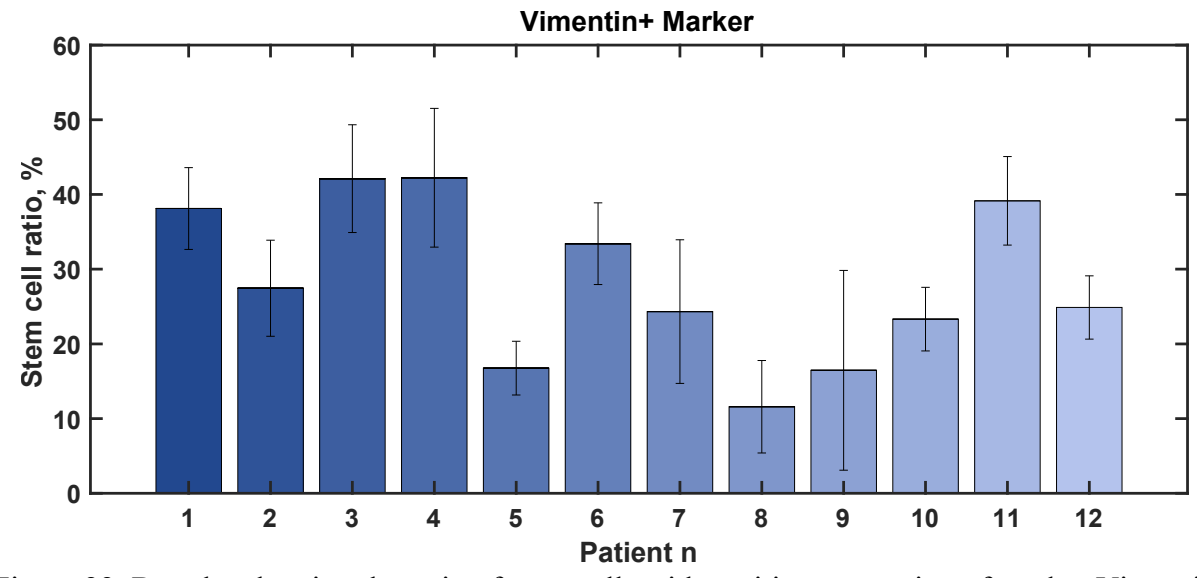


Figure 22. Bar plot showing the ratio of stem cells with positive expression of marker Vimentin to total number of cells in the tissue slide in all 12 patients.

As it is shown in the bar plots from Figures 20 to 22, it can be noticed that the stem cell markers expressed ratios were not consistent among patients and additional comparisons by sex or age did not provide any conclusive results. After receiving the total numbers, the expression of certain salivary epithelial cells markers in relation to the expression of stem cell markers was evaluated.

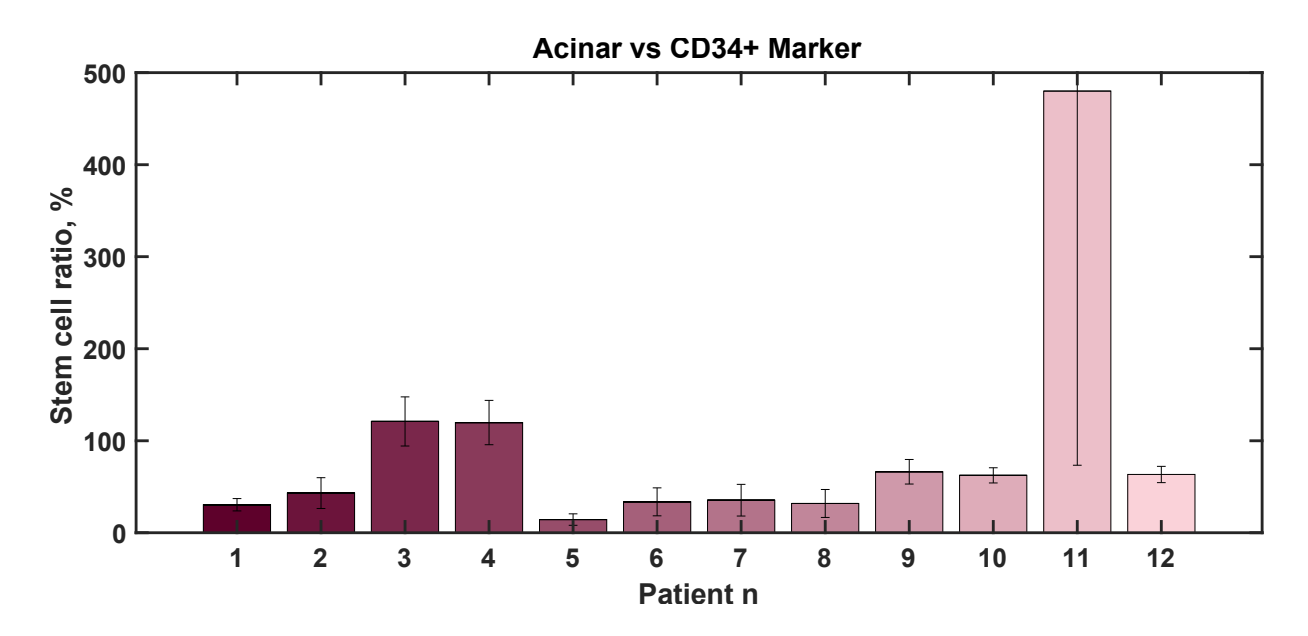


Figure 23. CD34 marker expression in 12 patients in relation to the acinar cells.

* The value of Patient 11 is very high due to the abnormally low number of acinar cells in the tissue.

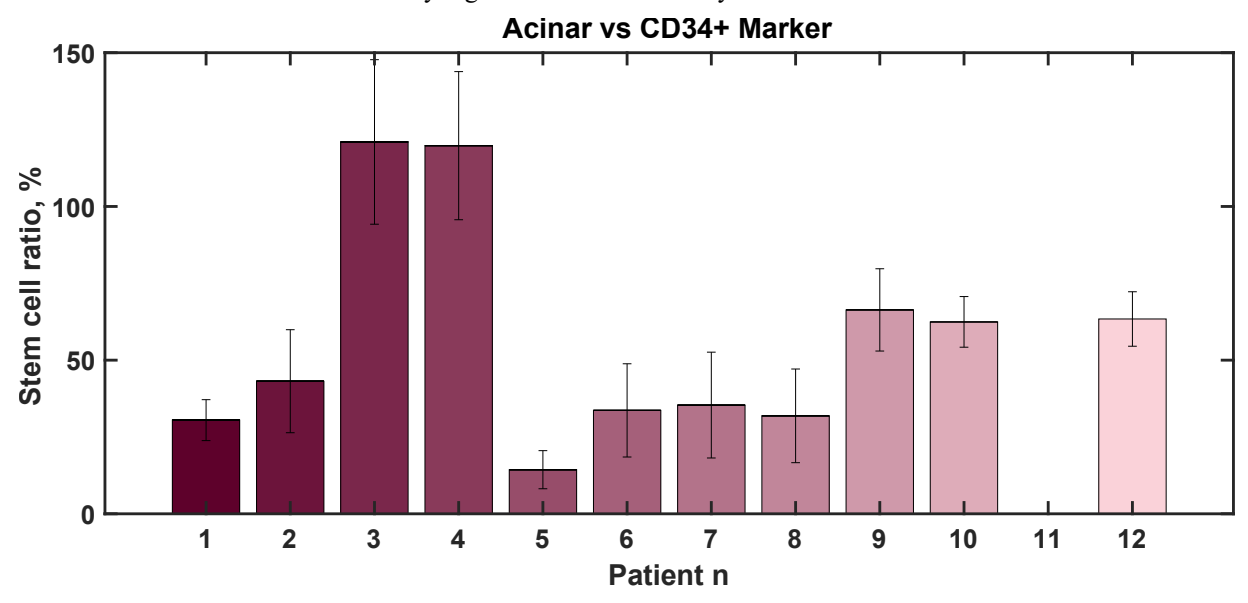


Figure 24. CD34 marker expression in 12 patients (excluding patient 11) in relation to the acinar cells.

Notably, the expression of CD34 positive cells in relation to the acinar cells (Figure 23-24) has been observed most abundantly in patient 3 and patient 4, which have the highest age among

^{*} The value of Patient 11 is very high due to the abnormally low number of acinar cells in the tissue.

the group (70 y.o. and 81 y.o., respectively). The relation to the sex and medical condition in this case had no relevance.

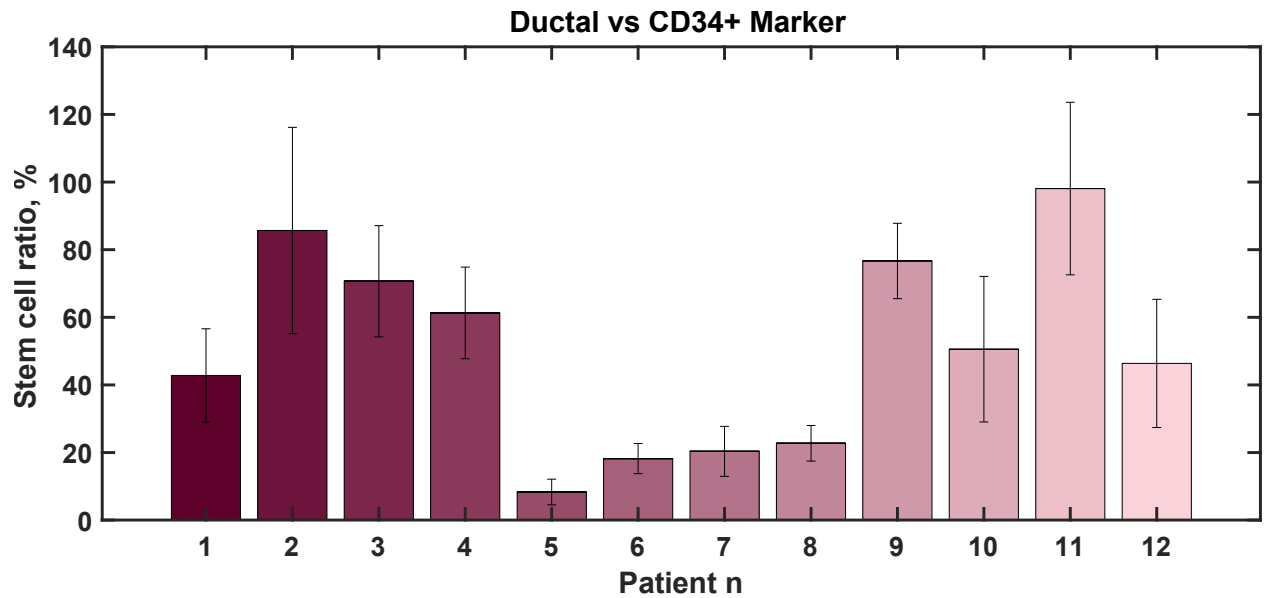


Figure 25. CD34 marker expression in 12 patients in relation to the ductal cells.

The expression of CD34 positive cells in relation to the ductal cells (Figure 25) was observed most abundantly in patient 2, 3,9 and 11. No relevance was noticed in relation to the clinical conditions or demographic factors.

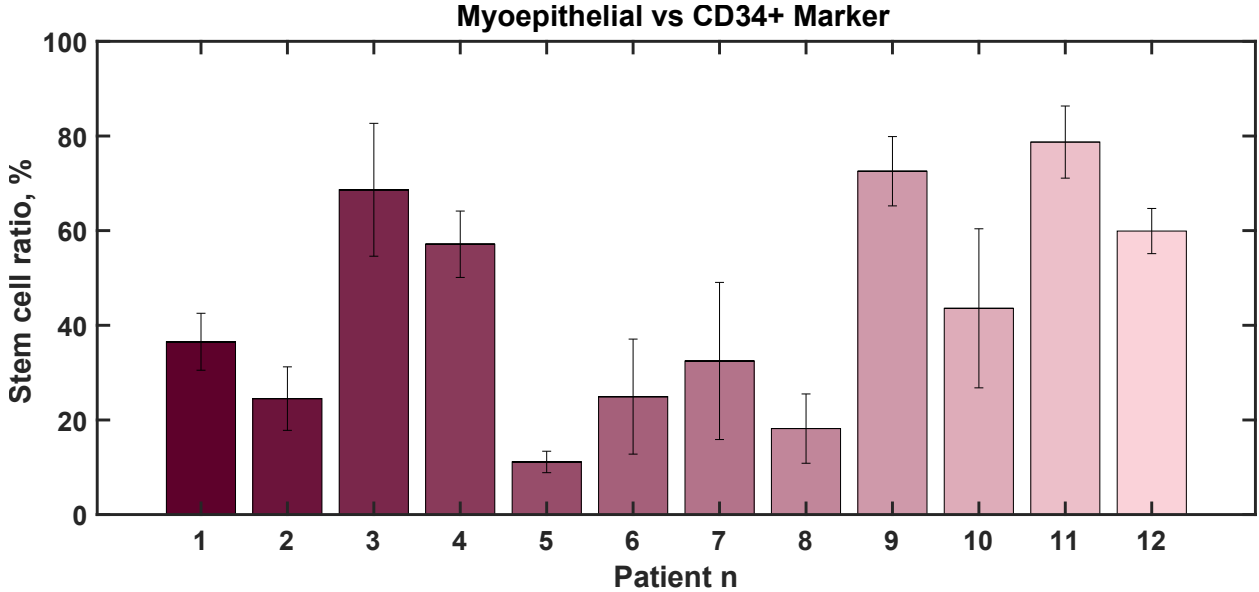


Figure 26. CD34 marker expression in 12 patients in relation to the myoepithelial cells.

Expression of CD34 positive cells in relation to the myoepithelial cells (Figure 26) was observed most abundantly in patients 3,9 and 11. No relevance was noticed in relation to the clinical conditions or demographic factors, but the trend of higher ratios can be outlined in the same patients as in the previous charts.

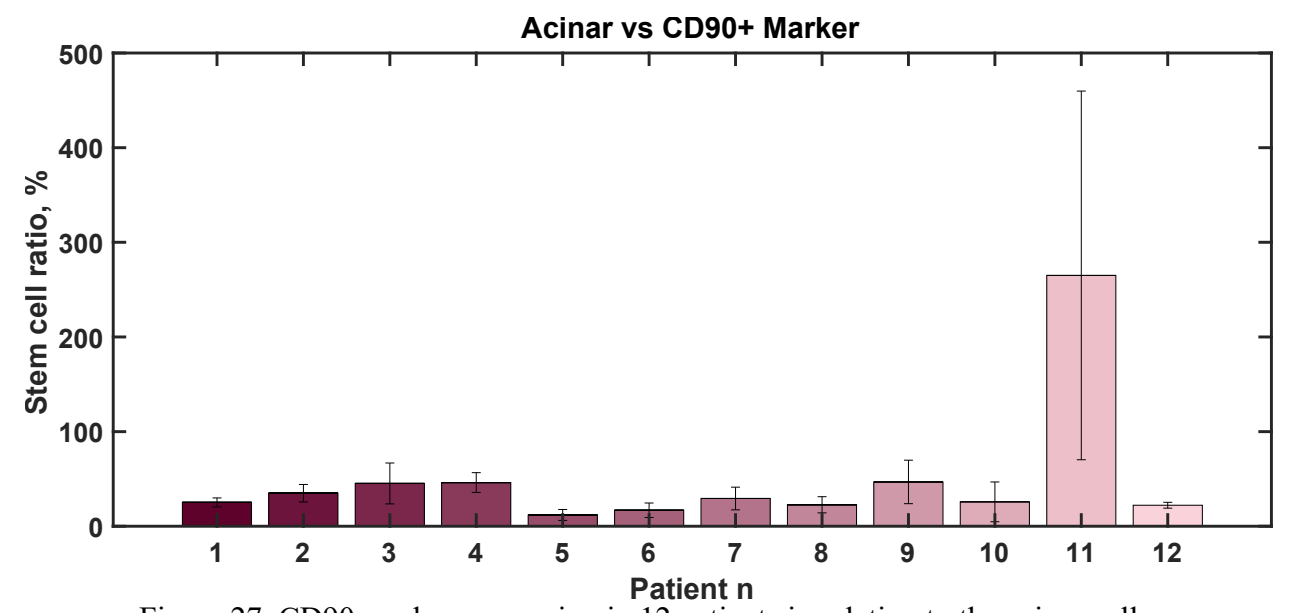


Figure 27. CD90 marker expression in 12 patients in relation to the acinar cells.

* The value of Patient 11 is very high due to the abnormally low number of acinar cells in the tissue.

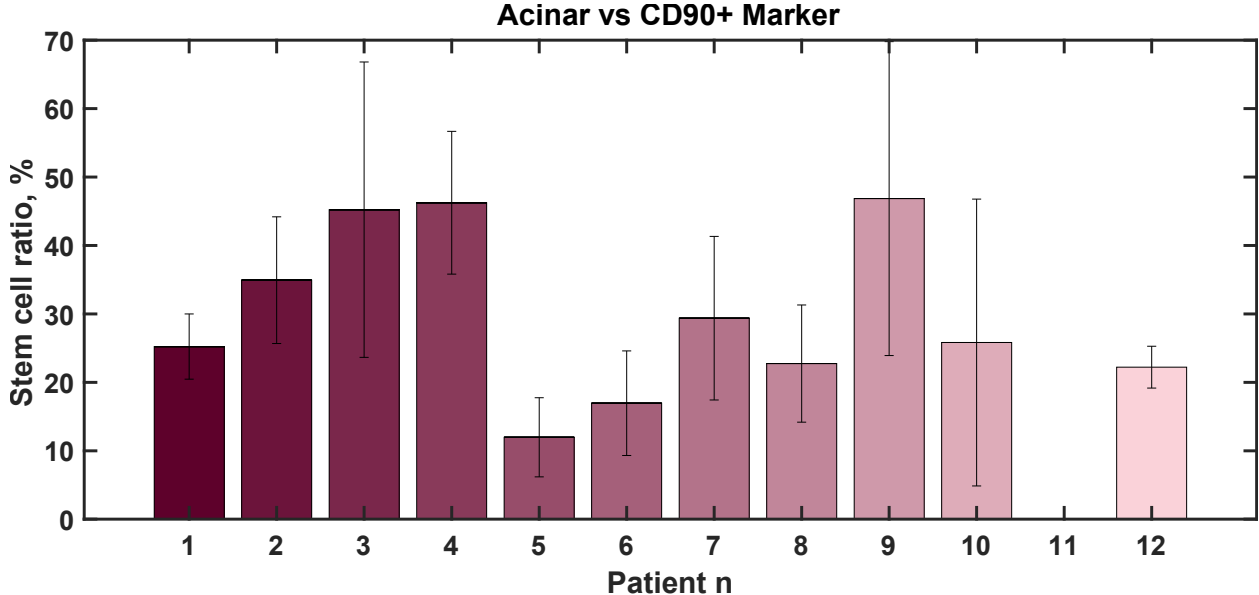


Figure 28. CD90 marker expression in 12 patients (excluding patient 11) in relation to the acinar cells.

^{*} The value of Patient 11 is very high due to the abnormally low number of acinar cells in the tissue.

In these plots (Figure 27-28) highest ratios of stem cells to acinar cells were observed in patients 3, 4 and 9. No relevance was noticed in relation to the clinical conditions or demographic factors.

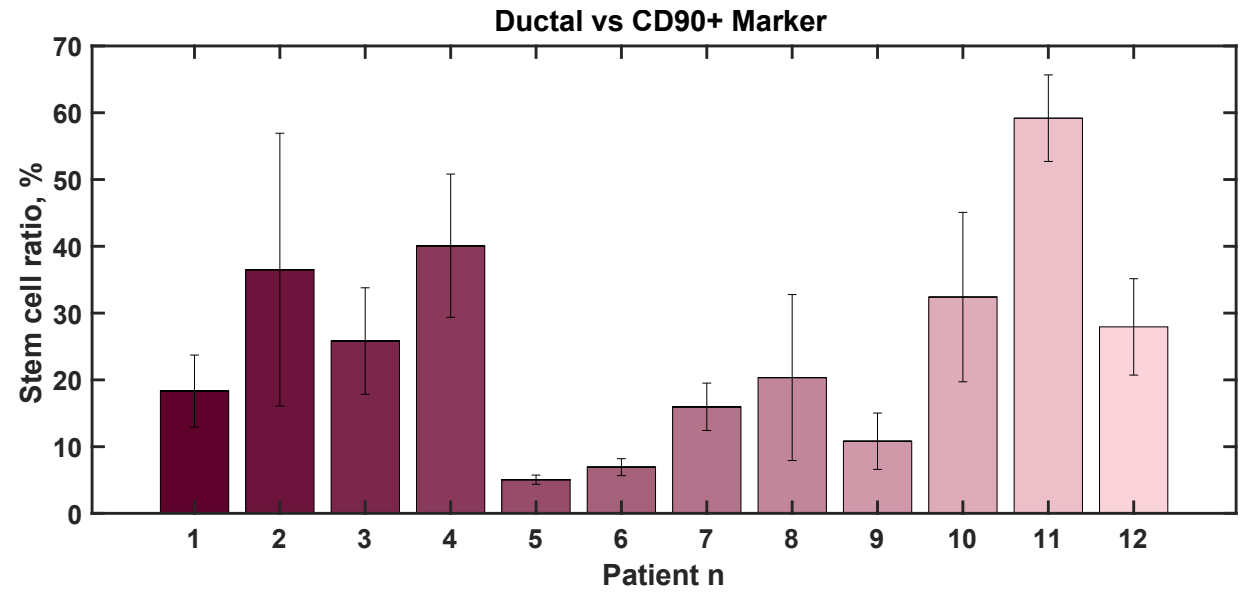


Figure 29. CD90 marker expression in 12 patients in relation to the ductal cells.

Upon examination of the plot, it becomes evident that Patients 2, 4, and 11 exhibit the highest ratios of ductal to stem cells (Figure 29). These patients are representative of different demographic and clinical groups, thereby indicating an absence of discernible correlation between factors.

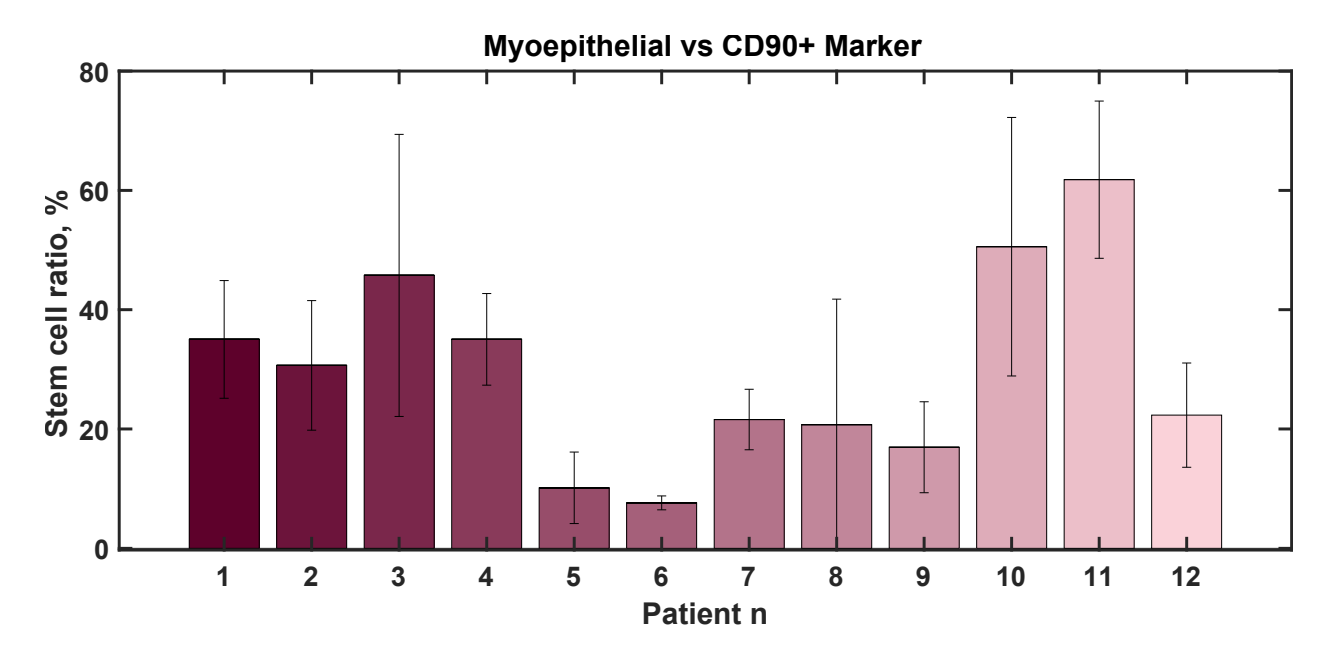


Figure 30. CD90 marker expression in 12 patients in relation to the myoepithelial cells.

In this plot showing the ratio of myoepithelial to stem cells (Figure 30), Patients 3, 10, and 11 stand out because they have the highest ratios compared to everyone else. Notably, these patients are categorized within the demographic group aged over 50 years old and also belong to the cancer cohort. This suggests there might be a connection between age, cancer, and the types of cells in the tissue samples which were studied. The higher ratio in these patients could mean that getting older and having cancer might change the balance of different types of cells in the body.

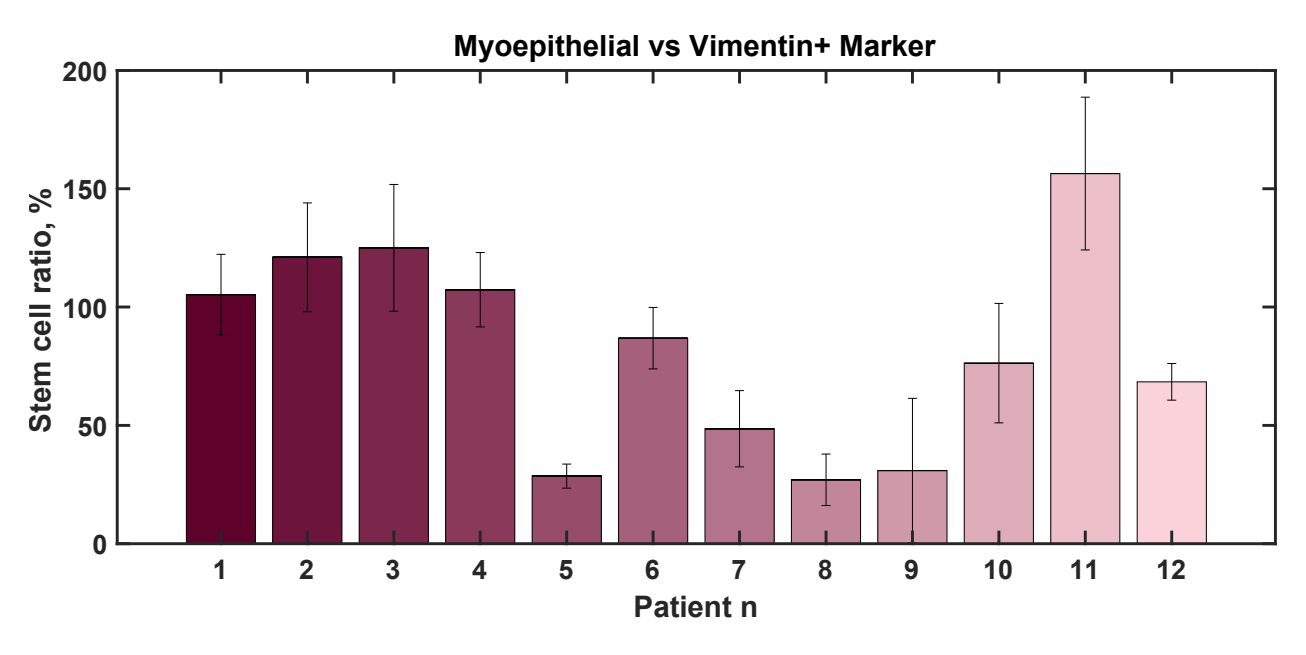


Figure 31. Vimentin marker expression in 12 patients in relation to the myoepithelial cells.

The highest ratios in this plot (Figure 31) were observed in patients 2,3 and 11. No relevance was noticed in relation to the clinical conditions or demographic factors.

After gathering initial data and observing certain trends, the need for a more in-depth investigation into the dataset was recognized. To facilitate this analysis, it was decided to create scattered plots using the Ashby variation technique. This method allows us to visualize and qualitatively analyze the relationships between different variables within the dataset. By plotting the data points on a graph with Ashby variation, aim was to uncover any patterns, correlations, or anomalies that may not be immediately apparent from the raw data.

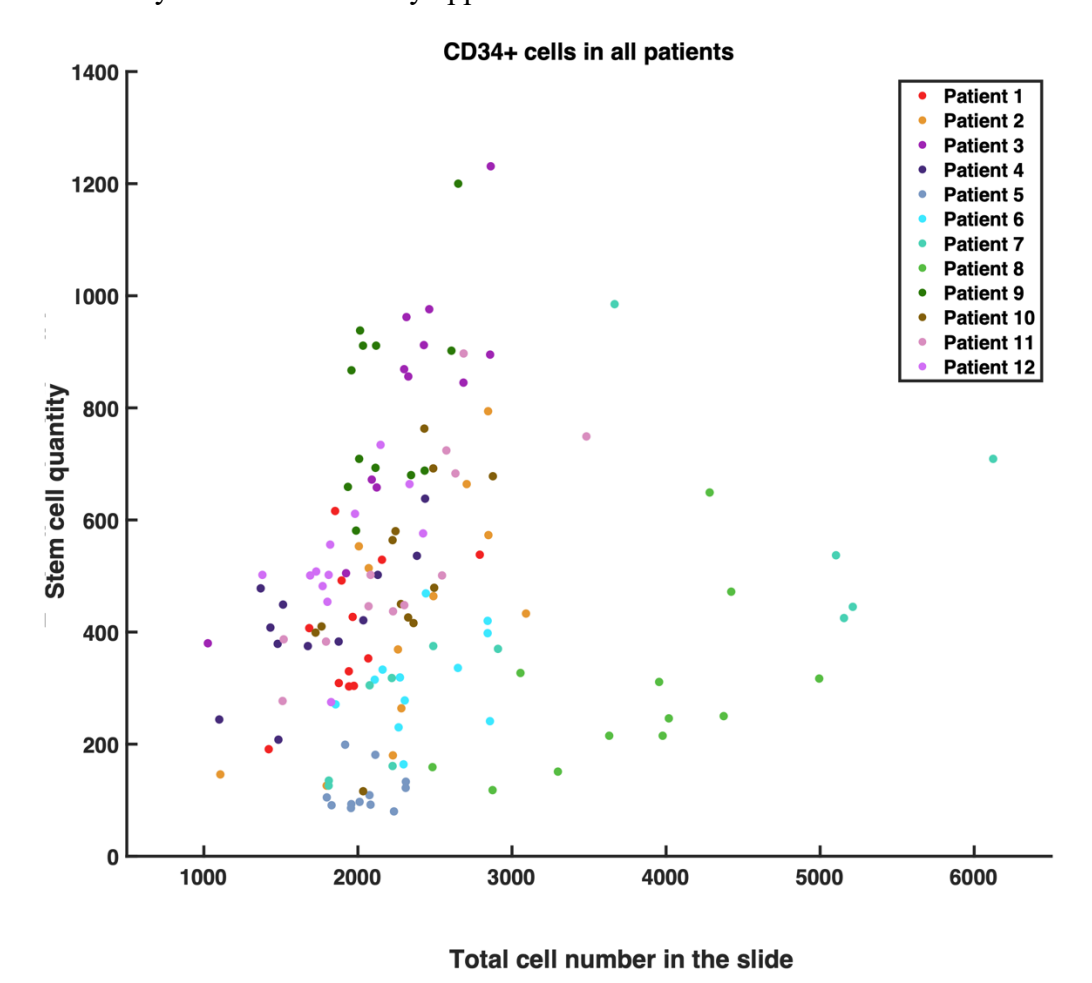


Figure 32. Scatter plot with data from all 12 patients representing the ratio between total cell number and CD34 positive stem cell quantity in the in the tissue slide.

The initial step involved generating a scatter plot, as illustrated in Figure 32, laying the groundwork for subsequent analyses. The dataset was organized into distinct groups based on three key factors: age (<50 y.o. and >50 y.o.), sex (male and female), and medical condition (healthy, benign tumor, and cancer). By segmenting the observations into these predefined groups, it was aimed to recognize any noticeable trends that could inform our further analysis and exploration of the dataset. This systematic grouping approach allows for a more detailed examination of the dataset, enabling us to identify potential patterns or correlations within specific demographic or clinical subsets.

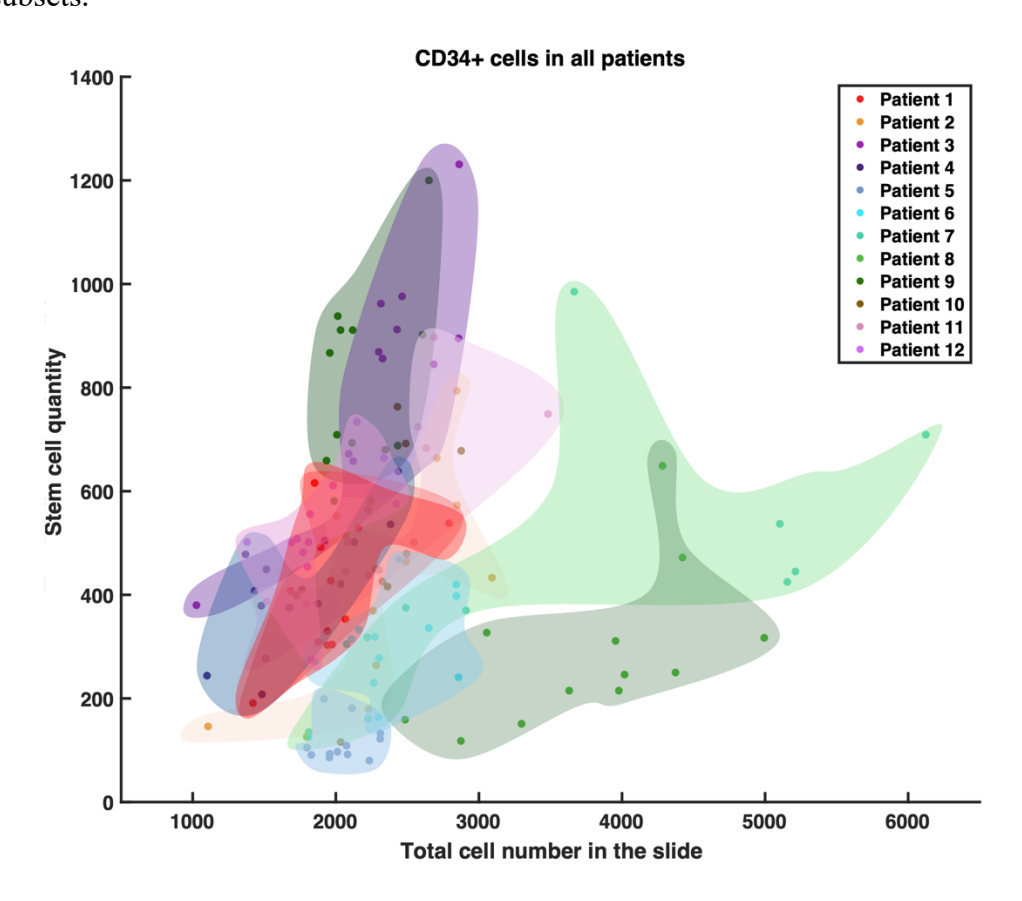


Figure 33. Ashby plot with data from all 12 patients representing the ratio between total cell number and CD34 positive stem cell quantity in the in the tissue slide. Each patient's data points are represented as a distinct cluster on the plot, with the position of the cluster indicating the patient's overall ratio of stem cells to total number of cells.

In Figure 33, was created an Ashby plot to visualize the expression of the CD34 marker. Since clear correlations between individual patients were not observed, it was decided to refine the analysis by grouping the patients according to the categories mentioned earlier. This breakdown into groups allowed for a more focused examination of the data and facilitated the identification of any potential trends or patterns that might not have been apparent at the individual patient level.

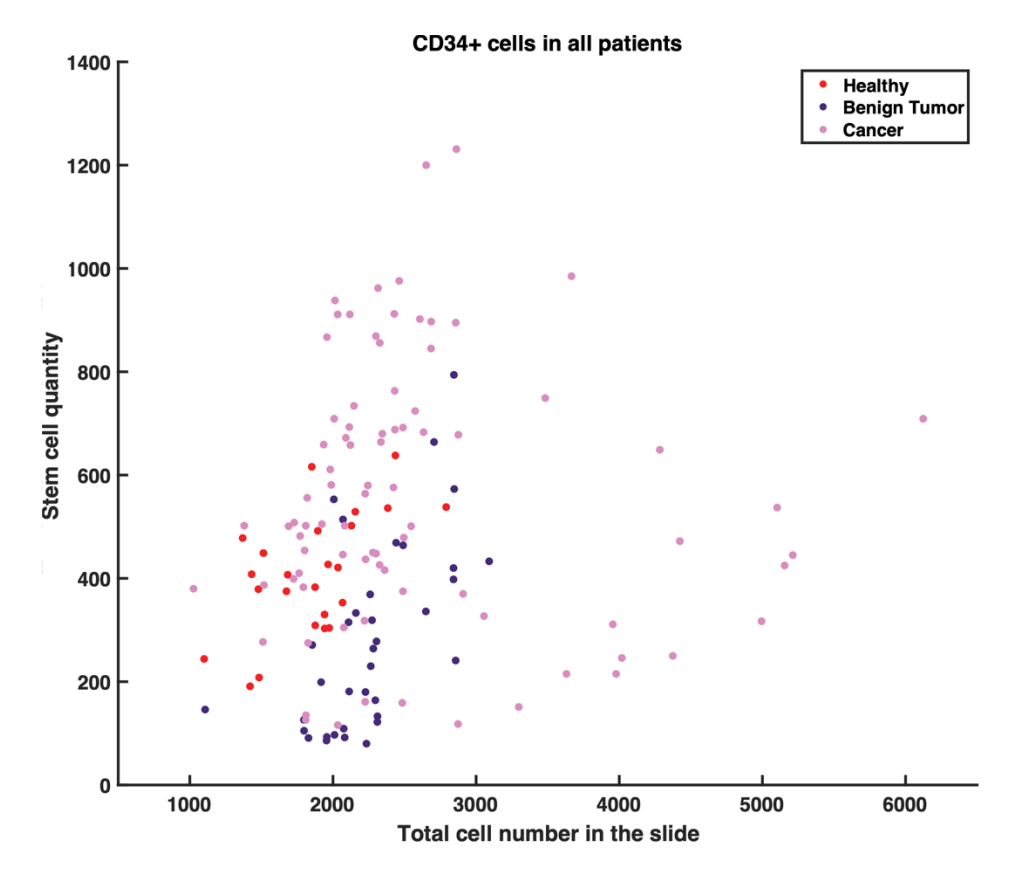


Figure 34. Scatter plot with data from all 12 patients divided into three groups (Healthy, Benign Tumor, Cancer), representing the ratio between total cell number and CD34 positive stem cell quantity in the in the tissue slide.

Following the creation of the scatter plot (Figure 34), we manually delineated distinct clusters on the plot to represent each group's data points. As illustrated in plot (Figure 35), noteworthy observations emerged regarding the ratio of stem cells to the total number of cells within each group.

For the Healthy group, the ratio was contained within a moderate range, indicating a balanced proportion of stem cells relative to the total cell count. Conversely, in the benign tumor group, the ratio was predominantly lower compared to the other two groups, suggesting a potential alteration in stem cell dynamics associated with benign tumor pathology.

Interestingly, the cancer group exhibited a scattered distribution, with data points clustering in three distinct regions of the plot. On average, the ratio of stem cells to total cells in the cancer group was higher than that observed in the Healthy and benign tumor groups. This dispersed clustering pattern within the cancer group suggests heterogeneity in stem cell ratios among cancer patients, highlighting the complexity and variability inherent in cancer biology.

Further analysis and exploration of these patterns may offer insights into the underlying mechanisms driving stem cell dynamics in different disease states.

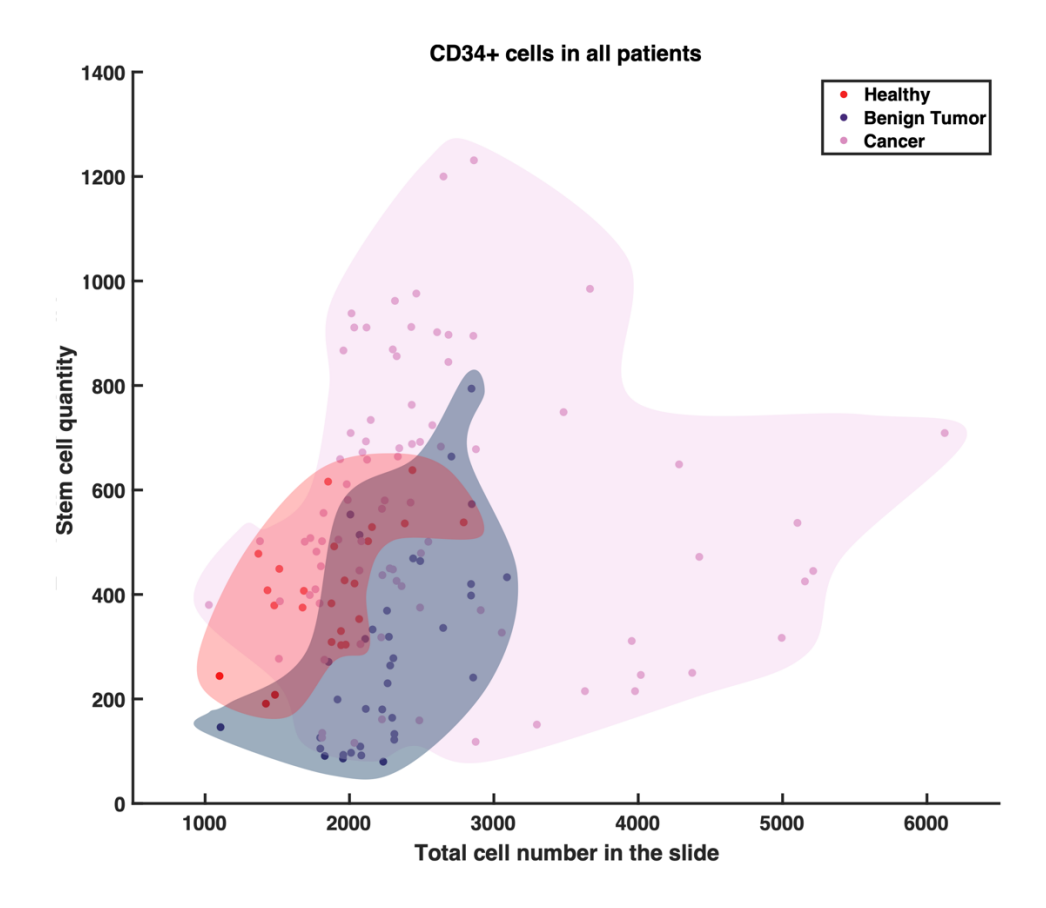


Figure 35. Ashby plot with data from all 12 patients divided into three groups (Healthy, Benign Tumor, Cancer), representing the ratio between total cell number and CD34 positive stem cell quantity in the in the tissue slide. Each patient's data points are represented as a distinct cluster on the plot, with the position of the cluster indicating the patient's overall ratio of stem cells to total number of cells.

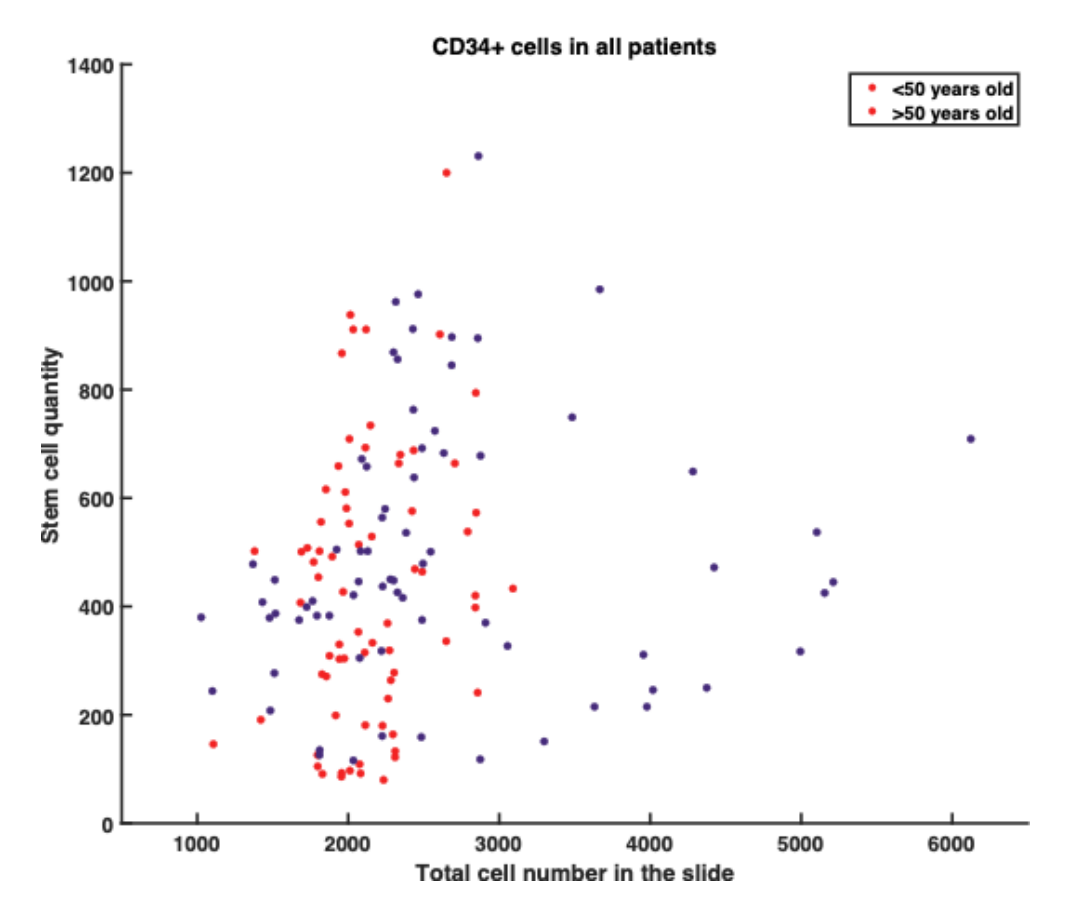


Figure 36. Scatter plot with data from all 12 patients divided into two groups (<50 years old, >50 years old), representing the ratio between total cell number and CD34 positive stem cell quantity in the in the tissue slide.

After noting correlations between medical conditions, our investigation progressed to examining age-related trends. Initially, a scatter plot (Figure 36) was constructed to visualize these associations. Building upon this, an Ashby plot (Figure 37) was developed to further explore the data.

Remarkably, the clustering of data points remained highly consistent across all patients, regardless of age. However, upon closer inspection, a slight deviation among patients aged over 50 years was observed. In this subgroup, the distribution of data points appeared more scattered compared to the younger group.

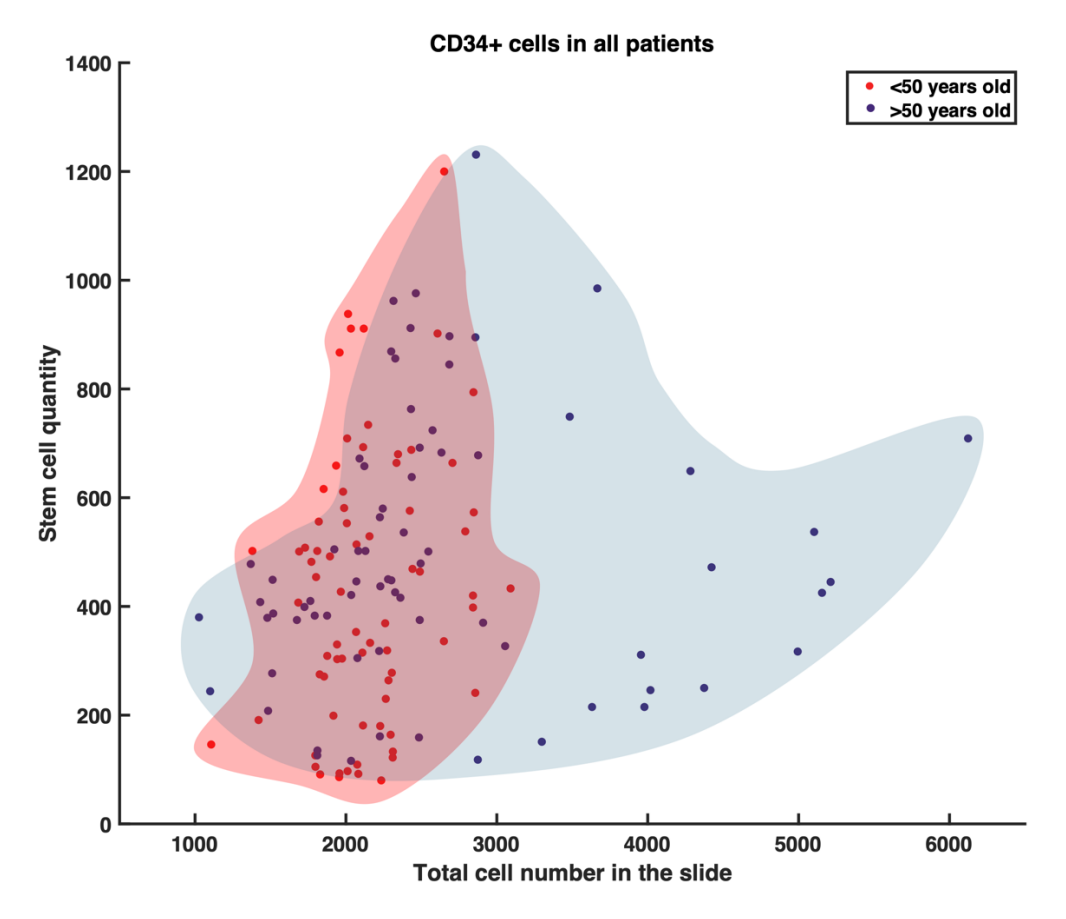


Figure 37. Ashby plot with data from all 12 patients divided into two groups (<50 years old, >50 years old), representing the ratio between total cell number and CD34 positive stem cell quantity in the in the tissue slide. Each patient's data points are represented as a distinct cluster on the plot, with the position of the cluster indicating the patient's overall ratio of stm cells to total number of cells.

The final category for comparison involved segregating patients by sex, distinguishing between female and male individuals. To initiate this analysis, a scatter plot (Figure 38) was utilized as a foundational framework, upon which the Ashby plot (Figure 39) was overlaid. Similar to the approach with age-based comparisons, it was aimed to observe patterns or discrepancies in the distribution of data points between the two sexes.

Interestingly, consistent clustering of data points within a specific region for both female and male patients was observed. However, upon closer examination, it became apparent that the data points for male patients exhibited a greater degree of scattering compared to their female counterparts.

This divergence in the distribution of data points between male and female patients suggests potential sex-related differences that may influence the variables under further investigation.

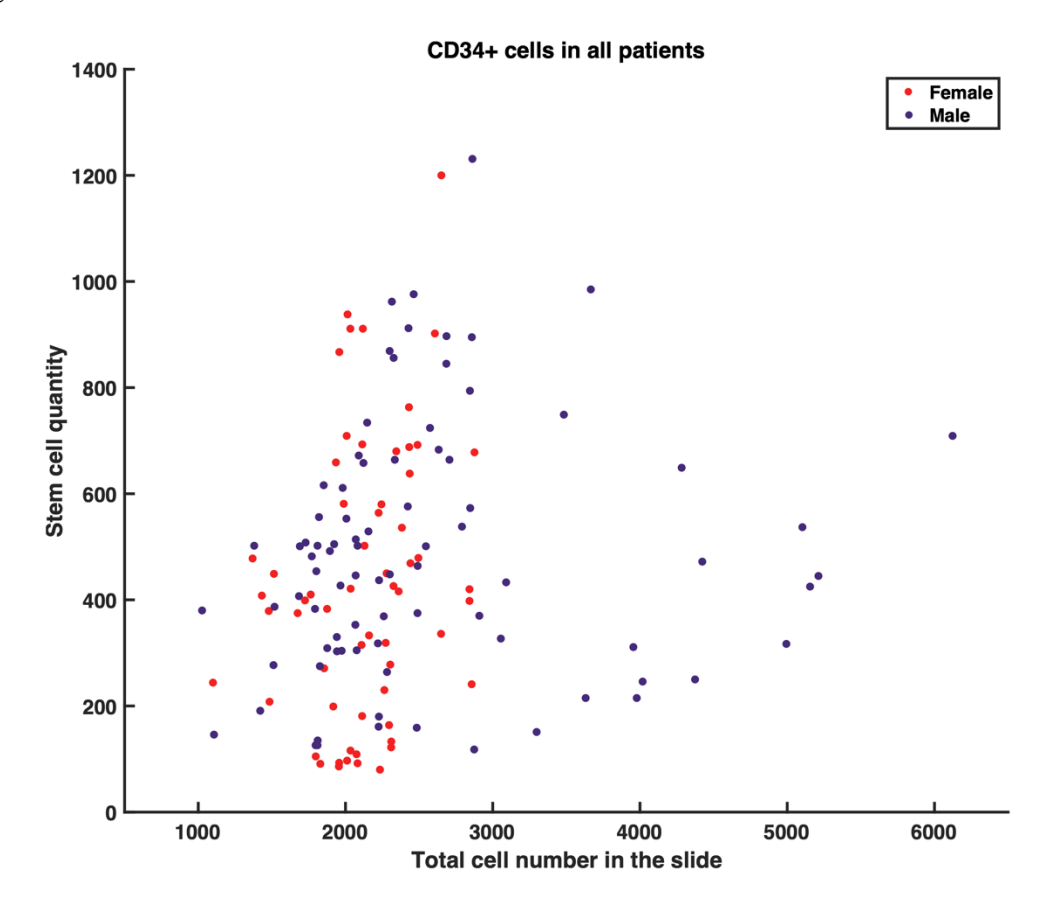


Figure 38. Scatter plot with data from all 12 patients divided into two groups (Female, Male), representing the ratio between total cell number and CD34 positive stem cell quantity in the in the tissue slide.

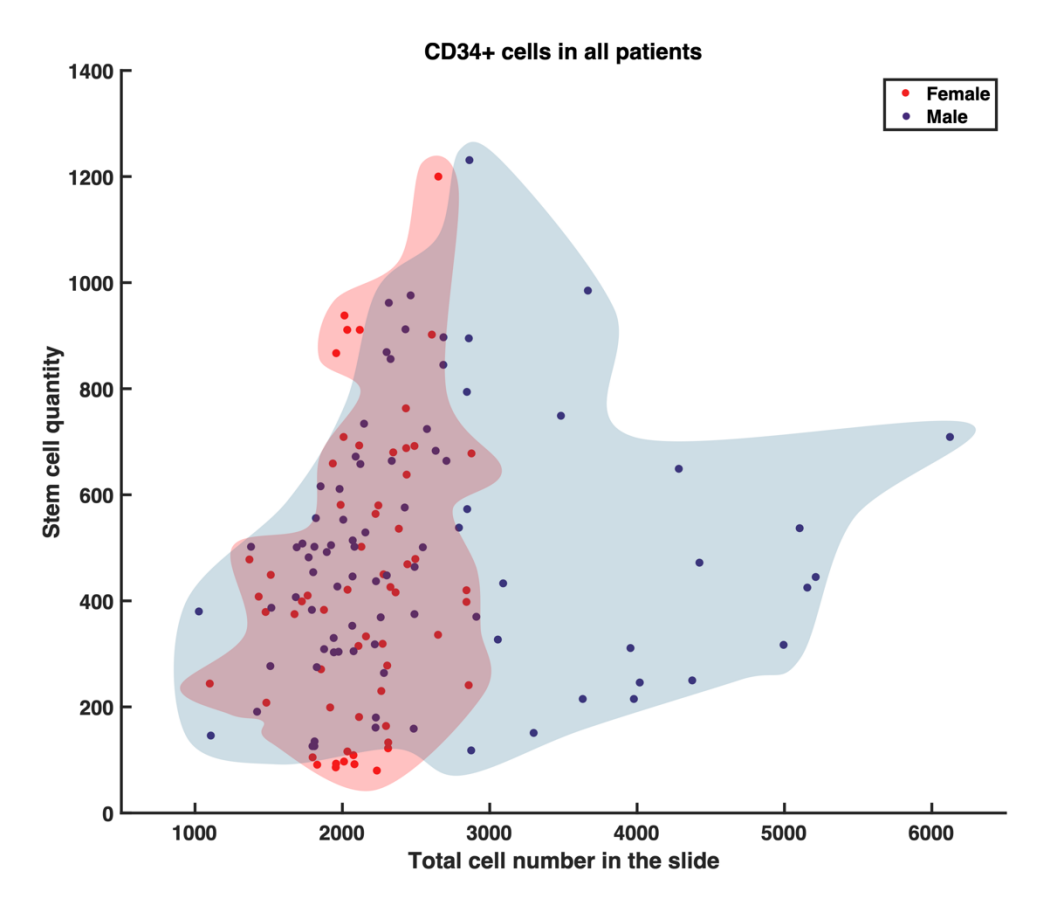


Figure 39. Ashby plot with data from all 12 patients divided into two groups (Male, Female), representing the ratio between total cell number and CD34 positive stem cell quantity in the in the tissue slide. Each patient's data points are represented as a distinct cluster on the plot, with the position of the cluster indicating the patient's overall ratio of stem cells to total number of cells.

Upon receiving qualitative data for the stem cell marker CD34, we embarked on a parallel analysis of another stem cell marker, CD90, employing a similar methodology. To ensure consistency and comparability with our previous analysis, the investigation was initiated by constructing a scatter plot (Figure 40). This plot served as the foundational framework for the subsequent analysis and allowed for visual examination of the distribution of CD90 marker expression across different groups.

Following the creation of the scatter plot, the data was categorized into the same groups as previously defined, ensuring a standardized approach to the analysis. This segmentation enabled for exploring the potential trends or variations in CD90 marker expression within specific demographic or clinical subsets, analogous to the analysis of the CD34 marker.

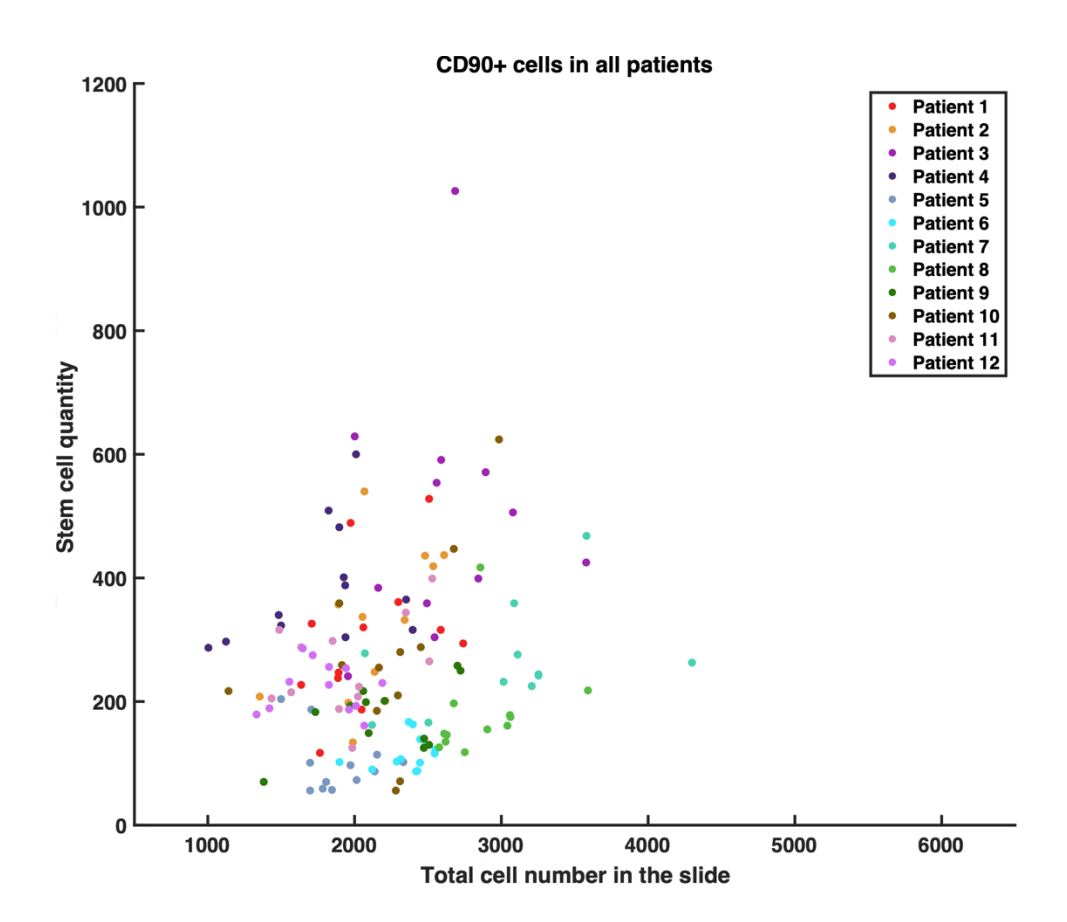


Figure 40. Scatter plot with data from all 12 patients representing the ratio between total cell number and CD90 positive stem cell quantity in the in the tissue slide.

In Figure 41, an Ashby plot was created to visualize the expression of the CD90 marker and proceeded to grouping the patients according to the categories.

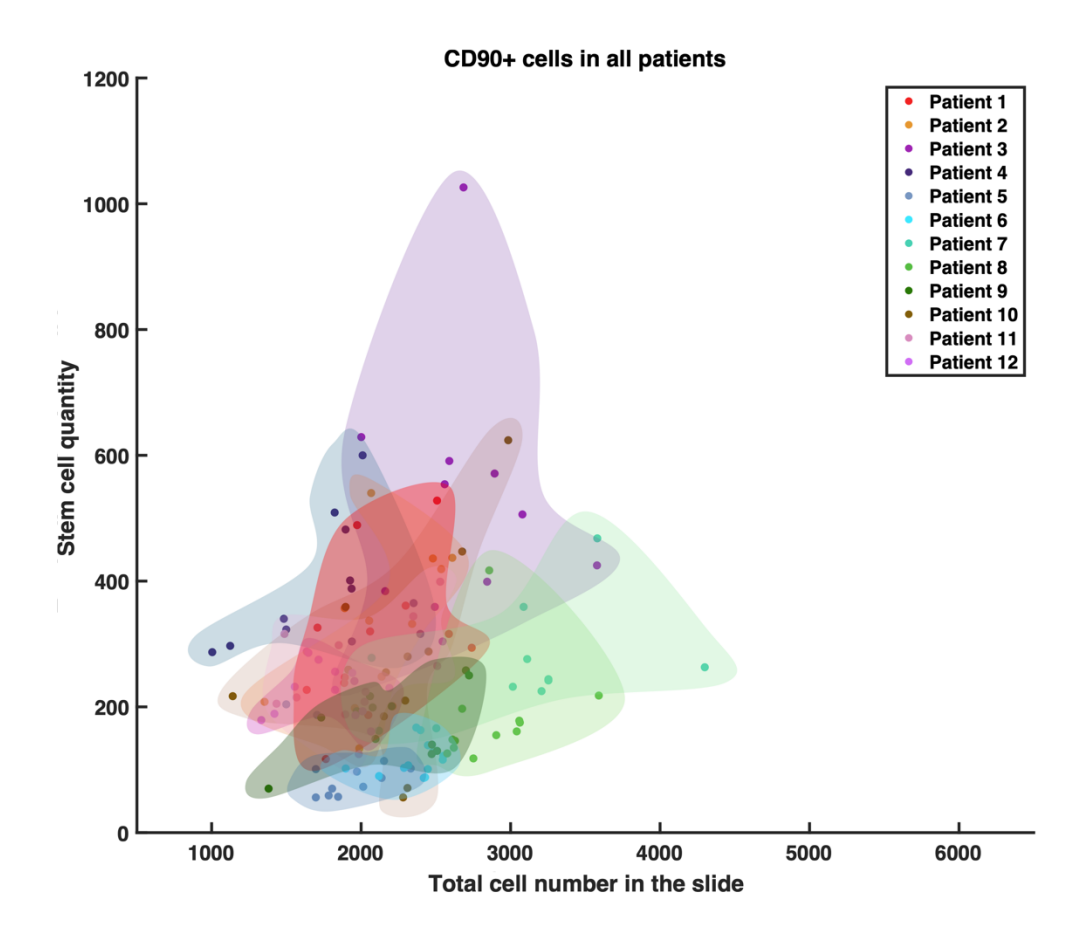


Figure 41. Ashby plot with data from all 12 patients representing the ratio between total cell number and CD90 positive stem cell quantity in the in the tissue slide. Each patient's data points are represented as a distinct cluster on the plot, with the position of the cluster indicating the patient's overall ratio of stem cells to total number of cells.

Following the creation of the scatter plot for the clinical conditions' groups (Figure 42), we manually delineated distinct clusters on the plot (Figure 43) to represent each group's data points and have obtained similar trends to the ones observed in plots with CD34 stem cell marker ratio. The observations which were encountered in CD34 stem cell marker ratios repeated in plots (Figure 44-47) for the stem cell marker CD90 for all the group types, which attributes to the consistency of the results.

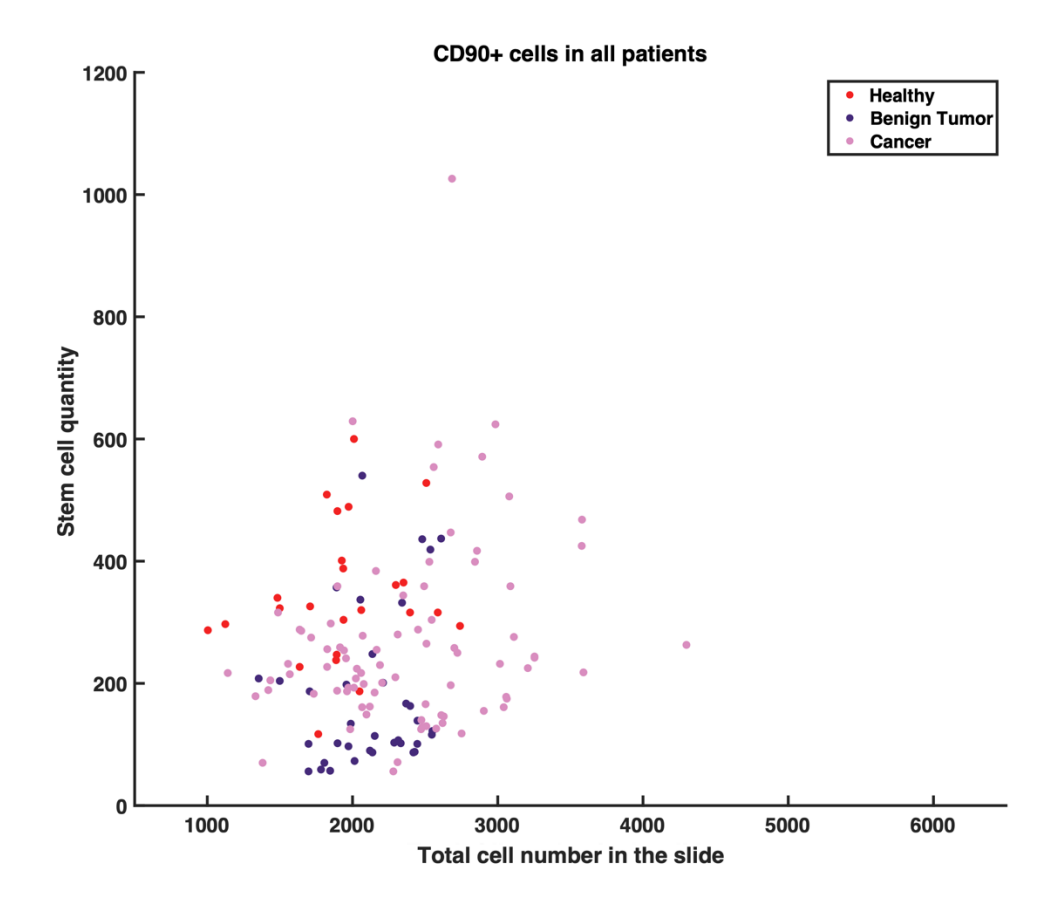


Figure 42. Scatter plot with data from all 12 patients divided into three groups (Healthy, Benign Tumor, Cancer), representing the ratio between total cell number and CD90 positive stem cell quantity in the in the tissue slide.

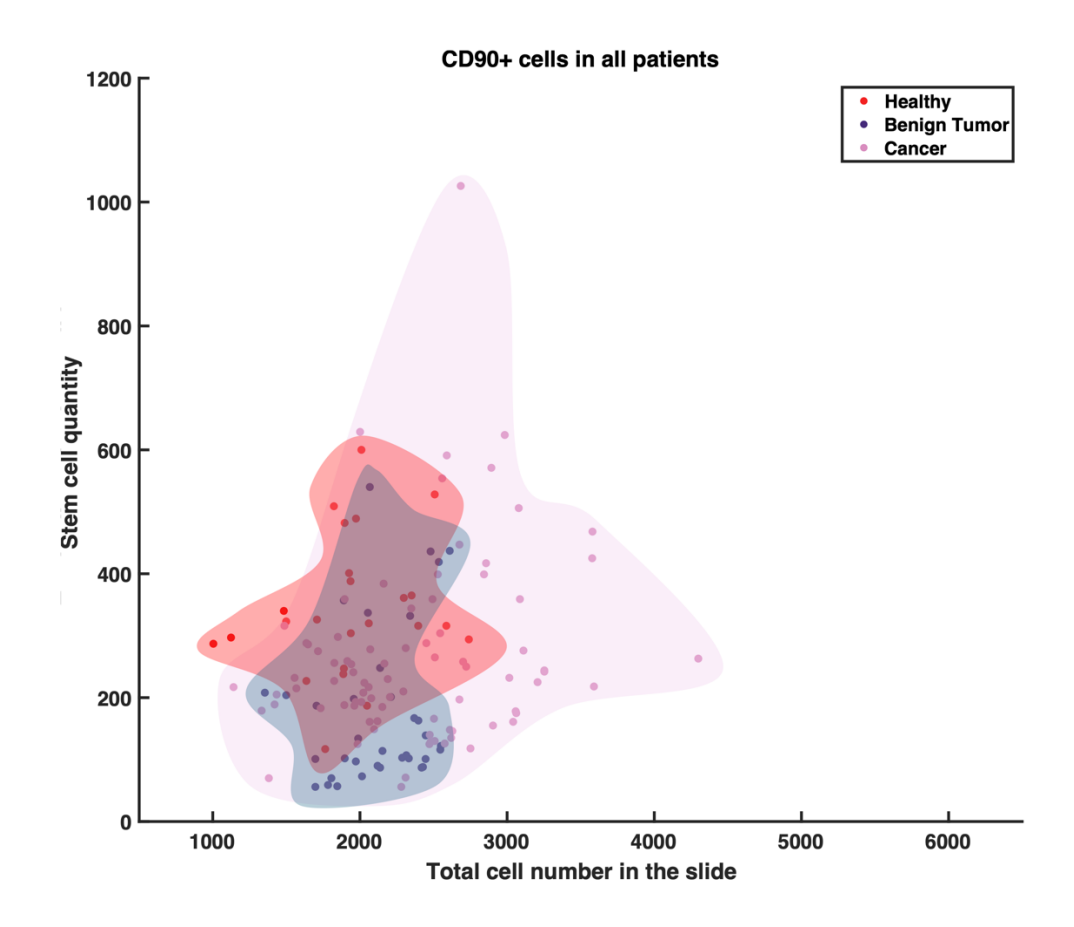


Figure 43. Ashby plot with data from all 12 patients divided into three groups (Healthy, Benign Tumor, Cancer), representing the ratio between total cell number and CD90 positive stem cell quantity in the in the tissue slide. Each patient's data points are represented as a distinct cluster on the plot, with the position of the cluster indicating the patient's overall ratio of stem cells to total number of cells.

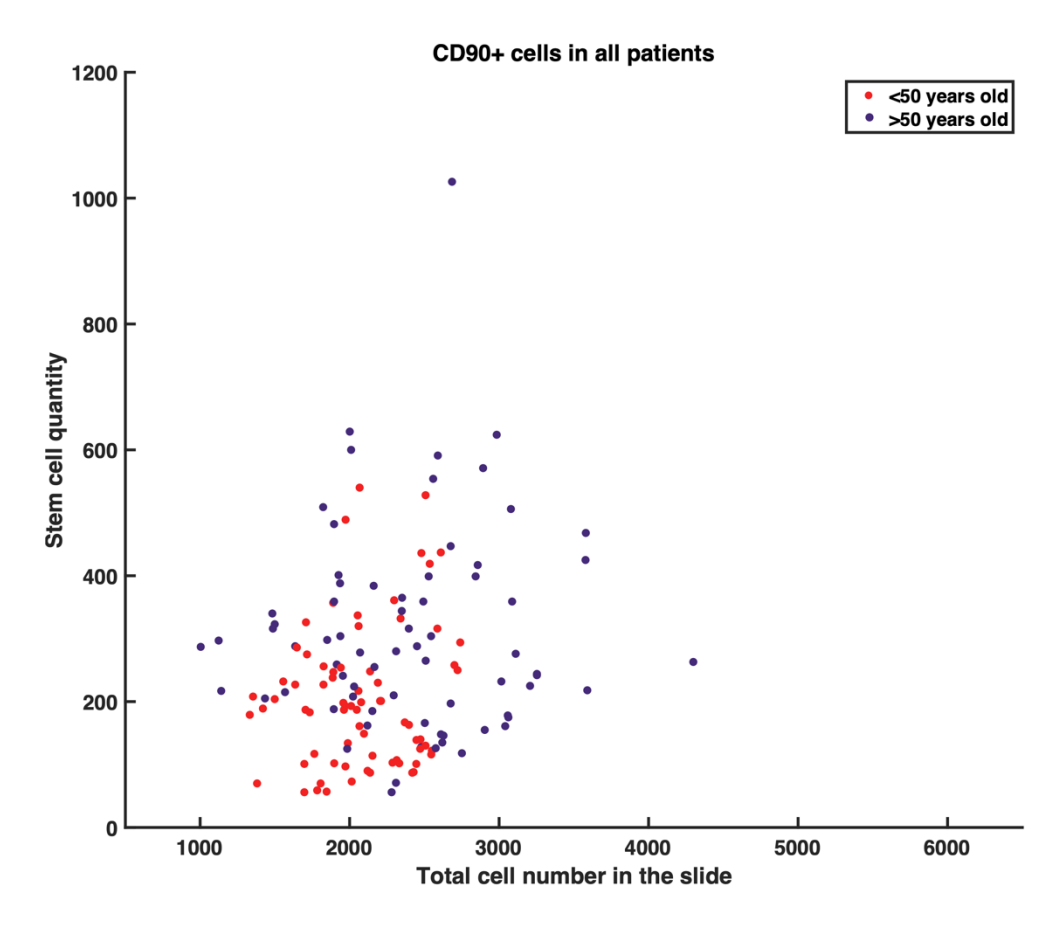


Figure 44. Scatter plot with data from all 12 patients divided into two groups (<50 years old, >50 years old), representing the ratio between total cell number and CD90 positive stem cell quantity in the in the tissue slide.

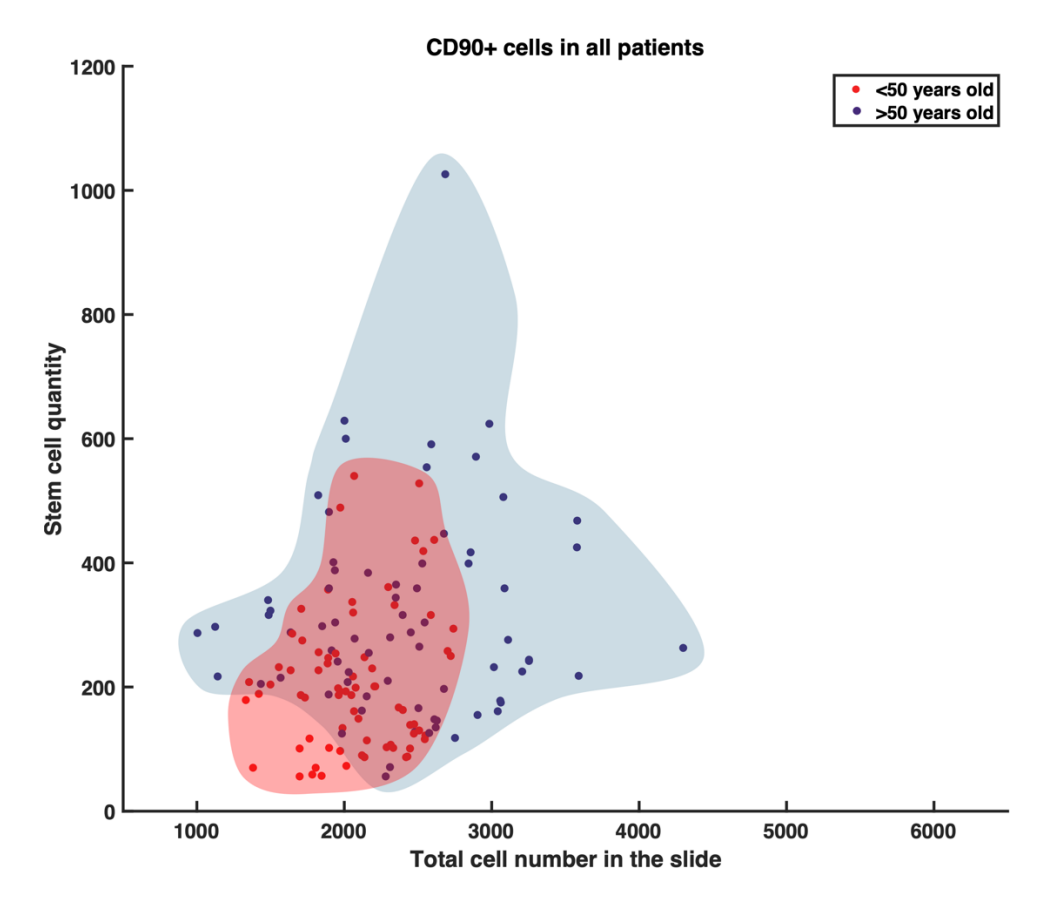


Figure 45. Ashby plot with data from all 12 patients divided into two groups (<50 years old, >50 years old), representing the ratio between total cell number and CD90 positive stem cell quantity in the in the tissue slide. Each patient's data points are represented as a distinct cluster on the plot, with the position of the cluster indicating the patient's overall ratio of stm cells to total number of cells.

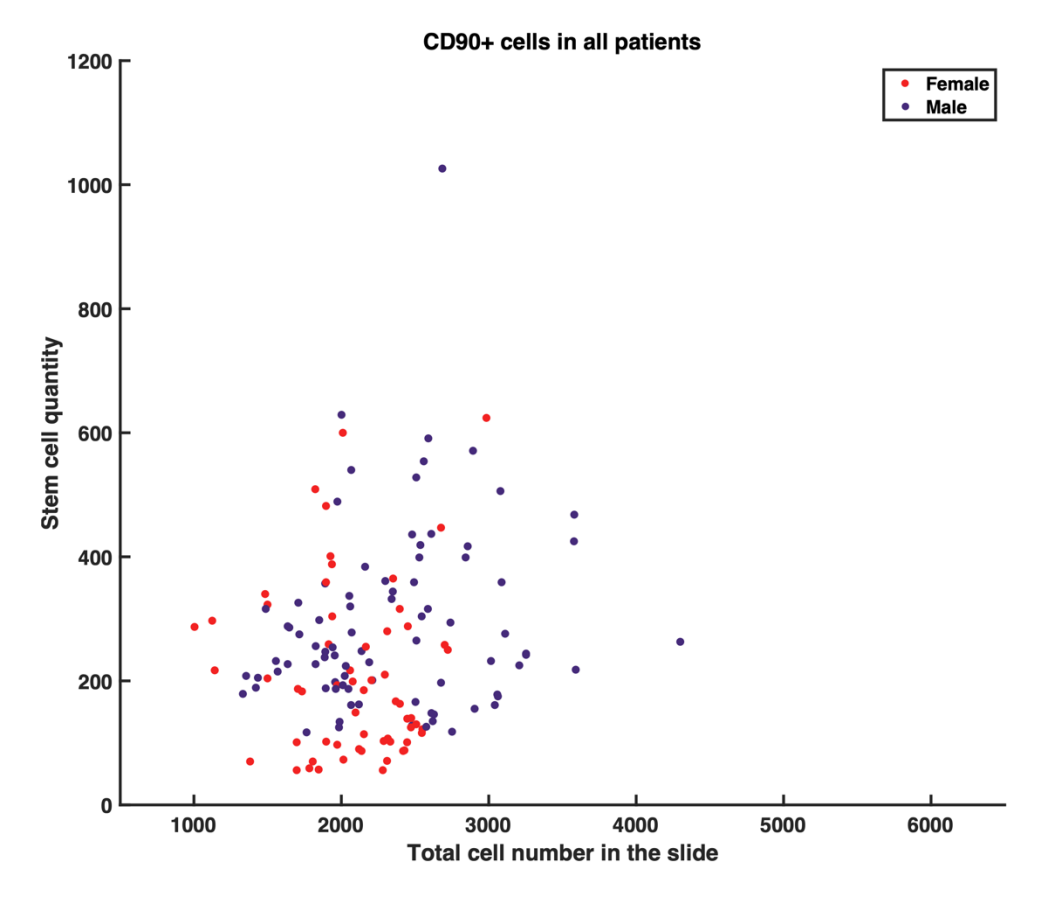


Figure 46. Scatter plot with data from all 12 patients divided into two groups (Female, Male), representing the ratio between total cell number and CD90 positive stem cell quantity in the in the tissue slide.

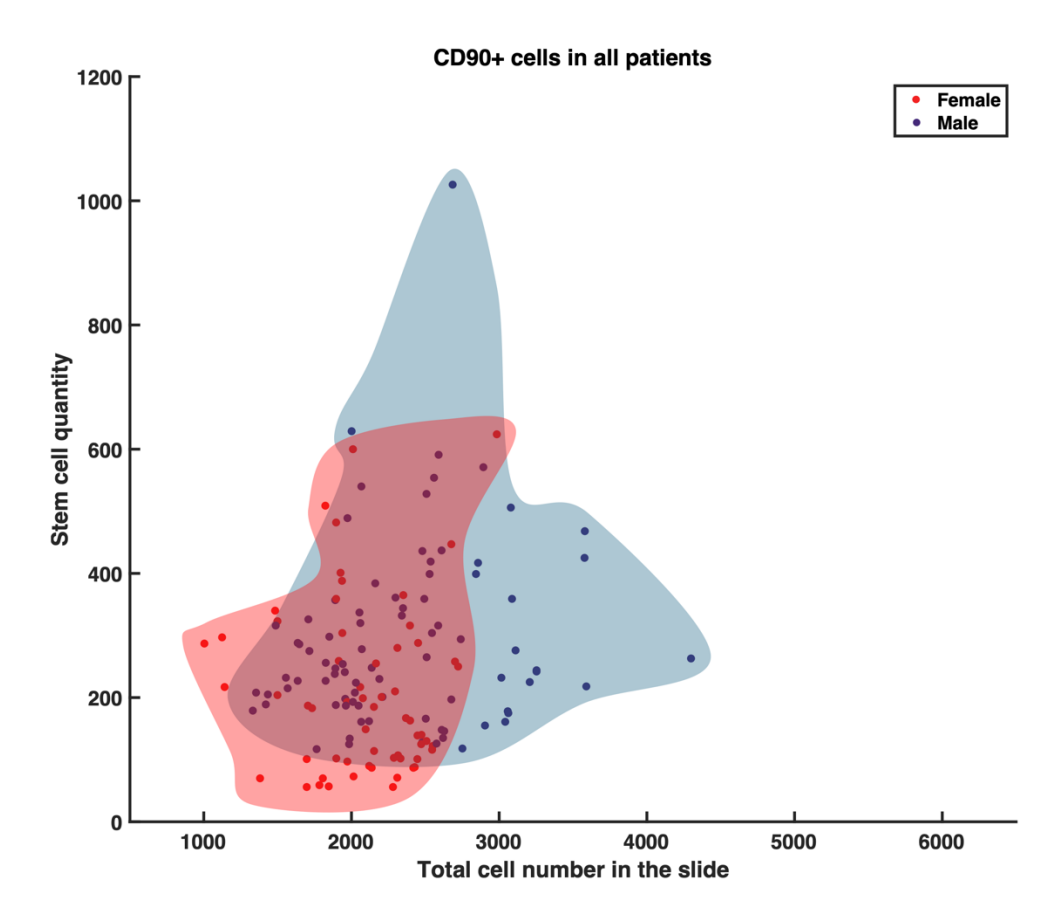


Figure 47. Ashby plot with data from all 12 patients divided into two groups (Male, Female), representing the ratio between total cell number and CD34 positive stem cell quantity in the in the tissue slide. Each patient's data points are represented as a distinct cluster on the plot, with the position of the cluster indicating the patient's overall ratio of stem cells to total number of cells.

Following the completion of our qualitative analysis, we transitioned to a quantitative approach utilizing curve fitting techniques. To accomplish this, a linear equation model represented by f(x) = p1*x + p2 was employed as the basis for the curve fitting process (Table 4-5).

Upon obtaining the coefficient values from the curve fitting procedure, we proceeded to construct a predictive model. This predictive model allowed to extrapolate and predict values beyond the observed data points, facilitating a deeper understanding of the underlying trends and relationships

within our dataset. By leveraging this predictive model, we were able to draw meaningful conclusions based on the projected outcomes.

Equation	Patient	R-Square	Adjusted R-square	Coefficient p values	Degree of freedom (DFE)
f(x)=p1*x+p2	1	0.2663 (27%)	0.1929 (19%)	p1=0.1996	10
				p2=7.8731	
	2	0.4385 (44%)	0.3824 (38%)	p1=0.2593	
				p2=-175.7911	
	3	0.7399 (74%)	0.7139 (71%)	p1=0.3992	
				p2=-98.0665	
	4	0.5526 (55%)	0.5078 (51%)	p1=0.2064	
				p2=58.8049	
	5	0.0059 (0.6%)	-0.0935(-9%)	p1=0.0170	
				p2=80.8582	
	6	0.1308 (13%)	0.0439 (4%)	p1=0.0958	
				p2=83.7608	
	7	0.4080 (41%)	0.3488 (35%)	p1=0.1005	
				p2=65.9218	
	8	0.3029 (30%)	0.2332 (23%)	p1=0.1122	
				p2=-138.3232	
	9	0.2035 (20%)	0.1238 (12%)	p1=0.3043	
				p2=147.1147	
	10	0.3561 (36%)	0.2917 (29%)	p1=0.3244	
				p2=-238.7979	
	11	0.6643 (66%)	0.6307 (63%)	p1=0.2705	
				p2=-82.0271	
	12	0.2903 (29%)	0.2193 (22%)	p1=0.2139	
				p2=125.5859	

Table 4. Curve fitting values for the predictive model of ratio of CD34+ stem cell quantity to total number of cells in the tissue. Basing on the R-square values, we can hypothesize that fit is relatively good with a couple of major deviations.

Equation	Patient	R-Square	Adjusted R-square	Coefficient p values	Degree of freedom (DFE)
f(x)=p1*x+p2	1	0.1838 (18%)	0.1022 (10%)	p1=0.1386	10
				p2=14.2576	
	2	0.2648 (26%)	0.1913 (19%)	p1=0. 1862	
				p2=-76.9395	
	3	0.0167 (1.7%)	-0.0816 (-8.2%)	p1=0.0578	
				p2=347.8495	
	4	0.1280 (13%)	0.0408 (4%)	p1=0.0816	
				p2=238.9865	
	5	0.1077 (11%)	0.0185(2%)	p1=-0.0665	
				p2=226.0867	
	6	0.0387 (4%)	-0.0263 (-3%)	p1=0.0387	
				p2=24.4719	
	7	0.2300 (23%)	0.1530 (15%)	p1=0.0694	
				p2=45.5082	
	8	0.0671 (7%)	-0.0262 (-3%)	p1=0.0704	
				p2=-20.3759	
	9	0.2290 (23%)	0.1519 (15%)	p1=0.0660	
				p2=31.1152	
	10	0.2177 (22%)	0.1395 (14%)	p1=0.1603	
				p2=-84.0478	
	11	0.1354 (14%)	0.0489 (5%)	p1=0.0746	
				p2=111.3897	
	12	0.000828 (0%)	-0.0991 (-9%)	p1=-0.0044	
				p2=230.3161	

Table 5. Curve fitting values for the predictive model of ratio of CD90+ stem cell quantity to total number of cells in the tissue. Based on the R-square values, the overall quality of the fit is lower.

Upon acquiring our dataset, we proceeded to construct curve fits for both CD34 and CD90 markers, as illustrated in Figure 48 and Figure 49 respectively. Our analysis revealed a discernible correlation between the ratios of stem cells to the total number of cells and the clinical conditions of the patients.

Healthy patients exhibited predictive curves that maintained a consistent and parallel median range for both CD34 and CD90 markers. This consistency suggests a stable relationship between stem cell ratios and overall cell composition in individuals without underlying health conditions.

Conversely, the ratios observed in the benign tumor group displayed a distinctive trend, with values generally falling below those of healthy patients. Within this group, the median value remained comparable to that of healthy patients, while two extremes were observed — one mirroring the ratios of healthy individuals and the other exhibiting notably lower or even negative values.

Remarkably, the curve fits for cancer patients showcased a scattered distribution, indicative of a greater variability in stem cell ratios within this cohort. Specifically, the CD34 marker displayed a prevalence towards higher values, suggesting a potential association with cancer pathology. In contrast, the CD90 marker maintained a distribution within the medium range, implying a different pattern of expression in cancer patients compared to healthy individuals and those with benign tumors.

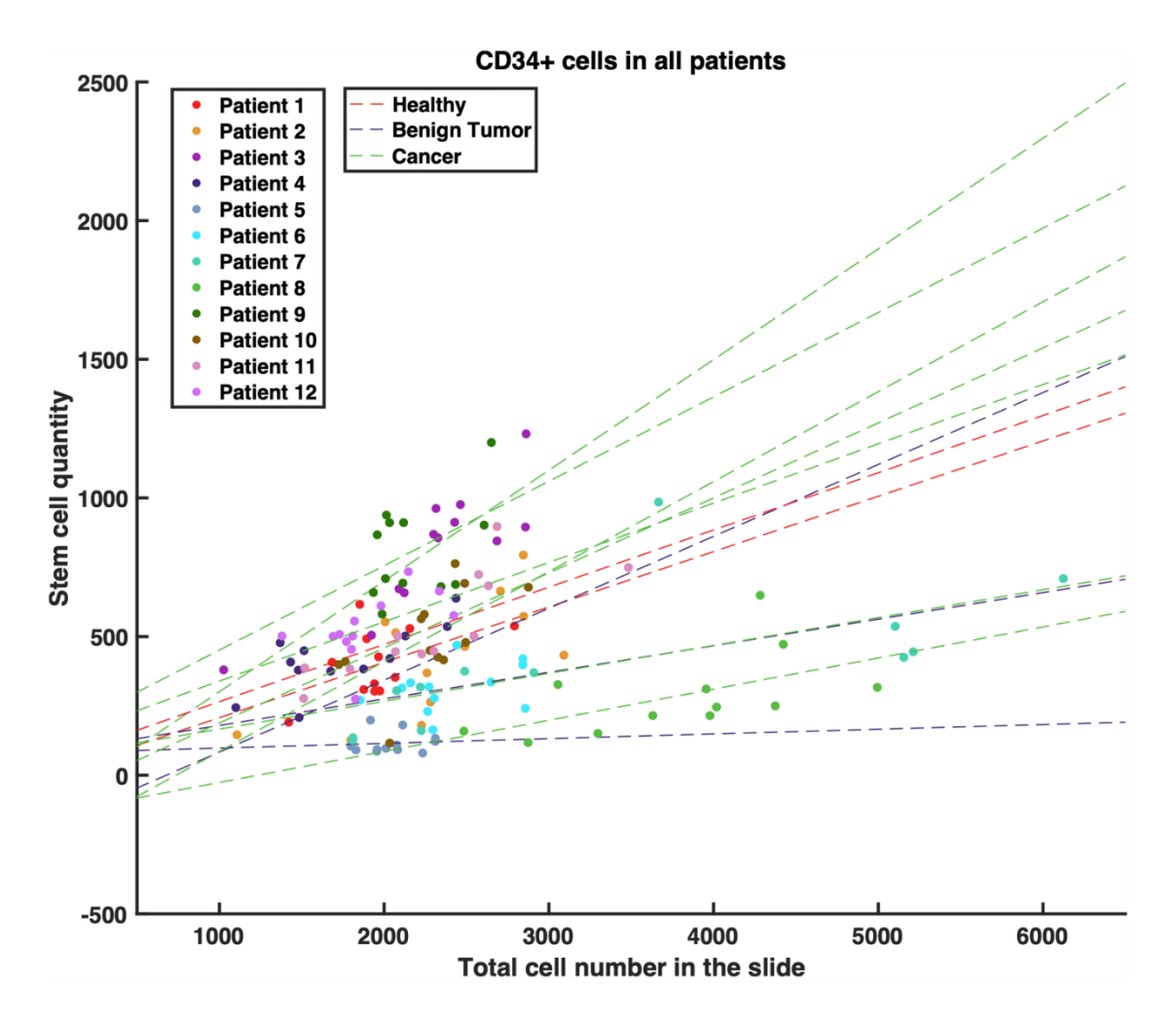


Figure 48. Curve fitting for the data from all 12 patients divided into three groups (Healthy, Benign Tumor, Cancer), representing the ratio between total cell number and CD34 positive stem cell quantity in the in the tissue slide.

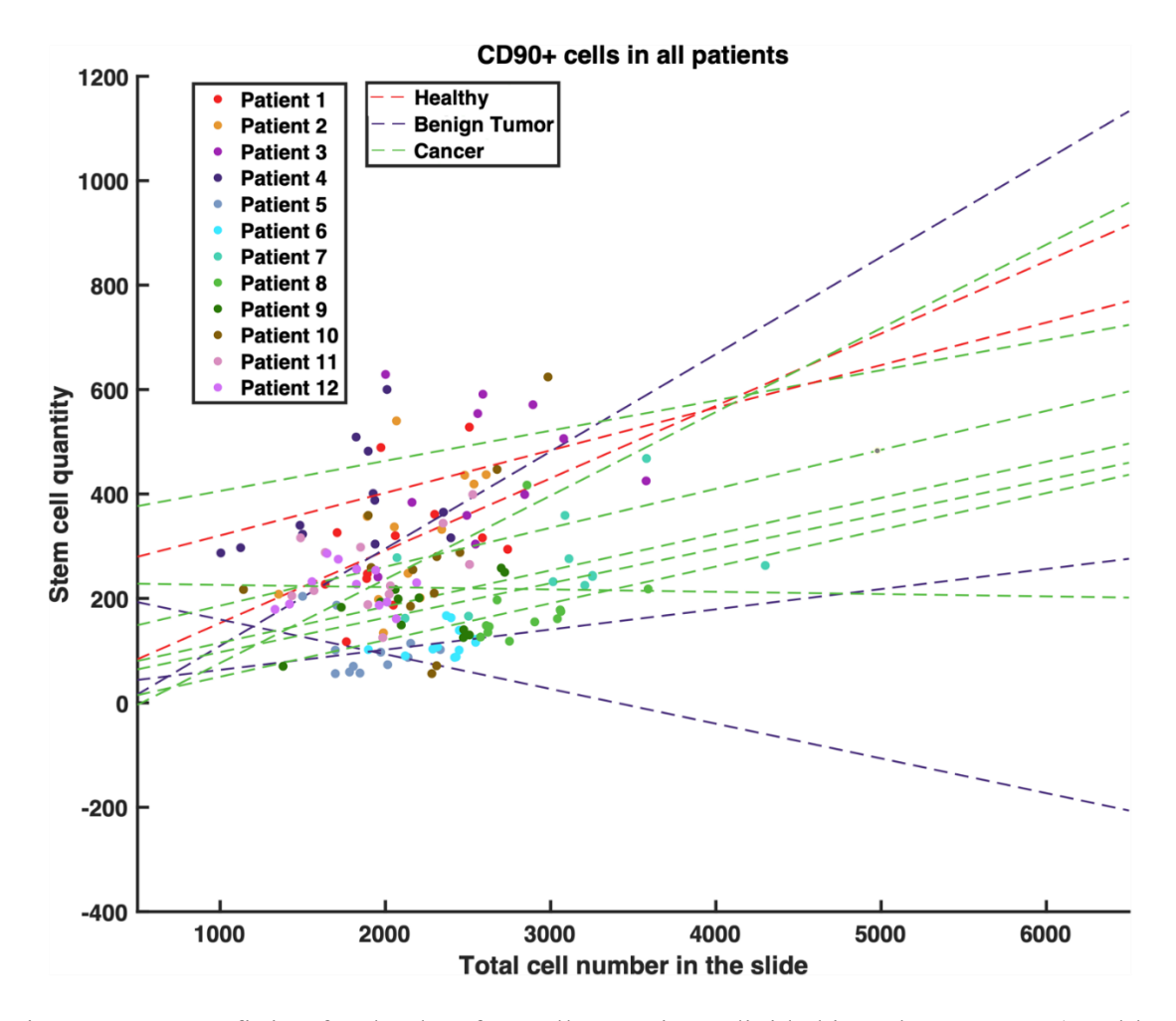


Figure 49. Curve fitting for the data from all 12 patients divided into three groups (Healthy, Benign Tumor, Cancer), representing the ratio between total cell number and CD90 positive stem cell quantity in the in the tissue slide.

Another aspect of our investigation involved examining the overlapping signals in our staining channels to ascertain the co-expression of epithelial and stem cell markers within individual cells. This analysis aimed to quantify the proportion of cells concurrently expressing both marker types, shedding light on potential cellular heterogeneity and phenotypic transitions within the studied population.

TOTAL OVERLAP COUNT

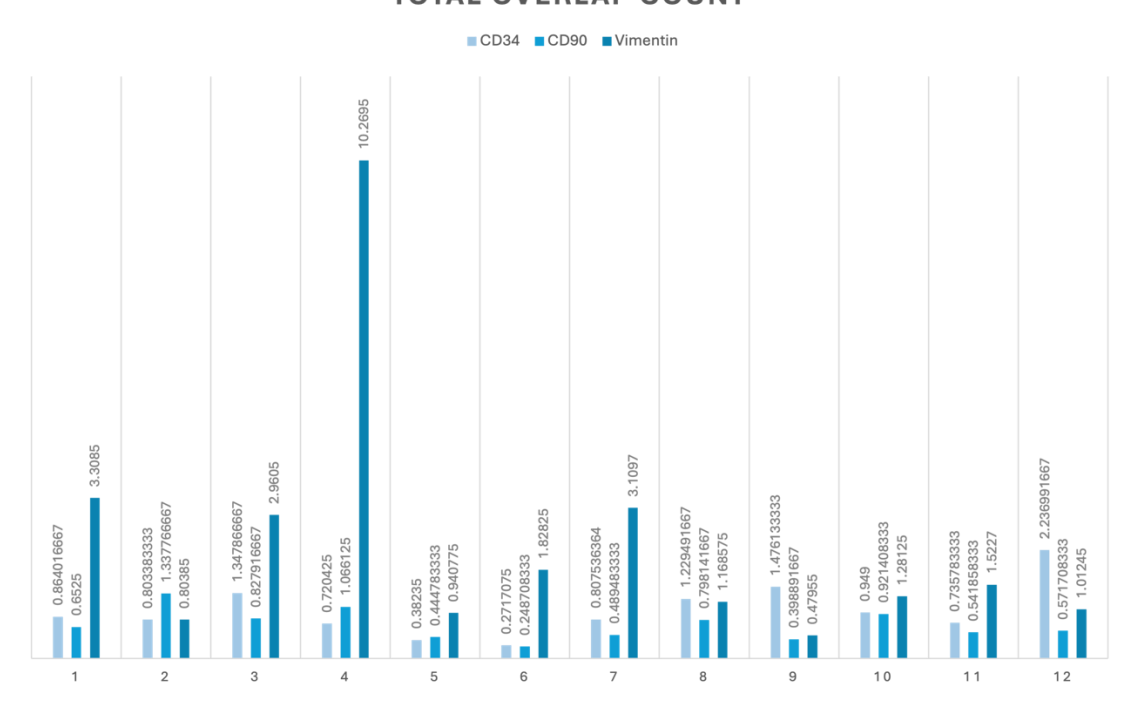


Figure 50. Bar plot showing the total overlap count of stem cells with 3 types of SG cells without separation for each type in the tissue slide in all 12 patients.

We conducted an analysis of overlapping signals and observed distinct patterns among patient groups. Notably, patients diagnosed with cancer (3, 7-12) exhibited a higher prevalence of co-expression of cells bearing the CD34 marker compared to both the healthy and benign tumor groups, as depicted in Figure 50. However, no significant correlation was discerned for the CD90 marker across the studied cohorts.

Interestingly, heightened expression of Vimentin was observed, primarily attributed to its role as a marker for both stem cells and myoepithelial cells. This dual functionality resulted in elevated expression levels, contributing to the overall increased numbers observed. To delineate the contributions of specific cell types to this phenomenon, we segregated our data and generated separate plots for each salivary gland epithelial cell type.

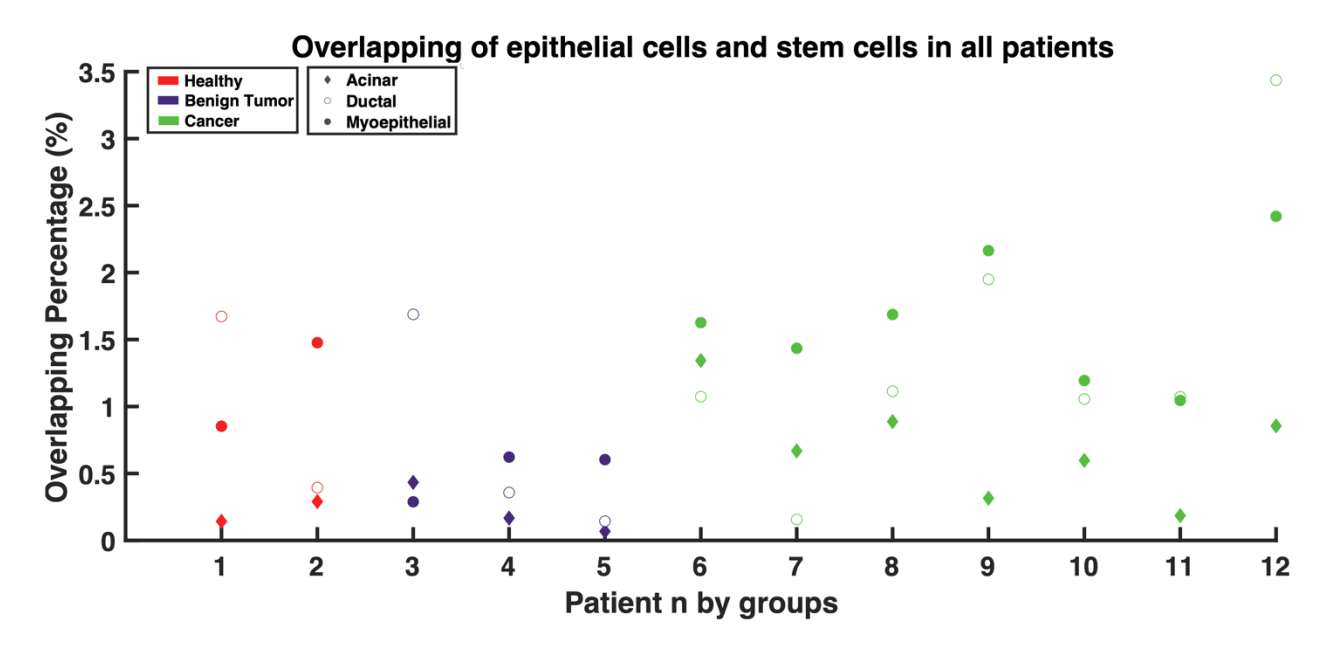


Figure 51. Overlap of epithelial markers with stem cell marker CD34 in all 12 patients.

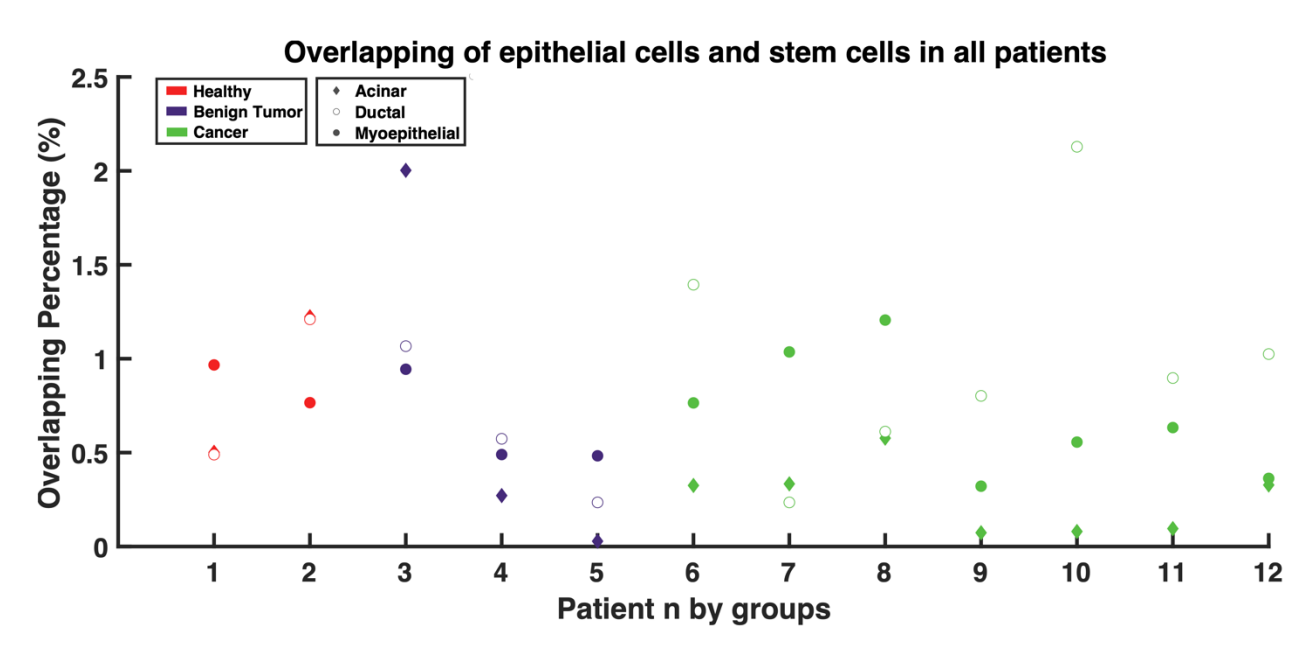


Figure 52. Overlap of epithelial markers with stem cell marker CD90 in all 12 patients.

Analysis of Figure 51 reveals noteworthy observations regarding the marker CD34. Specifically, elevated levels of overlapping signals were observed predominantly in ductal cells, while co-expression in acinar cells remained considerably low. The underlying mechanisms

driving this phenomenon require further investigation to understand its nature and significance within the context of cellular dynamics and disease pathology.

Conversely, examination of Figure 52 highlights comparable levels of overlapping signals across acinar and ductal cell populations in co-expression with marker CD90. Notably, the values for acinar and ductal cells intersected on multiple occasions, indicative of shared patterns of co-expression. Additionally, sporadic peaks of high overlapping numbers were observed specifically in the ductal cell population within the cancer patient group, suggesting potential alterations in co-expression patterns associated with disease progression or pathophysiological changes.

These findings underscore the complex relationships between cellular subtypes and marker expression patterns, offering valuable insights into the heterogeneous nature of cell populations and their contributions to disease processes.

4. Discussion

CD34 marker is usually tested in most studies for detection of hematopoietic stem cells, however, in a recent study [44] CD34 has been tested as a new promising marker for mesenchymal stem cells.

The high expression of CD90 has been explored in many studies, making it a trustworthy marker for determining mesenchymal stem cells.

Low use and presence of cKit expressing cells in human studies can be explained by the fact, that it is a marker for hematopoietic stem cells and as our search was MSCs oriented, our review of the literature did not retrieve enough records to have strong comparison, although, cKit was broadly present in rodent studies.

We observed a lack of expression of the marker CD45 as it is commonly used as a negative proof associated with hematopoietic cells. If cells were tested for stem cells nature, we would use cKit and CD45 co-expression, absence of CD45 marker and presence of cKit marker proves that found cells are hematopoietic stem cells.

In multiple studies, Vimentin was reported as a marker for mesenchymal stem cells.

The main reason for choosing a targeted source of stem cells in the submandibular glands is that stem cells was a discovery presented in studies by Okumura et al. (2012) and Aure et al. (2015). In these studies, stem cells populations reported showed the characteristics of adult or embryonic stem cells which are known to have the highest potential in tissue regeneration following injury or loss of cells in salivary glands. These stem cells have been identified primarily in human major salivary glands. It is still a subject of debate, whether the regeneration of the main salivary gland cells (acinar or ductal cells) is performed by stem cells, or if the possibility of

regeneration lays within the salivary cells themselves. In salivary glands which underwent radiation therapy, they presented 2 main stages of cellular damage: the mild damage, where the acinar cell resisted the damage via the mechanism of self-duplication. The second stage was the medium damage, where while most of the acinar cell population got lost and the plasticity of the ductal cells was able to initiate a new acinar cells population. While these factors may play an important role in tissue regeneration and repair, we still should consider the rising potential of stem cell therapy, which have proven to be efficient in the treatment many other organs and tissues [6].

In this project, we have used immunofluorescence method to test certain stem cell markers and we decided to use these markers based on previous studies highlighting the markers of different types of animal and human stem cells. It has been discussed in the paper by Scott Schachtele, et al. (2013), who reported that 2% or less of MSCs population should express CD34 and 95% or more should express CD90. At the same time, studies by Lin et al. (2012) and Kaiser et al. (2007) stated that CD34 negative status is variable depending on the cell culture conditions. In studies by Quirici et al. (2010), Yoshimura et al. (2006) and Pachón-Peña et al. (2011), it has been found that CD34+ cells were of MSC nature in the isolation stage but lost the expression in the culture.

Certain limitations are associated with the immunofluorescence method used in this study which includes the difficulty to accurately quantify the precise number of stem cells.

As CD34 is considered to be one of the salivary gland stem cell biomarkers, we have been able to reproduce the results and visualize its presence. The quantities of CD34+ cells were more abundant compared to the expression of CD90 stem cell marker. Despite our findings, we cannot rely on the immunofluorescence staining data only.

Salivary gland stem cells are considered one of the most readily available source of stem cells and have been tested widely [7], mesenchymal stem cells present as a very attractive option of

stem cell therapy due to their low level of immunogenicity, decreased risk of tumor formation and high ability to multiply and differentiate to multiple cell types. Therefore, we used the CD90 marker to detect if the cells of mesenchymal stem cell nature are present in our groups of patients. As per our literature search, we have discovered that c-KIT is considered to be the most used marker for detection of salivary gland stem cells, but it was suggested by literature [18], that population of cKIT+ cells declines with age. Patients age was one of the factors we were investigating in this project, alongside with sex, to determine any significant difference in the quantities as of salivary gland cells and stem cells.

One of our patients had highly abundant amount of CD34+ stem cells. In the search for the explanation, we have encountered the study by Won-Tae Kim et al. (2017), who reported that some normal adult and embryonic stem cells were expressed by cancer stem cells. Our patient who showed high expression of surface marker CD34 was being treated for squamous cell carcinoma of the larynx.

Konttinen et al. (2010) reported that salivary glands are sexually dimorphic organ that have been slowed down by the factor that humans as primates have more complex structures. Sjorgen syndrome has characteristic features that could not be conclusively explained yet. It has a skewed gender distribution with a tendency to affect 9 out of 10 female patients who are undergoing menopause. Our study was observing certain trends in correlations between the sex of the patients and the levels of stem cell markers expression, which was additionally similar to the stem cell markers expression in the disease groups we established.

The use of the custom MATLAB based application was motivated by the lack of present established protocols of automatic cell quantification for the immunofluorescence staining. Despite the existence of customized macros [49] which allowed using mask to count cells, it is

still an extension of ImageJ software which needs to be additionally installed and is still missing many necessary functions. With the development of our application, we have implemented additional functions, such as counting of cells depending on the channel, automatic labelling and custom changeable settings which will help to suit any image taken. In such manner we have been able to quantify separately the quantity of acinar, ductal and myoepithelial cells in addition to the stem cell marker expressing cells, by combining the blue channel with the red and the green, respectively. In addition, we added sliders with possibility to change necessary parameters depending on the magnification, quality and brightness of the image. Such parameters included sensitivity basing on the background noise, segmentation degree and area radius for the catching the channel color.

Due to the variability of diseases presented in our study we cannot conclusively state that age or gender were the main impacting factor for the reported quantity of stem cells and cells expressing salivary gland markers. In addition, it has been stated, that stem cell markers can pose as cancer markers and as per present data on patients in our study, some of them had various types of cancer or cancer-like diseases, this could also be an additional impact on the results.

5. Conclusions

This study aimed to assess the expression of stem cell markers in human submandibular salivary glands, particularly in relation to acinar, ductal, and myoepithelial stem cells, utilizing a custom application developed for this purpose. Specifically, we sought to determine the presence of stem cells in the submandibular salivary glands, quantify their abundance, determine their association with various salivary epithelial cell types, and compare stem cell expression across patients at different age, sex, and clinical conditions. Using MATLAB code, we developed the application enabling the quantification of targeted cell types and the possible overlaps of stem cells and salivary epithelial cells, facilitating comprehensive data analysis.

Our findings revealed a definite correlation between disease status and the quantity of stem cells present. However, establishing a clear relationship between age and stem cell quantity proved to be inconclusive due to the heterogeneous clinical conditions and demographic profiles of our patients. Notably, the absence of a clinically defined "healthy" control group posed a limitation, as patients categorized as healthy exhibited conditions other than cancer (e.g., post-stroke complications, submandibular reconstruction), thereby complicating direct comparisons.

Although statistical analysis yielded nonsignificant results (p value > 0.05), notable trends emerged. Stem cell expression in the healthy group consistently fell within a certain range, whereas the group of patients with benign tumors exhibited lower stem cell expression compared to other groups. Conversely, stem cell expression in the cancer group displayed significant variability, likely attributable to its larger size and heterogeneous composition in terms of age and sex distribution. Furthermore, higher expression of the hematopoietic stem cell marker CD34 in cancer patients underscored its role in cancer stem cell populations.

Our study highlights the correlation between stem cell quantity and demographic/clinical parameters, suggesting avenues for further investigation. Moreover, the development of our novel application represents a promising tool for automating cell quantification, offering new opportunities for both clinical and scientific researchers alike.

5.1 Future Directions

Moving forward, our research will focus on broadening the scope of our patient cohort to achieve greater clarity in differences between groups. By including a more diverse range of patients, we aim to achieve better understanding of the potential relationships between stem cell expression and various demographic and clinical variables. Additionally, we plan to conduct a comparative study targeting a specific demographic subset, such as students of similar age. This investigation will enable us to explore the influence of lifestyle factors, including smoking, alcohol consumption, and other habits, on stem cell expression. By examining these correlations, we can better understand the impact of environmental factors on salivary gland health and inform preventive measures to mitigate adverse effects. These future directions promise to enrich our understanding of stem cell dynamics in salivary glands and contribute to the development of targeted interventions for maintaining oral health.

6. References

- 1. Chibly, A.M., et al., *Salivary gland function, development, and regeneration*. Physiological Reviews, 2022. **102**(3): p. 1495-1552.
- 2. de Paula, F., et al., Overview of Human Salivary Glands: Highlights of Morphology and Developing Processes. The Anatomical Record, 2017. **300**(7): p. 1180-1188.
- 3. Emmerson, E. and S.M. Knox, Salivary gland stem cells: A review of development, regeneration and cancer. genesis, 2018. **56**.
- 4. Proctor, G.B., *The physiology of salivary secretion*. Periodontology 2000, 2016. **70**(1): p. 11-25.
- 5. Ogle, O.E., *Salivary Gland Diseases*. Dental Clinics of North America, 2020. **64**(1): p. 87-104.
- 6. Rocchi, C., L. Barazzuol, and R.P. Coppes, *The evolving definition of salivary gland stem cells.* npj Regenerative Medicine, 2021. **6**(1): p. 4.
- 7. Tran, O.N., et al., Chapter 14 Stem Cell-Based Restoration of Salivary Gland Function, in A Roadmap to Non-Hematopoietic Stem Cell-based Therapeutics, X.-D. Chen, Editor. 2019, Academic Press. p. 345-366.
- 8. Pringle, S., R. Van Os, and R.P. Coppes, *Concise Review: Adult Salivary Gland Stem Cells and a Potential Therapy for Xerostomia*. Stem Cells, 2013. **31**(4): p. 613-619.
- 9. Lombaert, I., et al., Concise Review: Salivary Gland Regeneration: Therapeutic Approaches from Stem Cells to Tissue Organoids. Stem Cells, 2016. **35**(1): p. 97-105.
- 10. Coppes, R. and M. Stokman, *Stem cells and the repair of radiation-induced salivary gland damage*. Oral diseases, 2011. **17**(2): p. 143-153.

- 11. Feng, J. and R.P. Coppes, Can we rescue salivary gland function after irradiation? ScientificWorldJournal, 2008. 8: p. 959-62.
- 12. Nanduri, L.S.Y., et al., *Regeneration of irradiated salivary glands with stem cell marker expressing cells*. Radiotherapy and Oncology, 2011. **99**(3): p. 367-372.
- 13. Pringle, S., et al., *Human Salivary Gland Stem Cells Functionally Restore Radiation Damaged Salivary Glands*. Stem Cells, 2016. **34**(3): p. 640-652.
- 14. Vissink, A., et al., Current ideas to reduce or salvage radiation damage to salivary glands.

 Oral Diseases, 2015. **21**(1): p. e1-e10.
- 15. Zawrzykraj, M., et al., *The effect of chemotherapy and radiotherapy on stem cells and wound healing. Current perspectives and challenges for cell-based therapies.* Biomedicine & Pharmacotherapy, 2023. **168**: p. 115781.
- 16. Marinkovic, M., et al., Autologous mesenchymal stem cells offer a new paradigm for salivary gland regeneration. International Journal of Oral Science, 2023. **15**(1): p. 18.
- 17. Mitroulia, A., et al., Salivary Gland Stem Cells and Tissue Regeneration: An Update on Possible Therapeutic Application. J Contemp Dent Pract, 2019. **20**(8): p. 978-986.
- 18. Tran, S.D., et al., *Adult stem cell therapy for salivary glands, with a special emphasis on mesenchymal stem cells.* Salivary Gland Development and Regeneration: Advances in Research and Clinical Approaches to Functional Restoration, 2017: p. 93-102.
- 19. Yoo, C., et al., Adult stem cells and tissue engineering strategies for salivary gland regeneration: a review. Biomaterials research, 2014. **18**(1): p. 9.
- 20. Im, K., et al., *An Introduction to Performing Immunofluorescence Staining*. Methods Mol Biol, 2019. **1897**: p. 299-311.

- 21. You, S., et al., *Isolation and Propagation of Mesenchymal Stem Cells from the Lacrimal Gland*. Investigative Ophthalmology & Visual Science, 2011. **52**(5): p. 2087-2094.
- 22. Yi, T., et al., Single Cell Clones Purified from Human Parotid Glands Display Features of Multipotent Epitheliomesenchymal Stem Cells. Scientific Reports, 2016. **6**(1): p. 36303.
- 23. Usui, S., H. Takahashi, and A. Tanaka, A Study of Submandibular Gland Changes in Mice of a Murine Model of Sjögren's Syndrome Administered Dental Pulp Stem Cell-Conditioned Medium. Journal of Hard Tissue Biology, 2023. **32**(2): p. 119-126.
- 24. Togarrati, P.P., et al., *Identification and characterization of a rich population of CD34+ mesenchymal stem/stromal cells in human parotid, sublingual and submandibular glands.*Scientific Reports, 2017. **7**(1): p. 3484.
- 25. Tiwari, S., et al., Establishing Human Lacrimal Gland Cultures with Secretory Function. PLOS ONE, 2012. 7(1): p. e29458.
- 26. Tatsuishi, Y., et al., *Human salivary gland stem/progenitor cells remain dormant even after irradiation*. Int J Mol Med, 2009. **24**(3): p. 361-366.
- 27. Sato, A., et al., *Isolation, Tissue Localization, and Cellular Characterization of Progenitors Derived from Adult Human Salivary Glands*. Cloning and Stem Cells, 2007. **9**(2): p. 191-205.
- 28. Rotter, N., et al., *Isolation and Characterization of Adult Stem Cells from Human Salivary Glands*. Stem Cells and Development, 2008. **17**(3): p. 509-518.
- 29. Redman, R.S. and J.C. Alvarez-Martinez, *Identifying stem cells in the main excretory ducts* of rat major salivary glands: adventures with commercial antibodies. Biotechnic & Histochemistry, 2023. **98**(4): p. 280-290.

- 30. Redman, R.S., An immunohistochemical study of the vasculature and stem cells and carbonic anhydrase IV in the ducts of irradiated and normal human submandibular salivary glands. Biotechnic & Histochemistry, 2023. **98**(6): p. 373-381.
- 31. Nelson, D.A., et al., *Quantitative single cell analysis of cell population dynamics during submandibular salivary gland development and differentiation.* Biology Open, 2013. **2**(5): p. 439-447.
- 32. Matsumoto, S., et al., *Isolation of Tissue Progenitor Cells from Duct-Ligated Salivary Glands of Swine*. Cloning and Stem Cells, 2007. **9**(2): p. 176-190.
- 33. Lu, L., et al., Characterization of a Self-renewing and Multi-potent Cell Population

 Isolated from Human Minor Salivary Glands. Scientific Reports, 2015. 5(1): p. 10106.
- 34. Lombaert, I.M.A., et al., Rescue of Salivary Gland Function after Stem Cell

 Transplantation in Irradiated Glands. PLOS ONE, 2008. 3(4): p. e2063.
- 35. Lee, S.J., et al., Comparative study on metabolite level in tissue-specific human mesenchymal stem cells by an ultra-performance liquid chromatography quadrupole time of flight mass spectrometry. Analytica Chimica Acta, 2018. **1024**: p. 112-122.
- 36. Kasamatsu, A., et al., Gibberellic acid induces α-amylase expression in adipose-derived stem cells. Int J Mol Med, 2012. **30**(2): p. 243-247.
- 37. Kang, S., et al., Adipose-derived mesenchymal stem cells promote salivary duct regeneration via a paracrine effect. Journal of Oral Biosciences, 2023. **65**(1): p. 104-110.
- 38. Jeong, J., et al., *Human salivary gland stem cells ameliorate hyposalivation of radiation-damaged rat salivary glands*. Experimental & Molecular Medicine, 2013. **45**(11): p. e58-e58.

- 39. I, T., et al., Resident CD34-positive cells contribute to peri-endothelial cells and vascular morphogenesis in salivary gland after irradiation. Journal of Neural Transmission, 2020. **127**(11): p. 1467-1479.
- 40. Furukawa, S., et al., Establishment of immortalized mesenchymal stem cells derived from the submandibular glands of tdTomato transgenic mice. Exp Ther Med, 2015. **10**(4): p. 1380-1386.
- 41. El-naseery, N.I., et al., Mesenchymal stem cells enhance AQP1 expression in the sublingual salivary gland of ovariectomized menopausal rat model. Annals of Anatomy Anatomischer Anzeiger, 2021. **236**: p. 151714.
- 42. Baek, H., et al., Autonomous isolation, long-term culture and differentiation potential of adult salivary gland-derived stem/progenitor cells. Journal of Tissue Engineering and Regenerative Medicine, 2014. 8(9): p. 717-727.
- 43. Andreadis, D., et al., *Minor salivary glands of the lips: a novel, easily accessible source of potential stem/progenitor cells.* Clinical Oral Investigations, 2014. **18**(3): p. 847-856.
- 44. Schachtele, S., C. Clouser, and J. Aho, *Markers and Methods to Verify Mesenchymal Stem Cell Identity*. Potency, and Quality.[(accessed on 29 January 2023)], 2016.
- 45. Okumura, K., M. Shinohara, and F. Endo, *Capability of Tissue Stem Cells to Organize into Salivary Rudiments*. Stem Cells International, 2012. **2012**: p. 502136.
- 46. Aure, M.H., S. Arany, and C.E. Ovitt, *Salivary Glands: Stem Cells, Self-duplication, or Both?* J Dent Res, 2015. **94**(11): p. 1502-7.
- 47. Lin, C.-S., et al., *Is CD34 truly a negative marker for mesenchymal stromal cells?*Cytotherapy, 2012. **14**(10): p. 1159-1163.

- 48. Kaiser, S., et al., *BM cells giving rise to MSC in culture have a heterogeneous CD34 and CD45 phenotype.* Cytotherapy, 2007. **9**(5): p. 439-450.
- 49. Yoshimura, K., et al., Characterization of freshly isolated and cultured cells derived from the fatty and fluid portions of liposuction aspirates. Journal of Cellular Physiology, 2006. **208**(1): p. 64-76.
- 50. Pachón-Peña, G., et al., Stromal stem cells from adipose tissue and bone marrow of agematched female donors display distinct immunophenotypic profiles. Journal of Cellular Physiology, 2011. **226**(3): p. 843-851.
- 51. Kim, W.-T. and C.J. Ryu, Cancer stem cell surface markers on normal stem cells. BMB reports, 2017. **50**(6): p. 285.
- 52. Konttinen, Y., et al., *Salivary glands* 'an unisex organ'? Oral Diseases, 2010. **16**(7): p. 577-585.
- 53. Cai, Z., et al., Optimized digital counting colonies of clonogenic assays using ImageJ software and customized macros: Comparison with manual counting. International Journal of Radiation Biology, 2011. **87**(11): p. 1135-1146.